

STEADY-STATE MODELING OF DETONATION PHENOMENON IN PREMIXED
GASEOUS MIXTURES AND ENERGETIC SOLID EXPLOSIVES

A THESIS SUBMITTED TO
THE GRADUATE SCHOOL OF NATURAL AND APPLIED SCIENCES
OF
MIDDLE EAST TECHNICAL UNIVERSITY

BY

FATİH CENGİZ

IN PARTIAL FULFILLMENT OF THE REQUIREMENTS
FOR
THE DEGREE OF MASTER OF SCIENCE
IN
MECHANICAL ENGINEERING

FEBRUARY 2007

Approval of the Graduate School of Natural and Applied Sciences

Prof. Dr. Canan ÖZGEN
Director

I certify that this thesis satisfies all the requirements as a thesis for the degree of Master of Science.

Prof. Dr. Kemal İDER
Head of Department

This is to certify that we have read this thesis and that in our opinion it is fully adequate, in scope and quality, as a thesis for the degree of Master of Science.

Bekir NARİN, M.Sc.
Co-Supervisor

Assoc. Prof. Dr. Abdullah ULAŞ
Supervisor

Examining Committee Members

Prof. Dr. Hüseyin VURAL (METU, ME) _____

Assoc. Prof. Dr. Abdullah ULAŞ (METU, ME) _____

Bekir NARİN, M.Sc. (TÜBİTAK, SAGE) _____

Prof. Dr. Yusuf ÖZYÖRÜK (METU, AEE) _____

Dr. Ahmet YOZGATLIGİL (METU, ME) _____

I hereby declare that all information in this document has been obtained and presented in accordance with academic rules and ethical conduct. I also declare that, as required by these rules and conduct, I have fully cited and referenced all material and results that are not original to this work.

Name, Last Name : **Fatih CENGİZ**

Signature :

ABSTRACT

STEADY-STATE MODELING OF DETONATION PHENOMENON IN PREMIXED GASEOUS MIXTURES AND ENERGETIC SOLID EXPLOSIVES

Cengiz, Fatih

M.Sc., Department of Mechanical Engineering

Supervisor : Assoc. Prof. Dr. Abdullah ULAŞ

Co-Supervisor: Bekir NARİN, M.Sc.

February 2007, 139 pages

This thesis presents detailed description of the development of two computer codes written in FORTRAN language for the analysis of detonation of energetic mixtures. The first code, named GasPX, can compute the detonation parameters of premixed gaseous mixtures and the second one, named BARUT-X, can compute the detonation parameters of C-H-N-O based solid explosives. Both computer codes perform the computations on the basis of Chapman-Jouguet Steady State Detonation Theory and in chemical equilibrium condition. The computed detonation point by the computer codes is one of the possible solutions of the Rankine–Hugoniot curve and it also satisfies the Rayleigh line.

By examining the compressibility of the gaseous products formed after detonation of premixed gaseous mixtures, it is inferred that the ideal-gas equation of state can be used to describe the detonation products. GasPX then calculates the detonation parameters complying with ideal-gas equation of state. However, the assumption of the ideal gas behavior is not valid for gaseous detonation products of solid explosives. Considering the historical improvement of the numerical studies in the

literature, the BKW (Becker-Kistiakowsky-Wilson) Equation of State for gaseous products and the Cowan & Fickett Equation of State for solid carbon (graphite) in the products are applied to the numerical model of BARUT-X.

Several calculations of detonation parameters are performed by both GasPX and BARUT-X. The results are compared with those computed by the other computer codes as well as the experimental data in the literature. Comparisons show that the results are in satisfactory agreement with experiments and also in good agreement with the calculations performed by the other codes.

Keywords: Detonation, Chapman-Jouguet, BKW, Cowan & Fickett, Explosives

ÖZ

KARARLI-DURUM KOŞULUNDA ÖN KARIŞIMLI GAZLARDA VE KATI FAZ PATLAYICILARDA PATLAMA TEPKİMESİNİN MODELLENMESİ

Cengiz, Fatih

Yüksek Lisans., Makina Mühendisliği Bölümü

Tez Yöneticisi : Assoc. Prof. Dr. Abdullah ULAŞ

Ortak Tez Yöneticisi: Bekir NARİN, M.Sc.

Şubat 2007, 139 sayfa

Bu tez kapsamında, FORTRAN dilinde yazılmış iki adet bilgisayar programı için yürütülmüş kod geliştirme çalışmaları ve uygulamaları detaylı bir şekilde anlatılmıştır. Geliştirilmiş iki adet programdan GasPX olarak adlandırılan, enerjik gaz karışımları için patlama tepkimesi noktasına ait parametreleri hesaplayabilmektedir. BARUT-X olarak adlandırılan program ise C-H-N-O tabanlı katı faz patlayıcılara ait patlama tepkimesi noktasına ait parametreleri hesaplamaktadır. Her iki program da, hesaplamaları Chapman-Jouguet patlama tepkimesi teorisi esasına uygun olarak, kimyasal denge koşulu için gerçekleştirmektedir. Hesaplanan patlama tepkimesi noktası Rankine-Hugoniot eğrisinin çözüm alanı içerisinde yer almakta ve aynı zamanda Rayleigh denklemini de sağlamaktadır.

Enerjik gaz karışımlarının patlaması sonucu ortaya çıkan, ürün gaz karışımı için yürütülen sıkıştırılabilirlik çalışması sonucunda, ideal-gaz durum denkleminin ürün gaz karışımı için yeterli olduğu sonucuna varılmıştır. Dolayısı ile GasPX programı ile yapılan hesaplamalar ideal-gaz denklemine uygun olarak gerçekleştirilmektedir. Buna karşın ideal gaz denklemi, katı faz patlayıcıların patlaması sonucu ortaya

ıkan rn gaz karıřımının durumunu tanımlamakta yetersiz kalmaktadır. Literatrde yer alan benzer programlara ait sayısal uygulamalar deęerlendirilerek, BKW (Becker-Kistiakowsky-Wilson) durum denklemi, katı faz patlayıcıların patlaması sonucu ortaya ıkan rn gaz karıřımını tanımlamak amacı ile BARUT-X programına uygulanmıřtır. Bununla birlikte, patlama sonrası rnler iinde meydana gelen katı karbonun tanımlanması amacıyla da Cowan & Fickett durum denklemi BARUT-X programına uygulanmıřtır.

Her iki programla da patlama tepkimesi noktasının belirlenmesine ynelik olarak bir ok hesaplama gerekleřtirilmiřtir. Elde edilen sonular literatrde yer alan deneysel deęerler ve dięer benzer programlara ait sonular ile karřılařtırılmıřtır. Bu karřılařtırmalar sonucunda, her iki programında mhendislik yaklařımı iersinde tatmin edici sonulara ulařtıęı, deęerlendirmesi yapılmıřtır.

Anahtar Kelimeler: Patlama, Chapman-Jouguet, BKW, Cowan & Fickett, Patlayıcı

To My Family

ACKNOWLEDGEMENTS

There are many people that I would like to thank for their guidance and motivation during the course of this thesis work. First, my supervisor Assoc. Prof. Dr. Abdullah ULAŞ has led and prodded me through a challenging and immensely rewarding graduate school experience. His advice, encouragement and support have been important factors in the completion of this thesis. And my co-supervisor Mr. Bekir NARİN has been a constant source of inspiration and insight in essential aspects of detonation theory and modeling. I am extremely grateful to Assoc. Prof. Dr. Abdullah ULAŞ and Mr. Bekir NARİN for their tremendous motivation on me.

I would also like to acknowledge my chief, Dr. Nadir SERİN from Terminal Ballistics Division at TÜBİTAK-SAGE, who has provided the convenient work environment and the motivation to pursue this work. I would also like to thank the Director of the Motor and Warhead Technologies Group at TÜBİTAK-SAGE, Dr. Mehmet Ali AK, for initializing and supporting this thesis. And I would like to express my sincere appreciation to my colleagues from Terminal Ballistics Division at TÜBİTAK-SAGE for their critical advice and unlimited friendship.

I would like to thank TÜBİTAK-SAGE (*The Scientific and Technological Research Council of Turkey – Defense Industries Research and Development Institute*) for its support of my academic endeavors.

I would also like to give my special appreciations to Dr. Muhammed SUĆESKA, from Laboratory of Thermal Analysis, Brodarski Institut, for his thoughtful contributions.

Lastly, I would like to thank my parents for their generous support over the past several years. They have always encouraged me in whatever challenges I have chosen to pursue. To my brothers, Alper, Çağatay and Ahmet, I would also like to thank them for their support.

TABLE OF CONTENTS

PLAGIARISM	iii
ABSTRACT	iv
ÖZ	vi
ACKNOWLEDGEMENTS.....	ix
TABLE OF CONTENTS	x
LIST OF TABLES	xiii
LIST OF FIGURES.....	xvi
LIST OF SYMBOLS	xviii
CHAPTER	
1. INTRODUCTION AND LITERATURE REVIEW.....	1
1.1. Introduction.....	1
1.2. Literature Review.....	2
1.3. Objectives.....	5
2. THERMODYNAMIC AND HYDRODYNAMIC THEORY OF DETONATION.....	7
2.1. Rayleigh Line Relation.....	11
2.2. Rankine-Hugoniot Curve	12
2.3. Chapman-Jouguet Point.....	15
3. DETONATION IN ENERGETIC GASEOUS MIXTURES	21
3.1. One-Dimensional Analysis.....	21
3.2. Equation of State	25

3.3.	Determination of the Chapman Jouquet Point.....	29
3.4.	Numerical Solution of Steady-State Detonation Properties for Premixed Gaseous Mixtures.....	32
3.4.1.	Thermodynamic Functions.....	34
3.4.2.	Thermodynamic Properties at States.....	37
3.4.3.	Chemical Equilibrium	39
3.4.4.	Algorithm of GasPX	42
3.4.5.	Sensitivity Analysis for GasPX.....	54
3.5.	Comparison of the Results	60
3.5.1.	Comparison of the Detonation Properties for Hydrogen-Oxygen Mixtures	60
3.5.2.	Comparison of the Detonation Properties for Acetylene-Oxygen Mixtures	67
3.5.3.	Comparison of the Detonation Properties for Cyanogen-Oxygen Mixtures	77
4.	DETONATION IN CONDENSED PHASE EXPLOSIVES.....	81
4.1.	One-Dimensional Analysis.....	81
4.2.	Equation of State	83
4.2.1.	Equation of State for Product Gas Mixture	83
4.2.2.	Equation of State for Solid Products.....	86
4.3.	Determination of the Chapman-Jouquet Point.....	86
4.4.	Numerical Solution of Steady-State Detonation Properties for Solid Explosives	87
4.4.1.	Thermodynamic Functions.....	89
4.4.1.1.	Thermodynamic Functions for Reactants	89
4.4.1.2.	Thermodynamic Functions for Gaseous Products.....	89
4.4.1.3.	Thermodynamic Functions for Solid Products	91

4.4.2.	Thermodynamic Properties at State of the Detonation Products	91
4.4.3.	Chemical Equilibrium	93
4.4.4.	Algorithm of BARUT-X	94
4.4.5.	Sensitivity Analysis for BARUT-X	107
4.5.	Comparison of the Results	113
5.	SUMMARY and CONCLUSIONS	128
5.1.	Summary and Conclusions	128
5.2.	Future Work	130
	REFERENCES	132
	APPENDICES	
A.	Properties of Explosives	139

LIST OF TABLES

TABLES

Table 1. Computed detonation properties and product composition of cyanogen-oxygen mixture stated in reference [48]	27
Table 2. Critical point properties.....	27
Table 3. Mole fractions and the covolumes of the components	29
Table 4. FORTRAN Format Used for Data in “thermo.inp”[54]	35
Table 5. Free FORTRAN format of “REACTIN.FOR”	43
Table 6. Free FORTRAN format of “PRODUCTIN.FOR”	45
Table 7. Experimental detonation velocity for acetylene-oxygen gaseous mixture [56]	54
Table 8. Constant parameters used in the computations performed for the sensitivity analysis of the pressure convergence factor (ε_p)	55
Table 9. Comparison of the computed Chapman-Jouguet detonation parameters by GasPX for the sensitivity analysis of the pressure convergence factor.....	55
Table 10. Effect of initial pressure values on computations	56
Table 11. Constant parameters used in the computations performed for the sensitivity analysis of the temperature convergence factor (ε_T)	57
Table 12. Comparison of the computed Chapman-Jouguet detonation parameters by GasPX for the sensitivity analysis of the temperature convergence factor.....	57
Table 13. Effect of initial temperature values on computations	58
Table 14. Constant parameters used in the computations performed for the sensitivity analysis of the tangency convergence factor (ε)	59
Table 15. Comparison of the computed Chapman-Jouguet detonation velocities by GasPX for the sensitivity analysis of the tangency convergence factor	59
Table 16. Parameters used in the computations performed by GasPX	60

Table 17. Comparison of GasPX predictions with experimental velocities of detonation wave of hydrogen and oxygen mixtures in a 10-cm diameter pipe.....	61
Table 18. Calculated and experimental velocities of detonation wave in hydrogen, oxygen and helium mixtures.....	64
Table 19. Comparison of the calculated velocities of detonation wave in hydrogen, oxygen and helium mixtures.....	66
Table 20. Comparison of the calculated equilibrium compositions.....	66
Table 21. Calculated and experimental velocities of detonation wave in acetylene and oxygen mixtures	68
Table 22. Calculated composition of the detonation products at C-J state	69
Table 23. Experimental and Calculated velocities of detonation wave after taking solid carbon formation into account.....	70
Table 24. Calculated composition of the detonation products including solid carbon at C-J state	71
Table 25. Comparison of the calculated velocities of detonation wave in acetylene and oxygen mixtures without solid carbon in products	73
Table 26. Comparison of the calculated velocities of detonation wave in acetylene and oxygen mixtures with solid carbon in products.....	75
Table 27. Computed heat of detonation in acetylene and oxygen mixtures with solid carbon in products.....	77
Table 28. Comparison of the computed detonation wave velocities by experimental and corrected data	78
Table 29. Comparison of the computed detonation wave velocities	79
Table 30. Comparison of the computed detonation wave velocities with corrected experimental data.....	80
Table 31. Covolumes of some gaseous detonation products.....	85
Table 32. Constants in BKW Equation of State.....	85
Table 33. Initial conditions for computation of BARUT-X	95
Table 34. Free FORTRAN format of "REACTIN.FOR".....	96
Table 35. Format of a row in the explosive data library, "EXPLOSIVE.FOR".....	97
Table 36. Free FORTRAN format of "PRODUCTIN.FOR"	98

Table 37. Experimental detonation parameters of RDX [35]	107
Table 38. Constant parameters used in the computations performed for the sensitivity analysis of the pressure convergence factor (ε_P)	108
Table 39. Comparison of the computed Chapman-Jouguet detonation parameters by BARUT-X for the sensitivity analysis of the pressure convergence factor.....	108
Table 40. Effect of initial pressure values on computations	109
Table 41. Constant parameters used in the computations performed for the sensitivity analysis of the temperature convergence factor (ε_T)	110
Table 42. Comparison of the computed Chapman-Jouguet detonation parameters by BARUT-X for the sensitivity analysis of the temperature convergence factor ...	110
Table 43. Effect of initial temperature values on computations	111
Table 44. Constant parameters used in the computations performed for the sensitivity analysis of the tangency convergence factor (ε)	112
Table 45. Comparison of the computed Chapman-Jouguet detonation velocities by BARUT-X for the sensitivity analysis of tangency convergence factor.....	112
Table 46. Parameters used in the computations performed by BARUT-X.....	113
Table 47. Values of constants in BKW Equation of State.....	114
Table 48. Comparison of calculated and experimental values of detonation parameters for different densities of HMX.....	116
Table 49. Comparison of calculated and experimental values of detonation parameters for different densities of TNT	118
Table 50. Comparison of calculated and experimental values of detonation parameters for different densities of RDX	120
Table 51. Comparison of calculated and experimental values of detonation parameters for different densities of PETN	122
Table 52. Comparison of calculated values of detonation heat.....	127
Table 53. Comparison of calculated mole numbers of detonation products per mole of explosive at C-J point	127

LIST OF FIGURES

FIGURES

Figure 1. Detonation Phenomenon Represented by a Closed Circle.....	7
Figure 2. One-Dimensional Stationary Detonation Wave.....	8
Figure 3. Rayleigh Line on the P - v diagram	12
Figure 4. Rankine-Hugoniot curve P versus $1/\rho$ plane	15
Figure 5. Rankine-Hugoniot curve and Chapman-Jouguet points.....	16
Figure 6. Velocities Defined Relative to the Observer Out of the Detonation Region	18
Figure 7. One-Dimensional Stationary Detonation Wave.....	21
Figure 8. Rankine-Hugoniot curves and Rayleigh line for gaseous detonation.....	30
Figure 9. Variation of the detonation velocity along the Rankine-Hugoniot curve	31
Figure 10. Data of the condensed titanium nitrate in the thermodynamic data library	36
Figure 11. Determination of the Chapman-Jouguet Point on the Rankine-Hugoniot curve by GasPX	48
Figure 12. Flow chart of GasPX	52
Figure 13. Comparison of the calculated and measured velocities of detonation wave for a 10-cm diameter pipe	62
Figure 14. Comparison of the calculated and measured velocities of detonation wave for a 1.2-cm diameter pipe	63
Figure 15. Comparison of the calculated and measured velocities of detonation wave in acetylene and oxygen mixtures.....	68
Figure 16. Comparison of the calculated and measured velocities of detonation wave by including the solid carbon formation into computations.....	70
Figure 17. Detonation velocities in acetylene-oxygen mixtures at 1 atm pressure...72	

Figure 18. Comparison of the calculated velocities of detonation wave without solid carbon formation into computations	74
Figure 19. Comparison of the calculated velocities of detonation wave with solid carbon formation into computations	75
Figure 20. Comparison of the detonation wave velocities computed by GasPX and experimental data.....	78
Figure 21. Comparison of the computed detonation wave velocities with corrected experimental data.....	80
Figure 22. Simplified Presentation of Condensed Phase Explosive Detonation Phenomenon	81
Figure 23. Determination of the Chapman-Jouguet Point on the Rankine-Hugoniot curve by BARUT-X.....	101
Figure 24. Flow chart of BARUT-X.....	105
Figure 25. Comparison of calculated and experimental values of detonation velocity for different densities of HMX.....	117
Figure 26. Comparison of calculated and experimental values of detonation pressure for different densities of HMX.....	117
Figure 27. Comparison of calculated and experimental values of detonation velocity for different densities of TNT.....	119
Figure 28. Comparison of calculated and experimental values of detonation pressure for different densities of TNT.....	119
Figure 29. Comparison of calculated and experimental values of detonation pressure for different densities of RDX.....	121
Figure 30. Comparison of calculated and experimental values of detonation pressure for different densities of RDX.....	121
Figure 31. Comparison of calculated and experimental values of detonation pressure for different densities of PETN.....	123
Figure 32. Comparison of calculated and experimental values of detonation pressure for different densities of PETN.....	123

LIST OF SYMBOLS

a_{ij}	number of atoms of element j in a molecule of species i in products
b_j	total number of atoms of element j in reactants
c	speed of sound (m/s)
$C_p(T)$	constants-pressure specific heat (J/kg K)
C_p	mean constant-pressure specific heat (J/kg K)
$C_v(T)$	constants-volume specific heat (J/kg K)
C_v	mean constant-volume specific heat (J/kg K)
D	detonation velocity (m/s)
e	specific internal energy pre unit mass (J/kg)
$F(x)$	gas imperfection factor in BKW EOS
g	specific Gibbs function per unit mass (J/kg)
g°	specific Gibbs function of formation per unit mass at standard state
G	Gibbs function
h	specific enthalpy pre unit mass (J/kg)
Δh_f°	enthalpy of formation at standard state (J/kg)
k	thermal conductivity (W/m ² K)
k_i	covolumes of the gaseous products
Ma	Mach number
\dot{m}''	mass flow rate per unit area (kg/m ² s)
MP_i	mass percentage of i^{th} solid explosive
MW	molecular weight (kg/kmol)
MW_g	molecular weight of gaseous mixture (kg/kmol)
MW_i	molecular weight of i^{th} component (kg/kmol)
MW_s	molecular weight of solid mixture (solid carbon) (kg/kmol)
MWR_i	molecular weight of i^{th} solid explosive
n	number of moles
n_g	total number of moles of gaseous components
n_s	number of moles of solid carbon
nr_i	number of moles of i^{th} solid explosives
P_a	Initiation pressure (Pa)

P	pressure (Pa)
P_C	pressure at critical point (bar)
P_{C-J}	pressure at Chapman-Jouguet point (Pa)
P_R	reduced pressure (P/P_C)
P_x	initially assumed pressure in computation of Chapman-Jouguet point calculation
q_R	heat of reaction ($q_R = (\Delta h_f^\circ)_1 - (\Delta h_f^\circ)_2$ kJ/kg)
R	gas constant of mixture (J/kg K)
R_u	universal gas constant (8.31457 kJ/kmol K)
s	specific entropy per unit mass (J/kg K)
s°	specific absolute entropy at standard reference pressure (J/kg K)
T	temperature (K)
T_C	temperature at critical point (K)
T_{C-J}	temperature at Chapman-Jouguet point (K)
T_R	reduced temperature (T/T_C)
u	velocity relative to stationary detonation wave (m/s)
U	any extensive property
v	specific volume (m^3/kg)
v_a	initiation specific volume (m^3/kg)
v_g	specific volume of gaseous mixture (m^3/kg)
v_s	specific volume of solid carbon (m^3/kg)
v_s°	specific volume of carbon at normal crystal density (cm^3/g)
v_{C-J}	specific volume of the products at Chapman-Jouguet point (m^3/kg)
\bar{V}_g	molal volume of gaseous mixture (cm^3/mole)
v_x	velocity relative to observer out of the detonation region
x	length (m)
x	mole fraction
x_i	mole fraction of the i^{th} gaseous component
x_s	mole fraction of the solid carbon
y_i	number of mols of the i^{th} gaseous component in equilibrium composition
y_s	number of mols of the solid carbon in equilibrium composition
Z	compressibility factor

Greek Symbols

α	BKW EOS parameter
β	BKW EOS parameter
γ	polytropic exponent
γ_{C-J}	polytropic exponent at Chapman-Jouguet point
Δ	change (= final minus initial)
ε	tangency convergence factor ($\varepsilon \rightarrow 0$)
ε_P	pressure convergence factor ($\varepsilon_P \rightarrow 0$)
ε_T	temperature convergence factor ($\varepsilon_T \rightarrow 0$)
η	compression of solid carbon relative to its normal crystal density
θ	BKW EOS parameter
κ	BKW EOS parameter
λ	phase control integer (indicator)
μ	chemical potential (J/kmol)
μ	viscosity (N s /m ²)
μ'	bulk viscosity (N s /m ²)
ρ	density (kg/m ³)
ρ_{C-J}	density at Chapman-Jouguet point (kg/m ³)

Subscripts

C-J	Chapman-Jouguet point
g	property of gaseous mixture
Ref, ref	reference value or state
RH	Rankine-Hugoniot
RL	Rayleigh line
s	property of solid carbon
1	initial state (state of reactants)
2	final state (state of products)

Superscripts

-	bar over symbol denotes property on molar basis
·	dot over symbol denotes time rate
'	denotes ideal part of thermodynamic functions
"	denotes property per unit area

- ° property at standard state or standard pressure
- * denotes imperfection part of thermodynamic functions

CHAPTER 1

INTRODUCTION AND LITERATURE REVIEW

1.1. Introduction

In premixed explosive gas mixtures based on C-H-N-O atoms, burning zone or combustion wave can be propagated in the form of a chemical reaction. Explosive gas mixtures are commonly mixtures of two reactants such as oxygen and fuel gaseous like methane, hydrogen, acetylene and etc.

The detonation of explosive gas mixtures can be studied in long pipes having one end closed and the other open. If the reaction develops at the closed end of the pipe as a result of an ignition source, then a propagation regime is observed, which is characterized by a very large wave velocity (2000-3000 m/s) through the unburned region and which is associated with an extremely large increase in pressure behind the reaction zone. This phenomenon of the supersonic wave propagation of the explosive gas mixture sustained by chemical reaction is called "detonation".

Detonation waves are shock waves, faster than sound (5-10 Mach). They are sustained by the energy released from the chemical reactions. Detonation is initiated by shock compression and the resulting high temperature. The difference between combustion waves and detonation waves is that a combustion wave propagates at a subsonic velocity by thermal and molecular diffusion.

The detonation phenomenon is valid not only in gas explosives, but also in condensed phase explosives. The theory on the detonation of condensed explosives has been constructed on the theory of gaseous detonation. However when the loading density of reactant is higher than 0.4 g/cm^3 , the pressure increases significantly due to the intermolecular forces of gases (attractive potential and repulsive potential). On the other hand, for explosive gas mixtures, the forces between molecules in the gas are negligible compared with the thermal effects of the gas, at relatively low pressures.

Thus, a detonation phenomenon is related to the interactions between hydrodynamic processes, the shock wave theory, and a thermochemical process, the combustion.

1.2. Literature Review

The earliest observations of detonation waves are performed by Berthelot and Veille [1] and independently Mallard and Le Chatelier [2]. These investigators discovered the speed of wave propagation of explosions in gas mixtures enormously greater than had been measured previously. The speeds of wave propagation in various explosive gas mixtures were able to be measured by means of chronoelectric [3] and photographic [4] methods. Many other scientists (complete list of reference are given in "Flame and Combustion in Gases" [5]) have continued to study and measure the detonation wave propagation velocity in a large number of explosive gas mixtures.

The detonation phenomenon is shock wave propagation sustained by chemical reaction. The theoretical interpretation of shock and detonation waves was comprehensively studied by Chapman [6], Jouguet [7], Becker [8], Ya. B. Zel'dovich [9, 10], Fickett [11] and other scientists.

The earliest and simplest theory, which interprets the detonation phenomena in a successful manner, is the Chapman-Jouguet Theory [6, 7]. The Chapman-Jouguet Theory discusses the detonation wave as a shock wave which has a discontinuity between the initial (upstream) and final (downstream) states. According to this theory, the expanding gases behind reaction zone possess the thermodynamic equilibrium after the spontaneous chemical reaction. The theory assumes that the flow is steady, inviscid, and one-dimensional with discontinuity. In addition, critical other assumptions are made: adiabatic condition, no shaft work, negligible body force and constant area across the detonation wave. In the Chapman-Jouguet Theory, the minimum wave velocity is observed at which detonation occurs [11]. Moreover, specifically, the theory assumes that the chemical reaction reaches the state of chemical equilibrium [12].

Experimental studies on the detonations caused by adiabatic compression by a shock in explosive gases were performed by some investigators, Laffitte [13], Wendlandt [14], Payman and Walls [15], Dixon [16, 17], and Bone [18]. Also, the

experimental detonation wave velocities were measured by these investigators in their work.

Besides these measurements, the first critical experimental study on the applicability of the Chapman-Jouguet Theory was carried out by Lewis and Friauf [19]. They performed both theoretical and experimental studies to determine the detonation wave velocity in mixtures of hydrogen and oxygen mixtures diluted with gases, nitrogen, argon and helium. Berets et al. [12] also conducted the both theoretical calculation and experimental determination of the detonation wave velocity in hydrogen and oxygen mixtures. An important conclusion from their study is that comparison of the velocities calculated by the Chapman-Jouguet Theory shows agreement only for mixtures with ratio of hydrogen to oxygen not far from stoichiometric. After Berets et al. considerable improvements in both computational and experimental work were developed. Duff et al. [20] studied on the measurement of the density in gaseous detonation by x-ray absorption. Edwards et al. [21] performed the measurement of the pressure by means of piezoelectric gauges. Peek and Thrapp [22] measured the detonation velocities in mixture of cyanogen and oxygen. White [23] performed a very comprehensive experimental study of hydrogen-oxygen mixture diluted with other gases.

On the basis of Chapman-Jouguet Theory, computer programs, which can solve steady-equilibrium detonation in premixed gaseous mixtures to obtain the state properties of reaction products, have been developed. Since gaseous explosives are well described by the ideal gas equation of state [11], these programs also treat the product gas mixture as ideal. One of these programs is BLAKE code [24] which can make calculations on the combustion gases formed by military propellants under gas chamber conditions. This program contains a subroutine based on an ideal gas equation of state. The other program, having a well-known reputation in academic platform, is NASA-Lewis code, CEA [25] (Chemical Equilibrium and Applications). The program can obtain chemical equilibrium compositions for assigned thermodynamic states, and also performs the calculations to obtain Chapman-Jouguet detonation properties. Detonation subroutine of CEA code is limited to gaseous reactants and uses the ideal gas equation of state.

In addition to the calculation of detonation parameters in gases, the study on the detonation phenomenon in condensed phase explosives, especially solid

explosives, is conducted by a large number of investigators. But condensed phase explosives are much harder to study. The ideal-gas equation of state is poor to describe the state of the product at high pressure, high temperature and also high density. Lack of satisfactory equation of state for the products hinders the simple comparison of theory and experiment.

In solid explosives, the measurement of detonation velocity is done in the conventional way, using cylinders, and removing the effects of finite charge diameter by extrapolation to infinite charge diameter [11]. The measurement of the Chapman-Jouguet detonation pressure were determined from experiments in which the pressure inferred from its measured effects in other material by Deal [26], Rivard [27], Davis and Venable [28], Mader and Craig [29], and Davis [30]. The other experimental technique is Aquarium Test which was developed to measure simultaneously detonation velocity and pressure, confinement effects, and the release isentrope from the Chapman-Jouguet state [31]. In this test, an explosive cylinder is placed in a water tank with two parallel transparent windows. By using the photographic exposures at the detonation time, the Chapman-Jouguet detonation properties of the explosives are deduced. C-J properties of several explosives were measured in Los Alamos Scientific Laboratory by this method [31].

The theoretical applications of detonation phenomenon are also conducted. The main problem of theoretical attempts was the equation of state which could satisfactorily be applied to gaseous products. A number of equations of state for products have been developed in the past. Virial [32], L-J (Lennard-Jones) [32], BKW (Becker-Kistiakowsky-Wilson) [33] and JCZ (Jacobs-Cowperthwaite-Zwissler) [34] Equations of State have been most commonly used in theoretical calculations. All these equations of state depend on the consideration of the molecular interactions (i.e., repulsive and attractive forces). The empirical constants used in them have been obtained from the experimental data as well as the experimental shock adiabat (Rankine-Hugoniot curve).

A large number of studies have been performed to calculate the detonation properties of solid explosives. In accordance with the theoretical models, some computer codes have been developed to determine the properties of detonation point. Those, of which have well-known reputations today, are FORTRAN BKW [35], RUBY [36], TIGER [37], CHEETAH [38], and EXPLO 5 [39]. The computations in

the codes commonly depend on the iterative calculation techniques. All these programs have performed the calculations of detonation properties on the basis of Chapman-Jouguet Theory by applying the BKW Equation of State to the gaseous products besides the newly developed equations of state. It can be deduced that the BKW Equation of State for gaseous products is sufficient even today.

Besides computer codes which are based on theoretical models, some empirical methods have also been developed to calculate the detonation parameters of solid explosives by Kamlet and Jackobs [40], Rothstein and Petersen [41]. Some of these empirical methods are still in use today.

1.3. Objectives

The work presented here aims to expand an improved understanding of numerical modeling of detonation phenomenon in premixed gaseous mixtures and condensed phase explosives. Two computer codes in FORTRAN language have been developed to determine detonation parameters of energetic gaseous and solid explosives on the basis of Chapman-Jouguet Theory and in chemical equilibrium condition. One named GasPX can compute the Chapman-Jouguet detonation parameters in premixed gaseous mixture and the other named BARUT-X can compute Chapman-Jouguet detonation parameters of solid explosives.

In order to compute equilibrium composition at the detonation point, a chemical equilibrium code has been developed. This code has an improved algorithm different than the other computer codes, which generally use the method developed by White et al. [42]. A commercial non-linear optimization solver coupled with FORTRAN has been adapted to the computation of chemical equilibrium. An objective function, which is a non-linear equation, is derived from Gibbs free energy function of the final state. This non-linear equation defined as an objective function is solved to determine the minimum value of Gibbs function by the commercial optimization solver while the mass balance is satisfied. The application of this chemical equilibrium algorithm to the detonation codes is explained in Chapter 3 and Chapter 4.

In Chapter 3, numerical model and algorithm of GasPX is presented in detail. Examining the compressibility and imperfection of the gaseous product mixture in gaseous detonation, it is inferred that the ideal gas behavior is enough to describe

the gaseous product mixture. So the ideal gas equation of state is applied to the GasPX. The computed detonation parameters by GasPX are at a point where the Rankine-Hugoniot curve is tangent to the Rayleigh line. The results computed by GasPX are compared with the experimental data and those obtained by the other codes as well as the theoretical methods.

In Chapter 4, the other computer code, BARUT-X, which has been developed to determine the detonation parameters of solid explosives, is presented in detail. Different than GasPX, BARUT-X uses the BKW Equation of State for gaseous detonation products due to the high density and high pressure of the gaseous product mixture. In addition, solid carbon formation in equilibrium composition is taken into account by BARUT-X. The equation of state developed by Cowan & Fickett is applied to the solid carbon under high pressure and temperature. The results computed by BARUT-X are compared with experimental data and those computed by EXPLO5 and FORTRAN BKW.

CHAPTER 2

THERMODYNAMIC AND HYDRODYNAMIC THEORY OF DETONATION

Detonation is a shock wave whose propagation is driven by the energy released from chemical reactions. Detonation phenomenon can be explained by a closed circle:

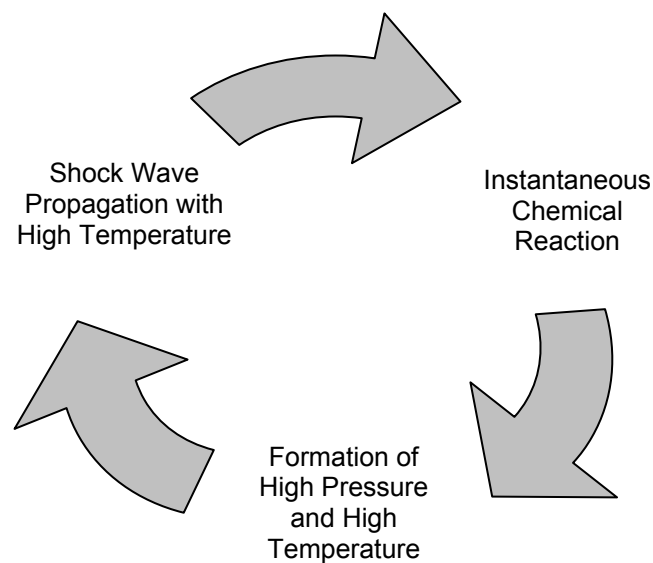


Figure 1. Detonation Phenomenon Represented by a Closed Circle

The earliest rigorous studies, which have explained the detonation theory, were performed by Chapman [6] in 1899. He approached the detonation phenomenon from the point of view of thermodynamics and hydrodynamics and was able to calculate the detonation velocities of various gaseous mixtures in good agreement. Being unaware of this earlier work, Jouguet [7], in 1905, made a considerable development on the detonation theory and reached a similar success. So, the first theory, which provides an extensive explanation to the detonation phenomenon, is accepted as the Chapman-Jouguet Theory.

The Chapman-Jouguet Theory assumes the following:

1. The flow is one-dimensional, steady and inviscid,

2. The detonation wave is a shock wave which has a discontinuity between initial (upstream) and final (downstream) states,
3. The products (expanding gases) behind reaction zone possess the thermochemical equilibrium after the spontaneous chemical reaction and are described with a thermodynamic equation of state,
4. The flow is adiabatic,
5. There is no shaft work and negligible body force,
6. Due to the thermochemical equilibrium and spontaneous chemical reaction, the theory assumes that the chemical reaction reaches the state of chemical equilibrium.

A schematic diagram of a one-dimensional combustion wave is shown in Figure 2. It is assumed that the control volume consists of the chemical-reaction zone (combustion wave or detonation wave) which has an infinitely thin planar structure. Actually, the combustion wave is moving at a constant velocity u_1 and the unburned gases are assumed as stationary. In a reference frame following the wave motion, the stationary unburned gases ahead of the wave can be considered to move at wave velocity (u_1) towards the detonation wave. The selection of this frame of reference transforms the propagating wave into a stationary wave, which is more convenient when the governing equations are applied [43].

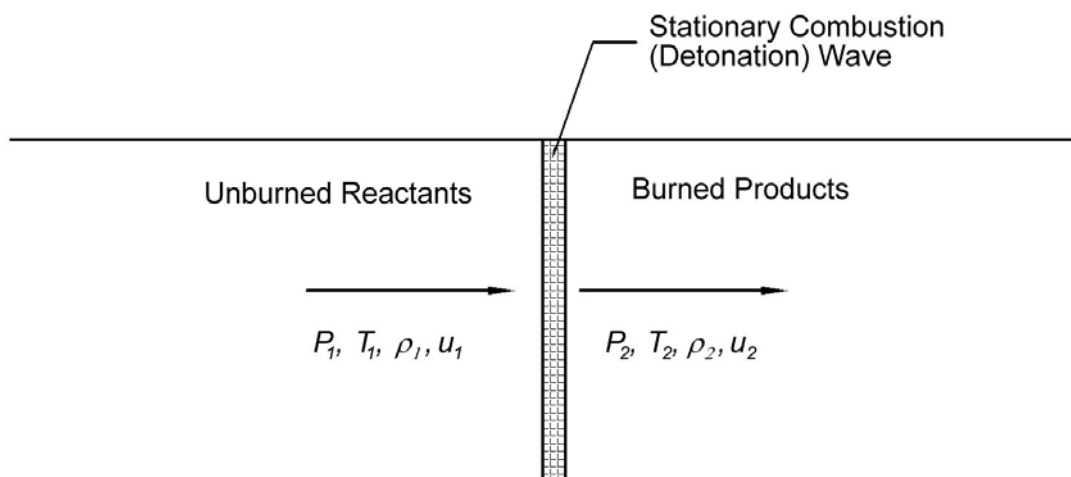


Figure 2. One-Dimensional Stationary Detonation Wave

Governing equations for steady one-dimensional flow, with no body forces, no shaft work, no external heat addition or heat loss, are as follows:

Continuity

$$\frac{d(\rho u)}{dx} = 0 \quad (1)$$

Momentum

$$\rho u \frac{du}{dx} = -\frac{dP}{dx} + \frac{d}{dx} \left[\left(\frac{4}{3} \mu + \mu' \right) \frac{du}{dx} \right] \quad (2)$$

where, μ : Viscosity, μ' : Bulk viscosity

Energy

$$\rho u \frac{dh}{dx} = \nabla \cdot (k \nabla T) + u \frac{dP}{dx} \quad (3)$$

In this form of the energy equation, due to the inviscid flow assumption, the viscous dissipation function is neglected.

From momentum equation,

$$\frac{dP}{dx} = -\rho u \frac{du}{dx} + \frac{d}{dx} \left[\left(\frac{4}{3} \mu + \mu' \right) \frac{du}{dx} \right] \quad (4)$$

and the heat conduction term in the energy equation can be written as

$$\nabla \cdot (k \nabla T) = \frac{d}{dx} \left(k \frac{dT}{dx} \right) \quad (5)$$

By substituting Eqn. 4 and Eqn. 5 into energy equation (Eqn. 3) we have

$$\rho u \frac{dh}{dx} = \frac{d}{dx} \left(k \frac{dT}{dx} \right) - \rho u^2 \frac{du}{dx} + u \frac{d}{dx} \left[\left(\frac{4}{3} \mu + \mu' \right) \frac{du}{dx} \right] \quad (6)$$

And the new form of energy equation,

$$\rho u \left[\frac{d}{dx} \left(h + \frac{u^2}{2} \right) \right] = \frac{d}{dx} \left(k \frac{dT}{dx} \right) + u \frac{d}{dx} \left[\left(\frac{4}{3} \mu + \mu' \right) \frac{du}{dx} \right] \quad (7)$$

The bulk viscosity μ' is usually very small and can be neglected [43].

Integrated continuity equation (Eqn. 1) is,

$$\rho u = \text{constant} \equiv \dot{m}'' \quad (8)$$

Eqn. 8 can be substituted into the momentum equation (Eqn. 2),

$$\rho u \frac{du}{dx} + u \frac{d\rho u}{dx} = -\frac{dP}{dx} + \frac{d}{dx} \left[\frac{4}{3} \mu \frac{du}{dx} \right] \quad (9)$$

Eqn. 9 becomes

$$\frac{d}{dx} \left[\rho u^2 + P - \frac{4}{3} \mu \frac{du}{dx} \right] = 0 \quad (10)$$

Integrating Eqn. 10,

$$\rho u^2 + P - \frac{4}{3} \mu \frac{du}{dx} = \text{constant} \quad (11)$$

Energy equation (Eqn. 7) becomes

$$\rho u \left[\frac{d}{dx} \left(h + \frac{u^2}{2} \right) \right] + \left(h + \frac{u^2}{2} \right) \frac{d(\rho u)}{dx} = \frac{d}{dx} \left(k \frac{dT}{dx} \right) + u \frac{d}{dx} \left[\frac{4}{3} \mu \frac{du}{dx} \right] \quad (12)$$

Due to the constant initial conditions ahead of the wave and the thermochemical equilibrium after the reaction zone, the velocity and temperature of reactants and products are constant respectively in the unburned and burned region. In other words, du/dx and dT/dx are both equal to zero ahead of the and behind the wave. Then, the following conservation equations are provided:

$$\rho_1 u_1 = \rho_2 u_2 = \dot{m}'' \quad (13)$$

$$P_1 + \rho_1 u_1^2 = P_2 + \rho_2 u_2^2 \quad (14)$$

$$h_1 + \frac{1}{2} u_1^2 = h_2 + \frac{1}{2} u_2^2 \quad (15)$$

2.1. Rayleigh Line Relation

When the continuity (Eqn. 13) and the momentum (Eqn. 14) equations are combined the following equation can be obtained:

$$P_2 - P_1 = \rho_1 u_1^2 - \rho_2 u_2^2 = \frac{\rho_1^2 u_1^2}{\rho_1} - \frac{\rho_2^2 u_2^2}{\rho_2} = \left(\frac{1}{\rho_1} - \frac{1}{\rho_2} \right) \dot{m}''^2 \quad (16)$$

Eqn. 16 can be written in terms of \dot{m}''^2 :

$$\dot{m}''^2 = \rho_1^2 u_1^2 = \rho_2^2 u_2^2 = \frac{P_2 - P_1}{\frac{1}{\rho_1} - \frac{1}{\rho_2}} \quad (17)$$

Using the specific volume, v , instead of density:

$$\frac{P_2 - P_1}{v_2 - v_1} = -\dot{m}''^2 \quad (18)$$

Simultaneous solution of the continuity and momentum equation yields the above relation (Eqn. 18). This equation is called the **Rayleigh line** relation.

By fixing initial pressure (P_1) and density (ρ_1), the **Rayleigh line** relation can be expressed in the generic linear relationship [44]:

$$P_2 = P_1 - \dot{m}''^2 (v_2 - v_1) \quad (19)$$

where the slope is \dot{m}''^2 .

Figure 3 shows the plot of a Rayleigh line relation for a given state 1 (fixed by P_1 and v_1). There are two limiting cases in the P - v diagram: If the Rayleigh line was vertical, the mass flux would go infinite. And if the Rayleigh line was horizontal, the mass flux would be zero. Moreover, since the sign of the \dot{m}''^2 can not be minus, regions A and B (formed by the dashed lines passing through the initial point (P_1 , v_1)) are physically inaccessible. Eventually, the region between horizontal and vertical asymptotes contains all possible mass fluxes and there are no solutions in the two quadrants labeled by A and B.

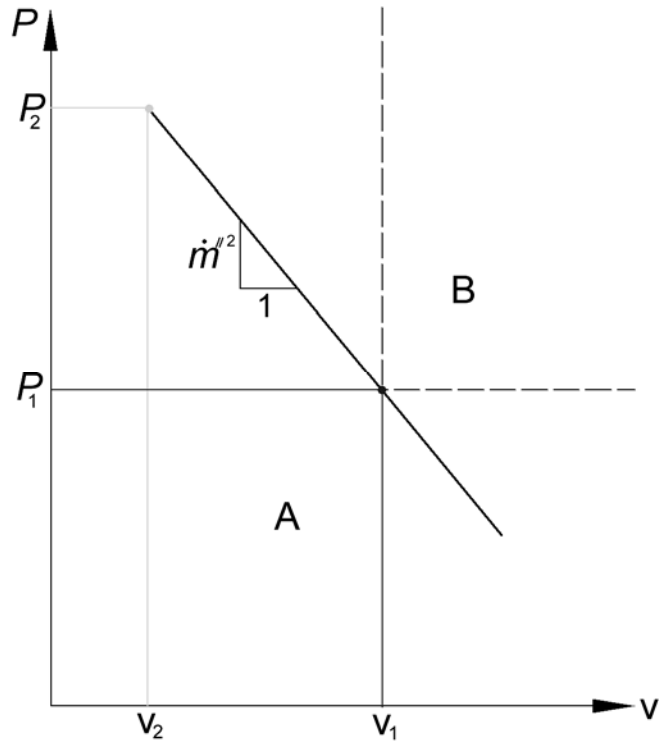


Figure 3. Rayleigh Line on the P - v diagram

2.2. Rankine-Hugoniot Curve

The energy equation (Eqn. 15) can be rewritten in the following form:

$$h_2 - h_1 = \frac{1}{2}u_1^2 - \frac{1}{2}u_2^2 \quad (20)$$

Combining Rayleigh-line relation (equation 17), the velocity terms in the energy equation (Eqn. 20) can be eliminated:

$$h_2 - h_1 = \frac{1}{2} \left(\frac{P_2 - P_1}{\frac{1}{\rho_1} - \frac{1}{\rho_2}} \right) \frac{1}{\rho_1^2} - \frac{1}{2} \left(\frac{P_2 - P_1}{\frac{1}{\rho_1} - \frac{1}{\rho_2}} \right) \frac{1}{\rho_2^2} \quad (21)$$

Rearranging Eqn. 21,

$$h_2 - h_1 = \frac{1}{2} \left(\frac{P_2 - P_1}{\frac{1}{\rho_1} - \frac{1}{\rho_2}} \right) \left(\frac{1}{\rho_1^2} - \frac{1}{\rho_2^2} \right) \quad (22)$$

Hence, the below relation is obtained,

$$h_2 - h_1 = \frac{1}{2}(P_2 - P_1) \left(\frac{1}{\rho_1} + \frac{1}{\rho_2} \right) \quad (23)$$

Simultaneous solution of the continuity, momentum and energy equations yields the above relation. This relation is called **Hugoniot** or **Rankine-Hugoniot** curve on the pressure (P) versus specific volume (v) diagram.

In Eqn. 23, the **Rankine-Hugoniot Relation** is expressed in terms of total (thermal plus chemical) enthalpy h .

$$h(T) = \Delta h_f^\circ + [h(T) - h(298)] \quad (24)$$

or

$$h(T) = \int_{298}^T C_p(T) dT + \Delta h_f^\circ \quad (25)$$

For mean value of specific heat (C_p), enthalpy term can be written as

$$h(T) = C_p (T - 298) + \Delta h_f^\circ \quad (26)$$

where Δh_f° is the enthalpy of formation at the *standard reference state* defined by $T_{ref} = 298.15$ K (25 °C) and $P_{ref} = 1$ atm.

This form of enthalpy (total enthalpy) is consistent with the thermodynamic data file which will be discussed later.

Regarding Eqn. 26, the Rankine-Hugoniot Relation can be rewritten as,

$$C_{p_2}(T_2 - 298) + (\Delta h_f^\circ)_2 - C_{p_1}(T_1 - 298) - (\Delta h_f^\circ)_1 = \frac{1}{2}(P_2 - P_1) \left(\frac{1}{\rho_1} + \frac{1}{\rho_2} \right) \quad (27)$$

In accordance with assumptions made for Chapman-Jouguet Theory and assuming the constant specific heat,

$$C_p(T_2 - T_1) - q_R = \frac{1}{2}(P_2 - P_1) \left(\frac{1}{\rho_1} + \frac{1}{\rho_2} \right) \quad (28)$$

where q_R is the heat of reaction,

$$q_R = (\Delta h_f^\circ)_1 - (\Delta h_f^\circ)_2 \quad (29)$$

Eqn. 28 can be redefined by using the ideal gas equation of state and the following relations,

$$C_v = C_p - R \quad (30)$$

$$\gamma = \frac{C_p}{C_v} \quad (31)$$

$$C_p = \frac{\gamma}{\gamma - 1} R \quad (32)$$

$$T = \frac{P}{\rho R} \quad (33)$$

Hence, we obtain

$$\frac{\gamma}{\gamma - 1} R \left(\frac{P_2}{\rho_2 R} - \frac{P_1}{\rho_1 R} \right) - q_R = \frac{1}{2} (P_2 - P_1) \left(\frac{1}{\rho_1} + \frac{1}{\rho_2} \right) \quad (34)$$

or

$$\frac{\gamma}{\gamma - 1} \left(\frac{P_2}{\rho_2} - \frac{P_1}{\rho_1} \right) - q_R = \frac{1}{2} (P_2 - P_1) \left(\frac{1}{\rho_1} + \frac{1}{\rho_2} \right) \quad (35)$$

Eqn. 35 is the one form of the Rankine-Hugoniot Relation in accordance with the characteristic nature of ideal gas state.

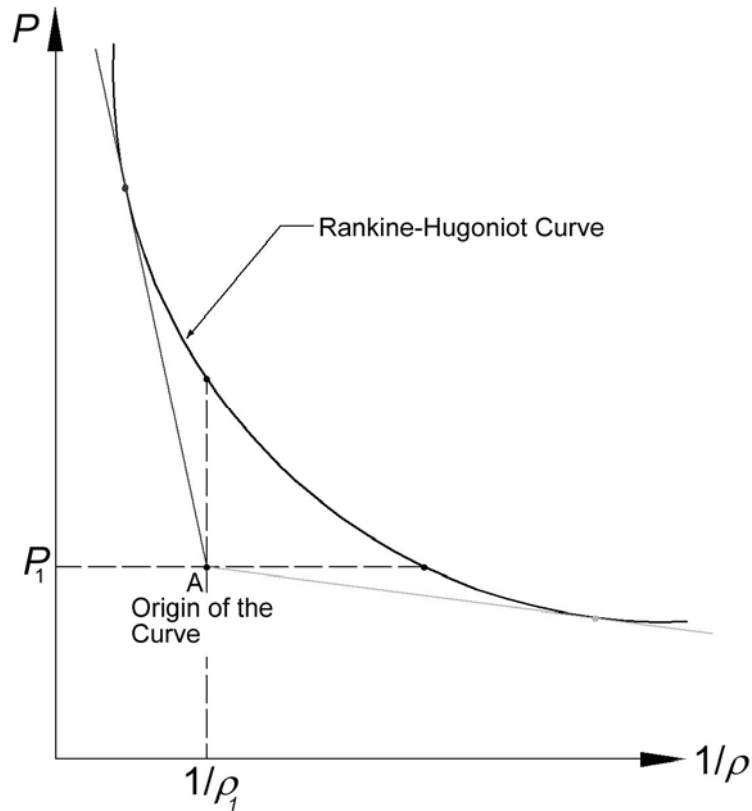


Figure 4. Rankine-Hugoniot curve P versus $1/\rho$ plane

Figure 4 shows the plot of the P as a function of density ($1/\rho$) or specific volume v for a given set of initial pressure (P_1), initial density (ρ_1) and the difference of the total enthalpies ($h_2 - h_1$). The point (P_1, ρ_1) or (P_1, v_1) is called the origin of the Hugoniot curve. However, the curve does not actually pass through the origin. Rankine-Hugoniot curve will be considered in detail in Section 2.3 (Chapman-Jouguet Point).

2.3. Chapman-Jouguet Point

Regarding the governing equations, it can be deduced that the Rayleigh line relation and the Hugoniot relation should be satisfied for any real process propagating state 1 to state 2. If two relations are plotted on the same pressure (P) and specific volume (v) diagram (Figure 5.), it can be noticed that there are tangencies between Rayleigh lines and Rankine-Hugoniot curve. These tangencies are called Chapman-Jouguet (C-J) points, point B and point E on the P - v diagram.

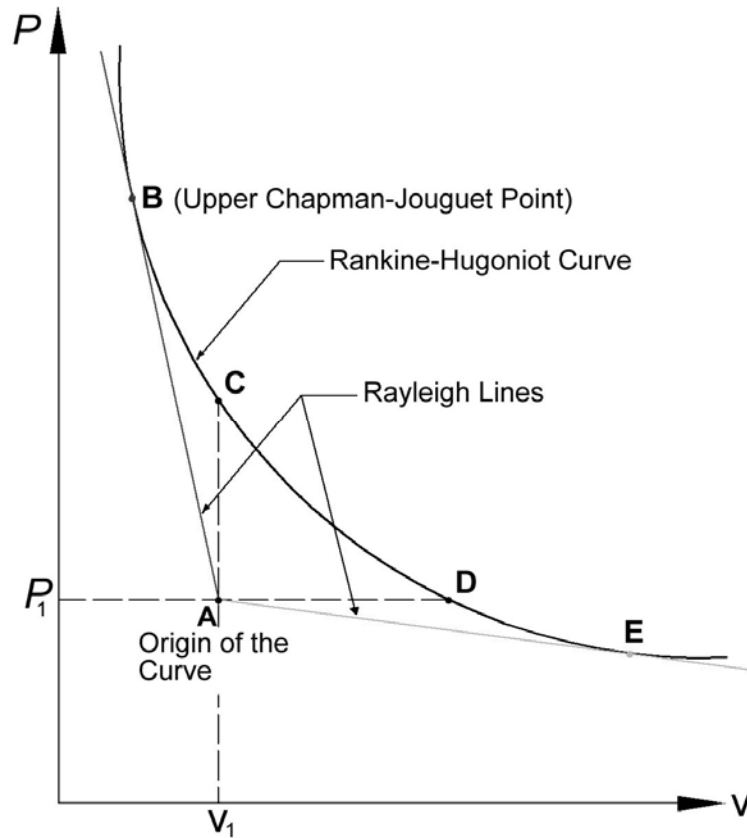


Figure 5. Rankine-Hugoniot curve and Chapman-Jouguet points

The point B is called upper C-J point and this point shows a reasonable approximation with the most detonation points observed by experimental studies [11, 43, and 44]. The solution of the detonation point on the Rankine-Hugoniot curve is consequently represented by the point B, upper Chapman-Jouguet point. At the Chapman-Jouguet point, the detonation wave proceeds at the minimum velocity and the computations according to the theory shows well agreement with the experiments [45]. According the Chapman-Jouguet Theory, the expansion process of the burned gas mixture behind the detonation plane continues isentropically and rarefaction wave moves at a velocity that never catches up the detonation wave. The isentropic expansion process represents the **isentrope** on the P - v diagram and the expansion isentrope is also tangent to the Rankine-Hugoniot curve and the Rayleigh line.

The Rankine-Hugoniot curve is divided into five regions by tangent Rayleigh lines and two limiting vertical and horizontal Rayleigh lines.

The region between vertical and horizontal lines (C-D) is physically inaccessible region, because, as stated in Section 2.1, no valid Rayleigh line can be drawn between point C and point D.

The region below point D represents the deflagration region where the combustion wave propagates at subsonic velocity. Across the flame, the velocity relative to the combustion wave increases greatly and also density of the burned products decreases notably. Because the deflagration region is out of the concern of this study, region below point D will not be considered.

The region above the point C is the detonation region and this region will be profoundly discussed in the following part.

It is already stated that there is tangency between Rayleigh line and Rankine-Hugoniot curve at the upper Chapman-Jouguet point on the P - v diagram (Figure 5).

For a fixed heat of reaction (q_R) and initial conditions designated by subscript 1, differentiating the Rankine-Hugoniot Relation (Eqn. 35) with respect to $1/\rho_2$,

$$\frac{d}{d\left(\frac{1}{\rho_2}\right)} \left[\frac{\gamma}{\gamma-1} \left(\frac{P_2}{\rho_2} - \frac{P_1}{\rho_1} \right) - q_R \right] = \frac{d}{d\left(\frac{1}{\rho_2}\right)} \left[\frac{1}{2} (P_2 - P_1) \left(\frac{1}{\rho_1} + \frac{1}{\rho_2} \right) \right] \quad (36)$$

From the above differentiation (Eqn. 36), the below relation is obtained,

$$\left[\frac{dP_2}{d\left(\frac{1}{\rho_2}\right)} \right]_{RH} = - \frac{P_2 \left(\frac{\gamma+1}{\gamma-1} \right) + P_1}{\left(\frac{\gamma+1}{\gamma-1} \right) \frac{1}{\rho_2} - \frac{1}{\rho_1}} \quad (37)$$

The slope of the Rayleigh line is,

$$\left[\frac{dP_2}{d\left(\frac{1}{\rho_2}\right)} \right]_{RL} = \frac{P_2 - P_1}{\frac{1}{\rho_2} - \frac{1}{\rho_1}} \quad (38)$$

Since there is a tangency between the Rankine-Hugoniot curve and the Rayleigh line at the C-J point, the slope of the two relations must be equal at the upper Chapman-Jouguet point. Equating Eqns. 37 and 38,

$$\frac{P_2 - P_1}{\frac{1}{\rho_2} - \frac{1}{\rho_1}} = -\frac{P_2 \left(\frac{\gamma + 1}{\gamma - 1} \right) + P_1}{\left(\frac{\gamma + 1}{\gamma - 1} \right) \frac{1}{\rho_2} - \frac{1}{\rho_1}} \quad (39)$$

Rearranging Eqn. 39, the below relation is obtained at the upper C-J point

$$\frac{P_2 - P_1}{\frac{1}{\rho_2} - \frac{1}{\rho_1}} = -\gamma \rho_2 P_2 \quad (40)$$

Rearranging the left-hand side of the Eqn. 40 according to the Rayleigh relation (Eqn. 17),

$$\rho_2^2 u_2^2 = \gamma \rho_2 P_2 \quad (41)$$

By means of the ideal-gas equation of state, Eqn. 41 yields,

$$u_2^2 = \gamma \frac{P_2}{\rho_2} = \gamma T_2 R = c_2^2 \quad (42)$$

where, c is the speed of sound. From Eqn. 42

$$u_2 = c_2 \quad (43)$$

Consequently, Mach number at the Chapman-Jouguet detonation points is equal to 1 (i.e., $Ma_2=1$).

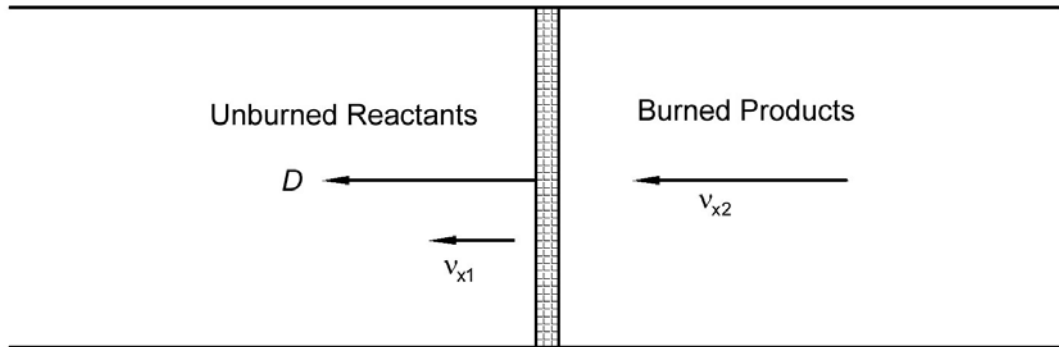


Figure 6. Velocities Defined Relative to the Observer Out of the Detonation Region

If detonation wave moving at velocity D is considered relative to the observer out of the detonation region, the concept of the absolute velocities of the state before and behind the detonation wave is taken into account in Figure 6. The below relations are the scale analysis of the absolute velocities (no vectorial consideration);

$$v_{x1} = D - u_1 \quad (44)$$

$$v_{x2} = D - u_2 \quad (45)$$

Where, u_1 and u_2 are the velocity of the burned and unburned states relative to the detonation wave (stationary wave condition).

By means of continuity equation (Eqn. 13) and $\rho_2 > \rho_1$ from the Hugoniot curve;

$$u_2 < u_1 \quad (46)$$

The unburned region can be assumed stationary, namely $u_1 = D$, so we can redefine the inequality (Eqn. 46),

$$u_1 - u_2 > 0 \quad \text{then } v_{x2} = u_1 - u_2 > 0 \text{ or } v_{x2} = D - u_2 > 0 \quad (47)$$

From Eqn. 43, $u_2 = c_2$, therefore;

$$D = c_2 + v_{x2} > c_2 \quad (48)$$

$$D > v_{x2} \quad (49)$$

The physical interpretation of the above analysis is that the burned gases behind the detonation region follow the detonation wave, but can never catch up with the detonation wave propagating at supersonic speed.

Now the detonation region, above the point C, can be discussed profoundly. The region above the point B, upper Chapman-Jouguet point, are the states representing **strong detonation**. In this region, the pressure of the burned gases is higher than that of the Chapman-Jouguet detonation point ($P_2 > P_{CJ}$). Through the strong detonation wave, however, the burned gas velocity relative to the reaction wave shows an essential reduction from supersonic speed to subsonic speed, the pressure and density increase. Strong detonation waves are seldom observed, since it requires a special experimental setup for generating overdriven shock waves in a very strong confinement [43].

Between point C and point B is the region of the **weak detonation** in which the pressure of the burned gases is lower than that of the Chapman-Jouguet point

($P_2 < P_{CJ}$). Through the weak detonation wave, although the burned gas velocity relative to the reaction wave slows down, it still has supersonic speed. Since the density of the burned gases approaches that of the unburned mixture, the detonation wave velocity increases significantly. Similar to the strong detonation case, to observe a weak detonation condition, an experimental test setup should be established to generate extremely fast chemical kinetics [43].

CHAPTER 3

DETONATION IN ENERGETIC GASEOUS MIXTURES

3.1. One-Dimensional Analysis

As it is stated previously in Chapter 2, the simplest but still acceptable one-dimensional theory also today was developed by Chapman and Jouguet known as the Chapman-Jouguet Theory.

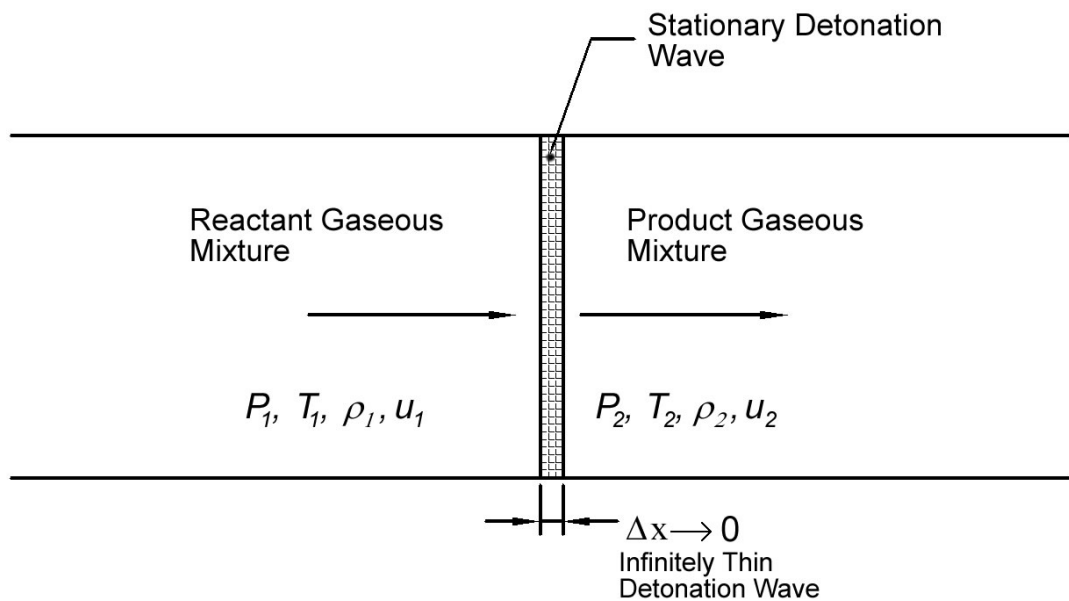


Figure 7. One-Dimensional Stationary Detonation Wave

One-dimensional detonation wave is depicted in Figure 7. According to this stationary wave reference frame, the governing equations are;

Continuity equation

$$\rho_1 u_1 = \rho_2 u_2 = \dot{m}'' \quad (50)$$

Momentum equation

$$P_1 + \rho_1 u_1^2 = P_2 + \rho_2 u_2^2 \quad (51)$$

Energy equation

$$h_1 + \frac{1}{2}u_1^2 = h_2 + \frac{1}{2}u_2^2 \quad (52)$$

Simultaneous solution of the continuity and momentum equation yields the above relation (Eqn. 53). This equation is called the **Rayleigh line** relation.

$$\dot{m}^2 = \rho_1^2 u_1^2 = \rho_2^2 u_2^2 = \frac{P_2 - P_1}{\frac{1}{\rho_1} - \frac{1}{\rho_2}} \quad (53)$$

The enthalpy terms in energy equation (Eqn. 52) can be define as the enthalpy of the state which is composed of Δh_f^o , associated with the total formation of the compound from its elements (total enthalpy of formation at the state), and Δh , associated with the change of enthalpy with respect to standard reference state defined by $T_{ref} = 298.15$, K, $P_{ref} = 1$ atm.

$$h(T) = \Delta h_f^o + [h(T) - h(T_{ref})] = \Delta h_f^o + \Delta h \quad (54)$$

The energy equation shall be redefined as,

$$[\Delta h_f^o + \Delta h]_1 + \frac{1}{2}u_1^2 = [\Delta h_f^o + \Delta h]_2 + \frac{1}{2}u_2^2 \quad (55)$$

$$\Delta h_1 + \frac{1}{2}u_1^2 + q_R = \Delta h_2 + \frac{1}{2}u_2^2 \quad (56)$$

This is the energy equation where Δh_1 and Δh_2 are the enthalpies of the initial (before reaction) and final (after reaction) states, respectively, and q_R is the heat of reaction.

$$q_R = \Delta h_{f_1}^o - \Delta h_{f_2}^o \quad (57)$$

The enthalpy term can be defined in terms of constant-pressure specific heat ($C_p(T)$),

$$h(T) = \Delta h_f^o + \int_{T_{ref}}^T C_p(T) dT \quad (58)$$

For a gas mixture obeying the ideal gas model, the constant pressure specific heat ($C_p(T)$) can be defined by the constant volume specific heat ($C_v(T)$) [46],

$$C_p(T) = C_v(T) + R \quad (59)$$

where R is the gas constant.

Integrating Eqn. 59 from reference temperature (T_{ref}) to temperature (T),

$$\int_{T_{ref}}^T C_p(T) dT = \int_{T_{ref}}^T C_v(T) dT + \int_{T_{ref}}^T R dT \quad (60)$$

The Eqn. 60 can be substituted into the energy equation (Eqn. 56),

$$\left[\int_{T_{ref}}^T C_v(T) dT + \int_{T_{ref}}^T R dT \right]_1 + \frac{1}{2} u_1^2 + q_R = \left[\int_{T_{ref}}^T C_v(T) dT + \int_{T_{ref}}^T R dT \right]_2 + \frac{1}{2} u_2^2 \quad (61)$$

Also the integrations can be solved,

$$\left[\int_{T_{ref}}^T C_v(T) dT + \int_{T_{ref}}^T R dT \right]_1 = \int_{T_{ref}}^{T_1} C_{v1}(T) dT + RT_1 - RT_{ref} \quad (62)$$

and

$$\left[\int_{T_{ref}}^T C_v(T) dT + \int_{T_{ref}}^T R dT \right]_2 = \int_{T_{ref}}^{T_2} C_{v2}(T) dT + RT_2 - RT_{ref} \quad (63)$$

From the definition of the ideal gas equation, Eqn. 62 and Eqn. 63 can be written as,

$$\int_{T_{ref}}^T C_v(T) dT + RT - RT_{ref} = \int_{T_{ref}}^T C_v(T) dT + \frac{P}{\rho} - \frac{P_{ref}}{\rho_{ref}} \quad (64)$$

Hence, the energy equation (Eqn. 61) yields

$$\int_{T_{ref}}^{T_2} C_{v2}(T) dT - \int_{T_{ref}}^{T_1} C_{v1}(T) dT - q_R = \frac{1}{2} u_1^2 - \frac{1}{2} u_2^2 + \frac{P_1}{\rho_1} - \frac{P_2}{\rho_2} \quad (65)$$

The Rankine-Hugoniot equation complying with the above energy equation (Eqn. 65) can be derived as follows,

$$\int_{T_{ref}}^{T_2} C_{v2}(T)dT - \int_{T_{ref}}^{T_1} C_{v1}(T)dT - q_R = \frac{1}{2}u_1^2 + \frac{P_1}{\rho_1} - \frac{2P_2 + \rho_2 u_2^2}{2\rho_2} \quad (66)$$

$$\int_{T_{ref}}^{T_2} C_{v2}(T)dT - \int_{T_{ref}}^{T_1} C_{v1}(T)dT - q_R = \frac{1}{2}u_1^2 + \frac{P_1}{\rho_1} - \frac{P_2 + P_2 + \rho_2 u_2^2}{2\rho_2} \quad (67)$$

By using momentum equation, the above Eqn. 67 can be rewritten as,

$$\int_{T_{ref}}^{T_2} C_{v2}(T)dT - \int_{T_{ref}}^{T_1} C_{v1}(T)dT - q_R = \frac{1}{2}u_1^2 + \frac{P_1}{\rho_1} - \frac{P_2 + P_1 + \rho_1 u_1^2}{2\rho_2} \quad (68)$$

$$\int_{T_{ref}}^{T_2} C_{v2}(T)dT - \int_{T_{ref}}^{T_1} C_{v1}(T)dT - q_R = -\frac{1}{2} \frac{P_2 + P_1}{\rho_2} + \frac{1}{2} \frac{P_1}{\rho_1} + \frac{1}{2} \left[-\frac{\rho_1 u_1^2}{\rho_2} + \frac{P_1}{\rho_1} + u_1^2 \right] \quad (69)$$

From the Rayleigh line equation (Eqn. 53),

$$\frac{P_2}{\rho_1} = u_1^2 - \frac{\rho_1 u_1^2}{\rho_2} + \frac{P_1}{\rho_1} \quad (70)$$

Substituting the Rayleigh line equation (Eqn. 70) into the energy equation (Eqn. 69),

$$\int_{T_{ref}}^{T_2} C_{v2}(T)dT - \int_{T_{ref}}^{T_1} C_{v1}(T)dT - q_R = -\frac{1}{2} \frac{P_2 + P_1}{\rho_2} + \frac{1}{2} \frac{P_1}{\rho_1} + \frac{1}{2} \frac{P_2}{\rho_1} \quad (71)$$

The Rankine-Hugoniot equation can be defined in terms of mean specific heat at constant volume, C_v ,

$$(T_2 - T_{ref}) \frac{\left[\int_{T_{ref}}^{T_2} C_{v2}(T)dT \right]}{T_2 - T_{ref}} - (T_1 - T_{ref}) \frac{\left[\int_{T_{ref}}^{T_1} C_{v1}(T)dT \right]}{T_1 - T_{ref}} - q_R = -\frac{1}{2} \frac{P_2 + P_1}{\rho_2} + \frac{1}{2} \frac{P_1}{\rho_1} + \frac{1}{2} \frac{P_2}{\rho_1}$$

then

$$(T_2 - T_{ref})C_{v2} - (T_1 - T_{ref})C_{v1} - q_R = -\frac{1}{2} \frac{P_2 + P_1}{\rho_2} + \frac{1}{2} \frac{P_1}{\rho_1} + \frac{1}{2} \frac{P_2}{\rho_1} \quad (72)$$

Hence, the Rankine-Hugoniot equation can be deduced as,

$$C_{v2}(T_2 - T_{ref}) - C_{v1}(T_1 - T_{ref}) - q_R = \frac{1}{2}(P_2 + P_1) \left(\frac{1}{\rho_1} - \frac{1}{\rho_2} \right) \quad (73)$$

3.2. Equation of State

There are three governing equations which are continuity (Eqn. 50), momentum (Eqn. 51) and energy (Eqn. 52) equations with five unknowns, P_2 , T_2 , ρ_2 , u_1 and u_2 .

By defining:

- 1) Enthalpy is a function of only the temperature, $h=h(T)$,
- 2) Heat of detonation is a function of pressure (P_2) and temperature (T_2) of the gaseous product mixture because the heat of reaction is defined by the product composition with initially assigned state of the reactant,
 $q_R = q_R(T_2, P_2)$,
- 3) One relation (Eqn. 74) is acquired from the definition of the Chapman-Jouguet point that there is a tangency between Rankine-Hugoniot curve and Rayleigh line [43].

$$\left[\frac{dP_2}{d\left(\frac{1}{\rho_2}\right)} \right]_{\text{Rayleigh Line}} = \left[\frac{dP_2}{d\left(\frac{1}{\rho_2}\right)} \right]_{\text{Rankine-Hugoniot}} \quad (74)$$

In order to determine the five unknowns, there is a need of one more state function which only depends on the state of the products. Also, the state function shall be an equation of state which includes the relation between pressure, temperature and density. The best satisfactory equation of state (EOS) which complies with the ideal gas behavior of the product gaseous mixture is ideal gas equation of state.

$$Pv = RT \quad (75)$$

In this equation, v is the specific volume (m^3/kg) of the gaseous mixture and R is the gas constant, $R = \frac{R_u}{MW_g}$, where R_u is the universal gas constant ($= 8.314 \text{ kJ/kmol}\cdot\text{K}$) and MW_g is the molar weight of the gaseous mixture in kg/kmol .

At relatively low pressure (1-2 MPa) and low loading density (density of the reactant or density of the gaseous explosive), the ideal gas equation of state and the ideal gas thermodynamic properties are sufficient to determine the detonation point and the state of the products. BLAKE code [24] and NASA-Lewis, CEA code [25] also use the ideal gas equation of state to determine the Chapman-Jouguet detonation point. Due to the relatively low pressure in gaseous detonation, the intermolecular forces in the gas mixture are negligible by comparing the thermal effects of the gas mixture. And the ideal gas equation of state assumes that no forces exist between molecules of the gaseous mixture. If the pressure becomes relatively high, about 20 GPa or higher, the intermolecular forces become significant and the compressibility effect comes to a non negligible level.

In order to evaluate if the ideal gas behavior is valid in gaseous detonation, the compressibility factor, Z , shall be checked by means of the generalized compressibility chart [47] and the BKW Equation of State which is evolved from the Virial equation of state by considering intermolecular interactions in gas.

$$\frac{Pv}{RT} = Z \quad (76)$$

A thermodynamic calculation of the state of the detonation products performed by Kistiakowsky et al. [48] is confirmed the ideal gas behavior in gaseous detonation by checking the compressibility factor. The detonation parameters of cyanogen-oxygen gaseous mixture computed by Kistiakowsky et al. are given in Table 1. The computation of the compressibility factor is performed according to final (equilibrium) composition in Table 1.

Table 1. Computed detonation properties and product composition of cyanogen-oxygen mixture stated in reference [48]

Initial Composition, % (Mole fraction)	C ₂ N ₂	49.9
	O ₂	49.9
Initial Pressure, atms		1
Final Pressure, atms		56.9
Final Temperature, K		6287
Detonation velocity, m/s		2779
Final Composition, % (Mole fraction)	N ₂	30.79
	N	2.56
	CO	62.24
	C	1.19
	O	1.76
	CN	0.60
	CO ₂	0
	NO	0
	O ₂	0
	Ar	0.16

Due to their relatively high percentages of mole numbers, nitrogen (N₂) and carbon monoxide (CO) are dominant species to determine the compressibility factor from the compressibility chart and the effect of the other species can be neglected.

Critical properties of N₂ and CO adapted from Critical Tables [46] are shown in Table 2:

Table 2. Critical point properties

	Critical Temperature (T_C) K	Critical Pressure (P_C) atm
N ₂	126.0	33.456
CO	133.0	34.540

Reduced temperature and pressure of N₂ respectively:

$$T_R = \frac{T_{\text{final}}}{T_C} = 49.89 \quad P_R = \frac{P_{\text{final}}}{P_C} = 1.7$$

At these T_R and P_R , the compressibility factor, Z , of nitrogen is almost 1.

Reduced temperature and pressure of CO respectively:

$$T_R = \frac{T_{\text{final}}}{T_C} = 47.27 \quad P_R = \frac{P_{\text{final}}}{P_C} = 1.64$$

At these T_R and P_R , the compressibility factor, Z , of carbon monoxide is also almost 1.

From these results, it can be deduced that the ideal gas behavior can satisfy the state of the product gas mixture for the gaseous detonation.

The other verification method of ideal gas behavior for product gas mixture is BKW (Becker-Kistiakowsky-Wilson) [33, 49] Equation of State. This equation of state will be explained in detail in Section 4.2.1.

$$\frac{P v_g}{RT} = F(x) = 1 + x e^{\beta x} \quad (77)$$

where P : pressure of the product gaseous mixture, v_g : Specific volume of the product gaseous mixture, T : final temperature, R : Gas constant, x_i : Mole fraction of the each component of the product gaseous mixture, $F(x)$: Gas Imperfection factor for gaseous products, where x is defined as following

$$x = \frac{\kappa \sum_i x_i k_i}{\bar{V}_g (T + \theta)^\alpha} \quad (78)$$

α , β , κ , θ are the empirical constants of BKW Equation of State, and k_i is the geometrical covolume which is defined as the volume occupied by a molecule rotating about 10.46 times its center of mass [35]. The values of constants [50]:

$$\alpha = 0.5, \beta = 0.09, \kappa = 11.85, \theta = 400.$$

The gas imperfection factor gives the compressibility effect. The calculated detonation properties and composition by Kistiakowsky et al. [48] can be held to discuss the BKW Equation of State in this case as well. The mole fractions and covolumes of the gaseous detonation products according to Table 1 are given in Table 3.

Table 3. Mole fractions and the covolumes of the components

Components	x_i	$*k_i$
N ₂	0.3079	380
N	0.0256	148
CO	0.6224	390
C	0.0119	180
O	0.0176	120
CN	0.0060	486
CO ₂	0	600
NO	0	386
O ₂	0	350
Ar	0.0016	**-

* The covolumes cited by Mader [35]

** Due to the relatively very low mole fraction, its effect can be neglected

According to the given constants and calculated detonation state, the imperfection factor, $F(x)$, corresponding to the compressibility factor, Z , is equal to 1.004.

Therefore, it is proven that the ideal gas behavior satisfies the thermodynamic solution of the detonation in energetic gaseous mixture. And also the ideal gas equation of state can be applied to the numerical calculation methods of the Chapman-Jouguet detonation point.

3.3. Determination of the Chapman Jouguet Point

There is a tangency between Rayleigh line and Rankine-Hugoniot curve (shock adiabat) of the detonation products at the Chapman-Jouguet point. And the detonation velocity has its minimum value, on the Rankine-Hugoniot curve of the detonation products, at the C-J point. Some programs in the literature use either the tangency between Rayleigh line and Rankine-Hugoniot curve or the minimum detonation velocity along the Rankine-Hugoniot curve.

FORTTRAN BKW [51] by Mader and EXPLO5 [39] by Sućeska use the minimum detonation velocity along the Rankine-Hugoniot curve (Shock adiabat of the

detonation products) to determine the C-J point. The shock or Hugoniot curve for products of detonation, Figure 8, is generated by iterative methods, and then the detonation wave velocities (Eqn. 79) are computed by using the density and the pressure along the Rankine-Hugoniot curve.

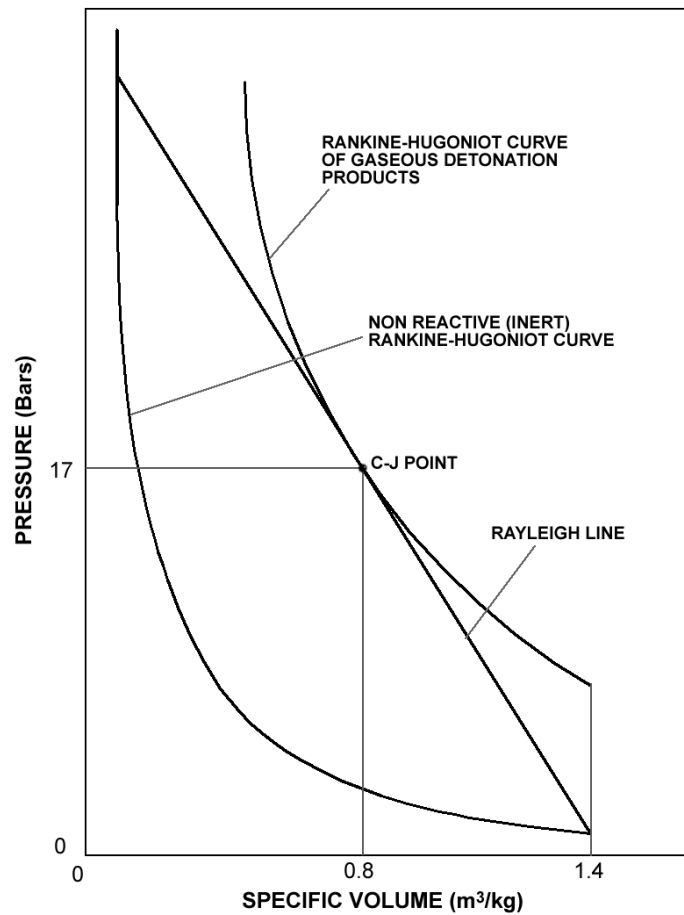


Figure 8. Rankine-Hugoniot curves and Rayleigh line for gaseous detonation

$$D = \left(\frac{1}{\rho_1} \right) \sqrt{\frac{P_2 - P_1}{\frac{1}{\rho_1} - \frac{1}{\rho_2}}} \quad (79)$$

The point at where the detonation wave velocity reaches its minimum value is the Chapman-Jouguet (C-J) point as shown in Figure 9.

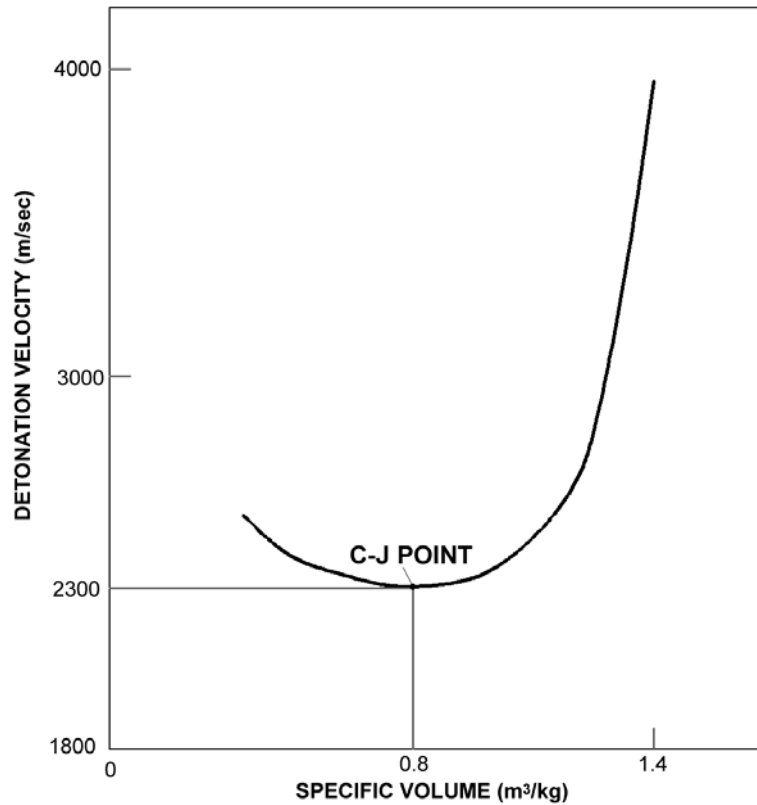


Figure 9. Variation of the detonation velocity along the Rankine-Hugoniot curve

AMRL code [52] uses the tangency between Hugoniot curve of detonation products and Rayleigh line, Figure 8.

$$\left[\frac{dP_2}{d\left(\frac{1}{\rho_2}\right)} \right]_{\text{Rayleigh line}} = \left[\frac{dP_2}{d\left(\frac{1}{\rho_2}\right)} \right]_{\text{Rankine-Hugoniot}} \quad (80)$$

Eqn. 80 shows the mathematical definition of the tangency at Chapman-Jouguet point. This equation can be solved by numerical methods. Due to the tangency, the slope of the Rankine-Hugoniot curve and that of Rayleigh line must be equal. The pressure, P_1 , and the density, ρ_1 , of the unreacted explosives are also known. After computation of the Rankine-Hugoniot curve, the slope of the Rankine-Hugoniot relation can be calculated by backward difference method.

$$\left| \frac{\left[\frac{P_2(i) - P_1}{v_2(i) - v_1} \right]_{\text{Rayleigh line}} - \left[\frac{P_2(i) - P_2(i-1)}{v_2(i) - v_2(i-1)} \right]_{\text{Rankine-Hugoniot}}}{\left[\frac{P_2(i) - P_2(i-1)}{v_2(i) - v_2(i-1)} \right]_{\text{Rankine-Hugoniot}}} \right| = \varepsilon \quad (81)$$

where the difference of the slopes goes to zero ($\varepsilon \rightarrow 0$, Eqn. 81) denotes the tangent point which is equal to the Chapman-Jouguet point.

3.4. Numerical Solution of Steady-State Detonation Properties for Premixed Gaseous Mixtures

On the basis of Chapman-Jouguet Theory, a numerical determination method of the detonation point for C-H-N-O based premixed gaseous mixtures has been developed. In accordance with this numerical method, a computer code named GasPX written in FORTRAN language has been developed for computing both the Chapman-Jouguet detonation point and the properties of the detonation products. GasPX uses double precision type of data in the computations. GasPX calculates the state of the reaction products of the detonation under assumptions of the thermal and chemical equilibrium. The products consist of any number of gaseous species. But in case mole number of the carbon is remarkably higher than that of oxygen in reactant gaseous mixture, the solid carbon formation can be observed in products, so the equilibrium composition of the products can include two phases.

The ideal-gas equation of state is applied to both reactant and product gaseous mixtures. Due to the low loading density and the low detonation pressure of the detonation product, no particular solid phase equation of state is applied for solid carbon formation. After computation of the state of the detonation, GasPX writes the post detonation properties into an output file in HTML form.

GasPX has four major subroutines, READ, REACTCALC, PRODCALC, PRODFINALCALC, and EQUILIBRIUM.

Subroutine READ reads the molecular properties and the thermodynamic coefficients of each gaseous and condensed phase species by using the library of the thermodynamic data, which is given as a data file named "thermo.inp" [53, 54]. This library contains thermodynamic data for over 2000 solid, liquid, and gaseous

chemical species as a function of temperature ranging from 200 to 2000 K. Subroutine READ not only reads the thermodynamic coefficients but also calculates the thermodynamic properties of each species such as specific enthalpy, h , specific entropy, s° , specific heat, C_p at constant pressure, specific Gibbs function, g , and enthalpy of formation, Δh_f° at standard state ($T_{ref}=298.15$ K and $P_{ref}=1$ atm). In addition to thermodynamic functions, identifying name, chemical formula, molecular weight and phase properties of each species are given in “thermo.inp” file. The “thermo.inp” file and calculation procedures are explained in detail in the following.

Subroutine REACTCALC calculates the thermodynamic properties of the reactant gaseous mixture. Heat of formation, enthalpy, entropy, internal energy, gas constant, molar weight, specific heats, and polytropic exponent of the reactant gaseous mixture at reference or initial state ($T_{ref}=298.15$ K and $P_{ref}=1$ atm) are calculated by REACTCALC. Density of the reactant gaseous mixture is calculated by means of the ideal gas equation.

Subroutine PRODCALC calculates and arranges the Gibbs free energy of the each species which can form after detonation reaction. The Gibbs free energy calculations are performed at a given arbitrary reaction temperature and pressure.

Subroutine EQUILIBRIUM performs the chemical equilibrium calculations by means of a commercial optimization solver. The equilibrium composition of the product gaseous mixture is calculated in accordance with minimization of Gibbs free energy principle. There is an objective function which comes from the minimization of Gibbs free energy and a constraint of mass balance. The commercial optimization solver reaches the local optimum point of equilibrium composition by using the objective function and simultaneously satisfying the mass balance. The codes cited in the literature [25, 39, 51] mostly used the optimization method developed by White et al. [42] or its modified version. This method depends on a steepest descent technique applied to a quadratic fit, and also is easy to apply to the numerical models of chemical equilibrium computation. This method also minimizes the Gibbs free energy at constant temperature and pressure subject to the conservation of mass constraint. However, this method needs user defined very near initial values of final equilibrium composition to catch the local optimum points. If appropriate initial values are not defined, the algorithm can compute an inconsistent solution set. Also

in this method, the increase of the gradients is taken as constant for each solution step. This feature undesirably affects the robustness of the proposed optimization method. But GasPX takes advantage of the commercial non-linear optimization programs which can successfully compute the equilibrium composition. Because this professional optimization programs have powerful non-linear optimization solvers, the robustness of the solutions and the global optimum determination efficiency are much better than that of using steepest descent method by White et al. Also, these commercial non-linear optimization solvers prevent any initially defined parameters in computations, whereas there is a need of initial guesses, which should be very close to the final solution, and a need of some decrement factors, which should be predefined by users, in the steepest descent method.

Subroutine PRODFINALCALC calculates the thermodynamic properties of the product gaseous mixture after the chemical equilibrium composition is determined. Heat of formation, enthalpy, entropy, internal energy, gas constants, molar weight, specific heats, and polytropic exponent of the product gaseous mixture are calculated at the detonation temperature and pressure by PRODFINALCALC. Ideal gas behavior and also the ideal thermodynamic functions are valid for the detonation products.

3.4.1. Thermodynamic Functions

GasPX calculates the ideal thermodynamic properties of the mixture at any states by means of “thermo.inp”, the thermodynamic data library. The set of thermodynamic variables, $\bar{e}(T)$, $\bar{s}^o(T)$, g , $\bar{C}_p(T)$ and $\bar{C}_v(T)$ on the molar basis are computed by using the given data, in the form of least-squares coefficients that have been calculated from tabular thermodynamic data states. Dimensionless forms of the thermodynamic functions, $\bar{C}_p(T)$, $\bar{h}(T)$, and $\bar{s}^o(T)$, are given in the following [54].

Specific heat at constant pressure:

$$\frac{\bar{C}_p(T)}{R_u} = a_1 T^{-2} + a_2 T^{-1} + a_3 + a_4 T + a_5 T^2 + a_6 T^3 + a_7 T^4 \quad (82)$$

Enthalpy:

$$\frac{\bar{h}(T)}{R_u T} = -a_1 T^{-2} + a_2 \frac{(\ln T)}{T} + a_3 + a_4 \frac{T}{2} + a_5 \frac{T^2}{3} + a_6 \frac{T^3}{4} + a_7 \frac{T^4}{5} + \frac{b_1}{T} \quad (83)$$

Entropy:

$$\frac{\bar{s}^o(T)}{R_u} = -a_1 \frac{T^{-2}}{2} - a_2 T^{-1} + a_3 \ln T + a_4 T + a_5 \frac{T^2}{2} + a_6 \frac{T^3}{3} + a_7 \frac{T^4}{4} + b_2 \quad (84)$$

where R_u is the universal gas constant, $R_u = 8.31457$ kJ/K.kmol. The above thermodynamic properties are valid only for ideal gas behavior.

Table 4. FORTRAN Format Used for Data in "thermo.inp"[54]

Record	Contents	Fortran format	Columns
1	Species name or formula	A16	1 to 16
	Comments and data source	A62	19 to 80
2	Number of T intervals	I2	1 to 2
	Optional identification code	A6	4 to 9
	Chemical formula-symbols and numbers (all capitals)	5(A2, F6.2)	11 to 50
	Zero for gas, nonzero for condensed	I2	51 to 52
	Molecular weight	F13.7	53 to 65
	Heat of formation at 298.15 K, J/mol	F15.5	66 to 80
3	Temperature range	2F11.3	1 to 22
	Number of coefficients for $\bar{C}_p(T)/R$	I1	23
	T exponents in empirical equation for $\bar{C}_p(T)/R$	8F5.1	24 to 63
	$[\bar{h}(298.15) - \bar{h}(0)]$, J/mol	F15.3	66 to 80
4	First five coefficients for $\bar{C}_p(T)/R$	5D16.9	1 to 80
5	Last two coefficients for $\bar{C}_p(T)/R$	2D16.9	1 to 32
	Integration constants b_1 and b_2	2D16.9	49 to 80
--	Repeat 3, 4, and 5 for each interval	----	----

Table 4 shows the general FORTRAN format of the “thermo.inp”, thermodynamic data library. The coefficients in this library have been obtained by using the least square fit techniques. Computations of specific heat (Eqn. 82), enthalpy (Eqn. 83) and entropy (Eqn. 84) are performed according to the coefficients. As seen in the table, the thermodynamic data library accommodate the coefficients with species name, data source, species chemical formula, phase indicator, species molecular weight and species heat of formation at the reference state. To explain “thermo.inp” file better, an example of the data of condensed titanium nitrate complied with the Table 4 is given in Figure 10.

```

1234 5678901234 5678901234 5678901234 5678901234 5678901234 5678901234 567890
   10         20         30         40         50         60         70         80
1  TiN(cr)           Chase, 1998 pp1612-4.           1
2  2 j 6/68 TI 1.00N 1.00 0.00 0.00 0.00 0.00 1 61.87374 -337648.800 2
3  200.000 800.0007 -2.0 -1.0 0.0 1.0 2.0 3.0 4.0 0.0 5487.000 3
4  -5.479117220D+05 9.328691110D+03 -6.386263890D+01 2.429925456D-01 -4.304234520D-04 4
5  3.792645100D-07 -1.317412256D-10 -8.424256140D+04 3.392988560D+02 5
6  800.000 3220.0007 -2.0 -1.0 0.0 1.0 2.0 3.0 4.0 0.0 5487.000 6
7  -3.656247060D+05 1.265730431D+03 3.831711190D+00 1.632900455D-03 -1.062786626D-07 7
8  1.310931390D-11 -5.770548410D-16 -5.027654400D+04 -1.652632899D+01 8
9  TiN(L)           Chase, 1998 pp1612-4.           9
10 1 j 6/68 TI 1.00N 1.00 0.00 0.00 0.00 0.00 2 61.87374 -337648.800 10
11 3220.000 6000.0007 -2.0 -1.0 0.0 1.0 2.0 3.0 4.0 0.0 5487.000 11
12 0.000000000D+00 0.000000000D+00 7.548249987D+00 0.000000000D+00 0.000000000D+00 12
13 0.000000000D+00 0.000000000D+00 -3.626039860D+04 -3.958296649D+01 13
1234 5678901234 5678901234 5678901234 5678901234 5678901234 5678901234 567890
   10         20         30         40         50         60         70         80

```

Figure 10. Data of the condensed titanium nitrate in the thermodynamic data library

For each species, heats of formation are combined with sensible heats, so the enthalpy calculated from coefficients can be defined as,

$$\bar{h}(T) = [\bar{h}(T) - \bar{h}(298.15)] + \Delta\bar{h}_f^o \quad (85)$$

where $\Delta\bar{h}_f^o$ is equal to the enthalpy of formation at reference state, $T_{ref} = 298.15$ K.

The specific enthalpy used by GasPXX consists of sensible enthalpy with respect to reference state and enthalpy of formation at reference state.

Because the unit of temperature is in K and the unit of the universal gas constant is in the form of kJ/K.kmol, the units of thermodynamic functions ($\bar{C}_p(T)$, $\bar{h}(T)$, and $\bar{s}^o(T)$) are kJ/K.kmol, kJ/kmol, and kJ/K.kmol, respectively.

The other thermodynamic functions are derived from computed thermodynamic functions by least-squares coefficients.

Specific Gibbs free energy function per mole or chemical potential,

$$\bar{g} = \bar{h} - T \bar{s}^o \quad (86)$$

$$\bar{g}(T) = [\bar{h}(T) - \bar{h}(298.15)] + \Delta \bar{h}_f^o - T \bar{s}^o(T) \quad (87)$$

Unit of specific Gibbs free energy is kJ/kmol on the molar basis.

Specific Internal energy,

$$e = h - P v \quad (88)$$

By combining definition of internal energy and ideal gas equation

$$\bar{e}(T) = \bar{h}(T) - R_u T \quad (89)$$

And internal energy can be calculated as,

$$\bar{e}(T) = \bar{h}(T) - \Delta \bar{h}_f^o - [R_u T - R_u 298] \quad (90)$$

Due to the sensible enthalpy with respect to the reference state, the internal energy becomes

$$\bar{e}(T) = \bar{e}(T) - \bar{e}(298) \text{ with unit, (kJ/K.kmol).} \quad (91)$$

For the solid species, from the definition of the internal energy of incompressible substance, the internal energy becomes

$$\bar{e}(T) = \bar{h}(T) - \Delta \bar{h}_f^o - v_s [P_2 - P_{ref}] MW_s \quad \text{with unit, (kJ/K.kmol)} \quad (92)$$

Where $\bar{h}(T) = [\bar{h}(T) - \bar{h}(298.15)] + \Delta \bar{h}_f^o$

Also v_s and MW_s are respectively, the specific volume and the molar weight of the solid components.

3.4.2. Thermodynamic Properties at States

In order to determine the thermodynamic properties at any state, first, mole numbers of the all species have to be known. If there is any solid component (solid carbon) other than gaseous at that instant, the total mole number of the species at different phase should be calculated separately.

For gas phase;

$$n_g = \sum_g n_i \quad (93)$$

n_i is the mole number of the each species at gas phase, n_g is the total mole number of the gaseous species,

The mole number of the solid carbon can be defined as n_s . Because only solid component is carbon, the total mole number of the components at condensed phase is also equal to mole number of carbon.

Total mole number, n , at the state,

$$n = n_g + n_s \quad (94)$$

Mole fraction of the gaseous species is,

$$x_i = \frac{n_i}{n_g} \quad (95)$$

The mole fraction of the gaseous mixture is,

$$x_g = \frac{n_g}{n} \quad (96)$$

The mole fraction of the carbon is,

$$x_s = \frac{n_s}{n} \quad (97)$$

Because GasPX uses the extensive thermodynamic properties per unit mass in numerical computations, the molar weight must be determined.

Molar weight of the gaseous mixture,

$$MW_g = \frac{\sum n_i MW_i}{n_g} \quad (98)$$

MW_i (kg/kmol) is the molecular weight of the each gas species. Assuming that only solid species is solid carbon, the molar weight of the mixture (kg/kmol) at the state is then,

$$MW = \frac{n_g MW_g + n_s MW_s}{n_g + n_s} \quad (99)$$

Subscript g denotes the gaseous phase and subscript s denotes the solid carbon (graphite).

If we define any extensive properties, \bar{U} , on molar basis, an extensive property of the system can be defined per unit mass (per kg) as,

$$U = \frac{\sum n_i \bar{U}_i + n_s \bar{U}_s}{n_g MW_g + n_s MW_s} \quad (100)$$

Internal energy, heat of formation, and similar extensive properties are computed per unit mass in GasPX.

Specific internal energy of the state, e (kJ/kg),

$$e = \frac{\sum n_i \bar{e}_i + n_s \bar{e}_s}{n_g MW_g + n_s MW_s} \quad (101)$$

Heat of formation of the state, Δh_f^o (kJ/kg)

$$\Delta h_f^o = \frac{\sum n_i (\Delta \bar{h}_f^o)_i + n_s (\Delta \bar{h}_f^o)_s}{n_g MW_g + n_s MW_s} \quad (102)$$

3.4.3. Chemical Equilibrium

The Chemical-Equilibrium computations are performed on the basis of minimization of Gibbs free energy by GasPX. Thanks to commercial non-linear optimization solvers, equilibrium composition after chemical reaction can be determined precisely and even very fast. A commercial optimization solver which can be run coupled with a FORTRAN subroutine can be successfully applied to GasPX code, if the chemical equilibrium calculation is defined as a set of non-linear equations.

The condition that an equilibrium state is the one having the minimum value of the Gibbs function can be expressed as an objective function of the non-linear optimization model.

For a specified temperature and pressure,

$$dG|_{T,P} \leq 0 \quad (103)$$

where G is the extensive form of the Gibbs function. If inequality (103) is defined as an objective function, it goes to a minimum ($G \rightarrow \min$).

Gibbs function can be written in terms of chemical potential on the molar base,

$$G = \sum n_i \mu_i \quad (104)$$

n_i is the mole number of the component i in a equilibrium composition which may include condensed phase products besides gaseous phase.

The chemical potential, μ_i , of component i in an ideal gas mixture is equal to its Gibbs function per mole of i , evaluated at the mixture temperature and the partial pressure of i in the mixture [46].

$$\mu_i = \bar{h}_i(T) - T \bar{s}_i(T, P_i) \quad (105)$$

$$\mu_i = \left[\left(\bar{h}_i(T) - \bar{h}_i(298.15) \right) + \Delta \bar{h}_{f,i}^o \right] - T \left[\bar{s}_i^o(T) - R_u \ln \frac{x_i P}{P_{ref}} \right] \quad (106)$$

$$\mu_i = \left[\left(\bar{h}_i(T) - \bar{h}_i(298.15) \right) + \Delta \bar{h}_{f,i}^o \right] - T \bar{s}_i^o(T) + R_u T \ln \frac{x_i P}{P_{ref}} \quad (107)$$

g is already defined by Eqn. 87,

$$\mu_i = \bar{g}_i + R_u T \ln \frac{x_i P}{P_{ref}} \quad (108)$$

where $P_{ref} = 1\text{atm}$ and x_i is the mole fraction of component i in a mixture at temperature T and pressure P . Because all components may not be in gas phase but be condensed, the Eqn. 108 can be written compactly as

$$\mu_i = \bar{g}_i + (1 - \lambda) R_u T \ln \frac{x_i P}{P_{ref}} \quad (109)$$

where λ is the phase control integer, $\lambda = 0$ for gas components, and $\lambda = 1$ for condensed component (solid carbon).

Hence the objective function becomes

$$\sum n_i \left[\bar{g}_i + (1 - \lambda) R_u T \ln \frac{x_i P}{P_{ref}} \right] \rightarrow \text{MIN} \quad (110)$$

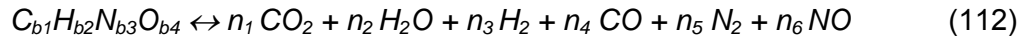
While reaching minimum value of the Gibbs function, the conservation of mass has to be satisfied. In other words, the optimization model has an objective function,

which is the minimum value of Gibbs free energy, with the conservation of mass constraint. The reactant total mass have to be kept after detonation reaction:

$$\sum_{i=1}^n a_{ij} n_i = b_j \quad (j=1, 2, \dots, m) \quad (111)$$

where there are m different types of atoms and a_{ij} are the formula numbers indicating the number of atoms of element j in a molecule of species i, n_i is the mole number of species i in equilibrium composition, and b_j is the total number of atoms of element j present in the reactant mixture [42].

As an example of how equation 111 is applied, consider the following reaction:



Conservation of carbon atom, C:

$$n_1 \cdot 1 + n_4 \cdot 1 = b_1 \quad (113)$$

Conservation of hydrogen atom, H:

$$n_2 \cdot 2 + n_3 \cdot 2 = b_2 \quad (114)$$

Conservation of nitrogen atom, N:

$$n_5 \cdot 2 + n_6 \cdot 1 = b_3 \quad (115)$$

Conservation of oxygen atom, O:

$$n_1 \cdot 2 + n_2 \cdot 1 + n_4 \cdot 1 + n_6 \cdot 1 = b_4 \quad (116)$$

Therefore, the non-linear optimization model is constructed on the objective function, minimum value of Gibbs function at specified temperature and pressure subject to the mass balance constraint. The chemical equilibrium computations in GasPX are performed according to this optimization model by means of a non-linear optimization solver coupled with FORTRAN language.

3.4.4. Algorithm of GasPX

The numerical model of GasPX basically depends on the iteration techniques. The computation of the detonation point performed by GasPX first starts with assuming initially a detonation pressure and a temperature. Then two main iteration loops run until determination of the C-J point; the pressure is calculated by the inner loop and the temperature is calculated by the outer one.

The algorithm of GasPX code which can perform the calculation of the detonation parameters has been built up in the following sequence:

1. Calculation starts with initially assumed C-J point temperature, T_2 , and pressure, P_2 .

Initial point: $P_2=0.1$ bar and $T_2=1000$ K

2. The input file, named REACTIN.FOR, which designates the reactant condition in FORTRAN format, is read. This file includes the temperature of the reactant, T_1 , pressure of the reactant, P_1 , number of reactants, number of different atoms forming reactants, descriptive formula which is commonly chemical formula, of the reactants, and mole numbers of the reactants. Because GasPX can calculate the detonation properties of only gas phase reactants, all reactant components must be in gas phase. REACTIN.FOR file can be composed by users in free FORTRAN format (Table 5).

Table 5. Free FORTRAN format of "REACTIN.FOR"

Line	Content	Columns
1	Temperature of the reactants in Kelvin, generally reference state temperature, $T_1 = 298.15$ K	1
	Pressure of the reactants in bar, generally reference state pressure, $P_1 = 1.01325$ bar	2
2	Number of reactant components limited up to 20	1
3	Number of different atoms forming reactants limited up to 10	1
4 – [a]	Symbols (all capitals) of different atoms forming reactants	1
[b] - [c]	Mole numbers of reactants	1
	Chemical formula of reactants (Symbols (all capitals) and numbers)	2

- a. Final line number depends on the number of different atoms and can not exceed the 13
 b. Line starts after the final line of symbols of different atoms forming reactants
 c. Final line depends on the number of reactant components and can not exceed the b+19

For example, for hydrogen, oxygen and argon mixture, and their mole numbers respectively, 49.9, 49.9, and 0.20, the input file (REACTIN.FOR) is

```

298.15 1.01325 ! TEMPERATURE (K) AND PRESSURE (bar)
3 ! NUMBER OF CHEMICAL COMPONENTS
6 ! NUMBER OF DIFFERENT ATOMS
C ! ATOMIC SYMBOLS
H
O
N
HE
AR
49.9 H2 ! MOLE NUMBERS AND CHEMICAL FORMULA
49.9 O2
0.2 Ar
    
```

3. After reading reactant condition, the thermodynamic properties of reactant mixture are calculated by using thermodynamic data library, "thermo.inp". Specific internal energy per unit mass, enthalpy of formation per unit mass,

mean specific heat at constant volume per unit mass and density of the reactant mixture are calculated at this step.

Calculation of the thermodynamic properties of mixture was explained in Section 3.4.2.

Specific internal energy per unit mass (kJ/kg):

$$e_1 = \frac{\sum_g n_i \bar{e}_i}{\sum_g (n_i MW_i)} \quad (117)$$

Heat of formation per unit mass (kJ/kg):

$$\Delta h_{f1}^o = \frac{\sum_g n_i (\Delta \bar{h}_f^o)_i}{\sum_g (n_i MW_i)} \quad (118)$$

Specific internal energy per unit mass (kJ/kg):

$$e_1 = e_1(T_1) - e_1(298.15) \quad (119)$$

If $T_1 = 298.15$ K, then $e_1 = e_1(T_1) - e_1(298.15) = 0$ (kJ/kg)

The density of the reactant mixture is calculated as follows. Gas constant of the reactant mixture:

$$R_1 = \frac{R_u \sum_g n_i}{\sum_g (n_i MW_i)} \quad (120)$$

By using ideal gas equation of state, the density is calculated:

$$\rho_1 = \frac{P_1}{R_1 T_1} \quad (121)$$

If units of P_1 , R_1 , and T_1 are kPa, kJ/kg·K and K respectively, the unit of density, ρ_1 , is kg/m³.

4. The input file, named PRODUCTIN.FOR, which the product components are designated within, is read. The product components, which may be formed after detonation reaction, are composed within the PRODUCTIN.FOR in the free FORTRAN format by users (Table 6). Only solid carbon can be condensed phase in product components, the others must be in gaseous

phase. The number of the components, limited to up to 20 species, and the descriptive names (commonly chemical formulas) of the product components are written within PRODUCTIN.FOR.

Table 6. Free FORTRAN format of "PRODUCTIN.FOR"

Line	Content	Columns
1	Number of reactant components limited up to 20	1
2-[a]	Chemical formula of products	1

a. Final line number depends on the number of components and can not exceed the 21

Example of "PRODUCTIN.FOR":

```

19 ! NUMBER OF CHEMICAL COMPONENTS
H2O
H2
OH
H2O2
H
O2
O
CO2
CO
C
C3H8
N2
N
CN
NO
He
Ar
C(gr)
C2N2

```

5. After reading of the product components, the chemical equilibrium calculation is performed at P_2 and T_2 by means of a commercial optimization solver running coupled with FORTRAN. P_2 and T_2 are changed by iteration manner until reaching the C-J detonation point. For the determination of chemical equilibrium composition, the only component property is the molal

standard dimensionless chemical potential derived from the Gibbs free energy function.

$$\frac{\mu_i}{R_u T_2} = \frac{\bar{g}_i}{R_u T_2} + (1 - \lambda) \ln \frac{x_i P_2}{P_{ref}} \quad (122)$$

Where $P_{ref} = 1$ atm and λ is 1 for condensed components and is 0 for gas components. x_i is the mole fraction of the gaseous component i and also the value of x_i is unknown.

$$x_i = \frac{y_i}{\sum_s y_i} \quad (123)$$

where y_i is the equilibrium mole number of the gaseous product component i and y_s is the equilibrium mole number of the solid carbon, which will be determined after equilibrium calculation.

For specified T_2 , the Gibbs free energy function (\bar{g}_i) of each component is determined by using thermodynamic data. Then Gibbs free energy functions are defined in dimensionless form.

The objective function becomes

$$\sum_s y_i \left[\frac{\mu_i}{R_u T_2} \right] + y_s \left[\frac{\mu_s}{R_u T_2} \right] \rightarrow \text{MIN} \quad (124)$$

with the constraint coming from the mass balance (Eqn. 111).

The commercial optimization solver computes the equilibrium composition by satisfying the minimum value of Gibbs free energy of product composition with the constraint of mass conservation for assumed detonation pressure P_2 , and temperature, T_2 .

6. After determination of the equilibrium composition, the thermodynamic properties of the production mixture are calculated for T_2 and P_2 by using thermodynamic data library, "thermo.inp" file. Because the equilibrium composition can include solid carbon besides gaseous species, the specific internal energy per unit mass, enthalpy of formation per unit mass, mean specific heat at constant volume per unit mass, and gas constant of the product mixture are calculated by considering the different phases (gas and solid) by GasPX.

Specific internal energy per unit mass (kJ/kg):

$$e_2 = \frac{\sum^g y_i \bar{e}_i + y_s \bar{e}_s}{y_g MW_g + y_s MW_s} \quad (125)$$

where y_i is the mole number of the gaseous component and y_s is the mole number of solid carbon.

Heat of formation of the state, Δh_f^o (kJ/kg)

$$\Delta h_{f2}^o = \frac{\sum^g y_i (\Delta \bar{h}_f^o)_i + y_s (\Delta \bar{h}_f^o)_s}{y_g MW_g + y_s MW_s} \quad (126)$$

Constant-volume mean specific heat per unit mass (kJ/kg):

$$e_2 = e_2(T_2) - e_2(298.15) \quad (127)$$

$$C_{v2} = \frac{e_2(T_2) - e_2(298.15)}{T_2 - 298.15} \quad (128)$$

The density of the gaseous product mixture is calculated as follows,

Gas constant of the reactant mixture:

$$R_2 = \frac{R_u \sum^g y_i}{\sum^g (y_i MW_i)} \quad (129)$$

And at this step, the heat of reaction, q_R , is calculated per unit mass as well:

$$q_R = \Delta h_{f1}^o - \Delta h_{f2}^o \quad (\text{kJ/kg})$$

7. After determination of the equilibrium composition and thermodynamic properties of the equilibrium mixture, parameters of the state (pressure and temperature) will be calculated along the Rankine-Hugoniot curve by decreasing the specific volume starting from initial density (density of the unreacted gaseous mixture) to the final density (density of the detonation product mixture) with a certain decrement of the specific volume (Figure 11).

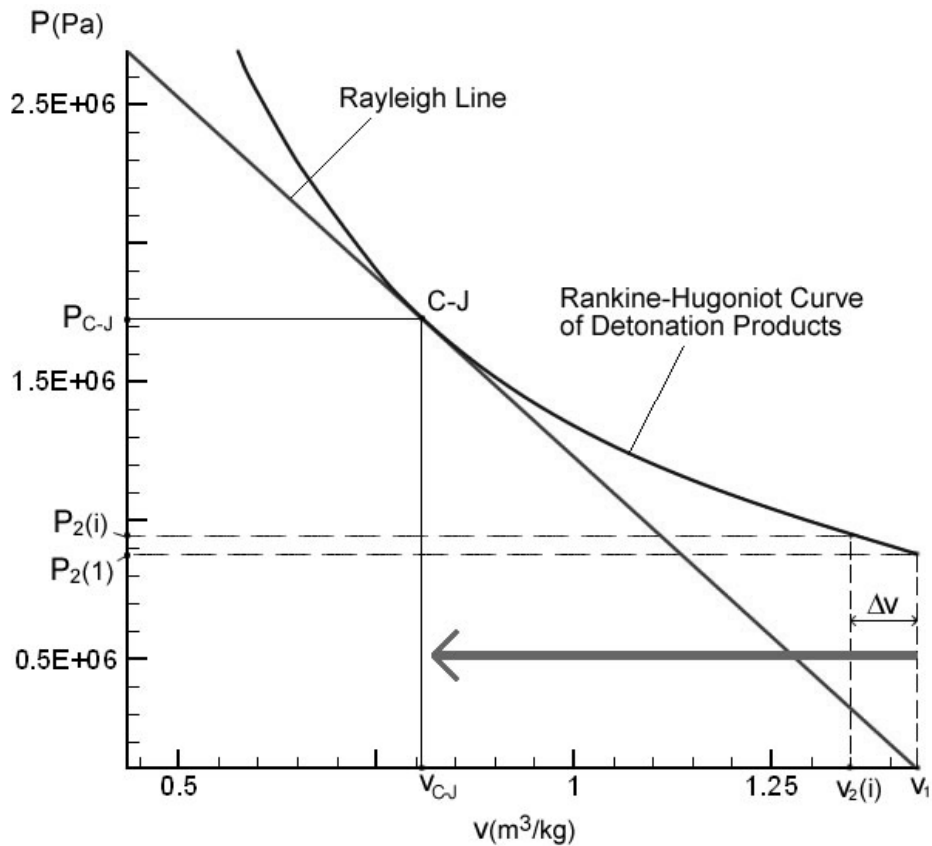


Figure 11. Determination of the Chapman-Jouguet Point on the Rankine-Hugoniot curve by GasPX

Calculation of the specific volume for certain decrement:

$$v_2(i) = v_1 - i \Delta v$$

$$v_1 = \frac{1}{\rho_1}$$

and

$$\Delta v = 5 \times 10^{-3} \text{ (m}^3/\text{kg) for GasPX}$$

8. The Chapman-Jouguet point is calculated by solving the Rankine-Hugoniot equation and ideal gas equation simultaneously. An initial pressure is needed for this calculation. This initial pressure P_x is 2×10^5 Pa in GasPX.
9. The temperature of the detonation products for calculated specific volume is calculated from the Rankine-Hugoniot Relation (Eqn. 73). Mean specific heats of the both reactant and product mixture, heat of reaction, and specific volumes of the both reactant and product mixture were defined in the

previous steps. Also the pressure of the product mixture was reckoned previously, but it will be checked later if it satisfies the ideal gas equation of state.

$$T_2(i) = \frac{q_R + \frac{1}{2}(P_x + P_1)(v_1 - v_2(i)) + C_{v1}(T_1 - T_{ref})}{C_{v2}} + T_{ref} \quad (130)$$

where heat of reaction is in kJ/kg, the pressures are in kPa, the specific heats are in kJ/kg·K and, the temperatures are in K.

- 10.** After determination of the temperature, the pressure which corresponds to the specific volume on the Rankine-Hugoniot curve is calculated by means of the ideal gas equation. Due to the ideal gas equation of state, if any solid carbon forms in the equilibrium composition, the specific volume of the gaseous product is calculated as follows,

The normal crystal density of the solid carbon is 2250 kg/m³, and the normal crystal specific volume is 0.444x10⁻³ m³/kg.

$$v_s = 0.444 \times 10^{-3} \text{ m}^3/\text{kg}$$

$$v_g = \frac{v_2(i) \left[\sum_g y_i MW_i + y_s MW_s \right] - v_s y_s MW_s}{\sum_g y_i MW_i} \quad (131)$$

If there is no formation of the condensed species, the specific volume of the gaseous product becomes,

$$v_g = v_2(i)$$

The gas constant and the temperature of the product mixture was calculated previously (in the step 6 and step 9 respectively)

$$P_g = \frac{R_2 T_2}{v_g} \quad (132)$$

If $|P_g - P_x| \rightarrow 0$ then $P_2(i) = P_g$ and proceed to the next step (step 11). Else, new $P_x = P_g$ and with this new P_x go to step 9, and repeat all process up to current step.

- 11.** Because the Rayleigh line is tangent to the Rankine-Hugoniot curve at the Chapman-Jouguet point, the difference of their slopes goes to zero. The determination method (Eqn. 81) was explained in Section 3.3 in detail.

If ε goes to zero then define $P_{C-J} = P_2(i)$, $T_{C-J} = T_2(i)$ and $v_{C-J} = v_2(i)$ and pass through the next step (step 12). Else go to step 7 and repeat all steps up to current step by new specific volume defined in step 7.

- 12.** The pressure, P_2 , at which the state of the product composition calculated, is compared with the pressure, P_{C-J} calculated by the determination methods of the Chapman-Jouguet point in step 11. If ε_P goes to zero where $\varepsilon_P = \left| \frac{P_2 - P_{C-J}}{P_{C-J}} \right|$ then pass through the next step (step 13). Else define $P_2 = P_{C-J}$ and go to step 5 and repeat all steps up to current step by new P_2 .

- 13.** The temperature, T_2 , at which the state and the thermodynamic properties of the product composition are calculated, is compared with the temperature, T_{C-J} calculated by Rankine-Hugoniot equation in step 9 and also satisfies the Chapman-Jouguet point in step 11. If ε_T goes to zero where $\varepsilon_T = \left| \frac{T_2 - T_{C-J}}{T_{C-J}} \right|$ then pass through the next step (Step 14).

Else $T_2 = T_2 + \Delta T$ and go to step 5 and repeat all steps up to current step by new T_2 .

- 14.** The temperature and the pressure, at which all state properties of the detonation composition are calculated, satisfy the Rankine-Hugoniot curve, ideal gas equation, and also the Rayleigh line. In other words, the Chapman-Jouguet point is determined. Also the properties of the Chapman-Jouguet point can be calculated.

Chapman-Jouguet temperature is T_{C-J} (K)

Chapman-Jouguet pressure is P_{C-J} (Pa)

Specific volume of the product mixture at C-J point is v_{C-J} (m^3/kg)

Density of the product mixture at C-J point is ρ_{C-J} (kg/m^3)

Also the composition of the detonation product and the heat of reaction, q_R , at C-J point were already determined.

The detonation velocity, D , can be calculated by Eqn. 79,

Therefore, the computations of the detonation point and detonation properties of energetic gaseous mixture are completed.

The flow chart of GasPX is given in Figure 12 in accordance with the previously explained algorithm.

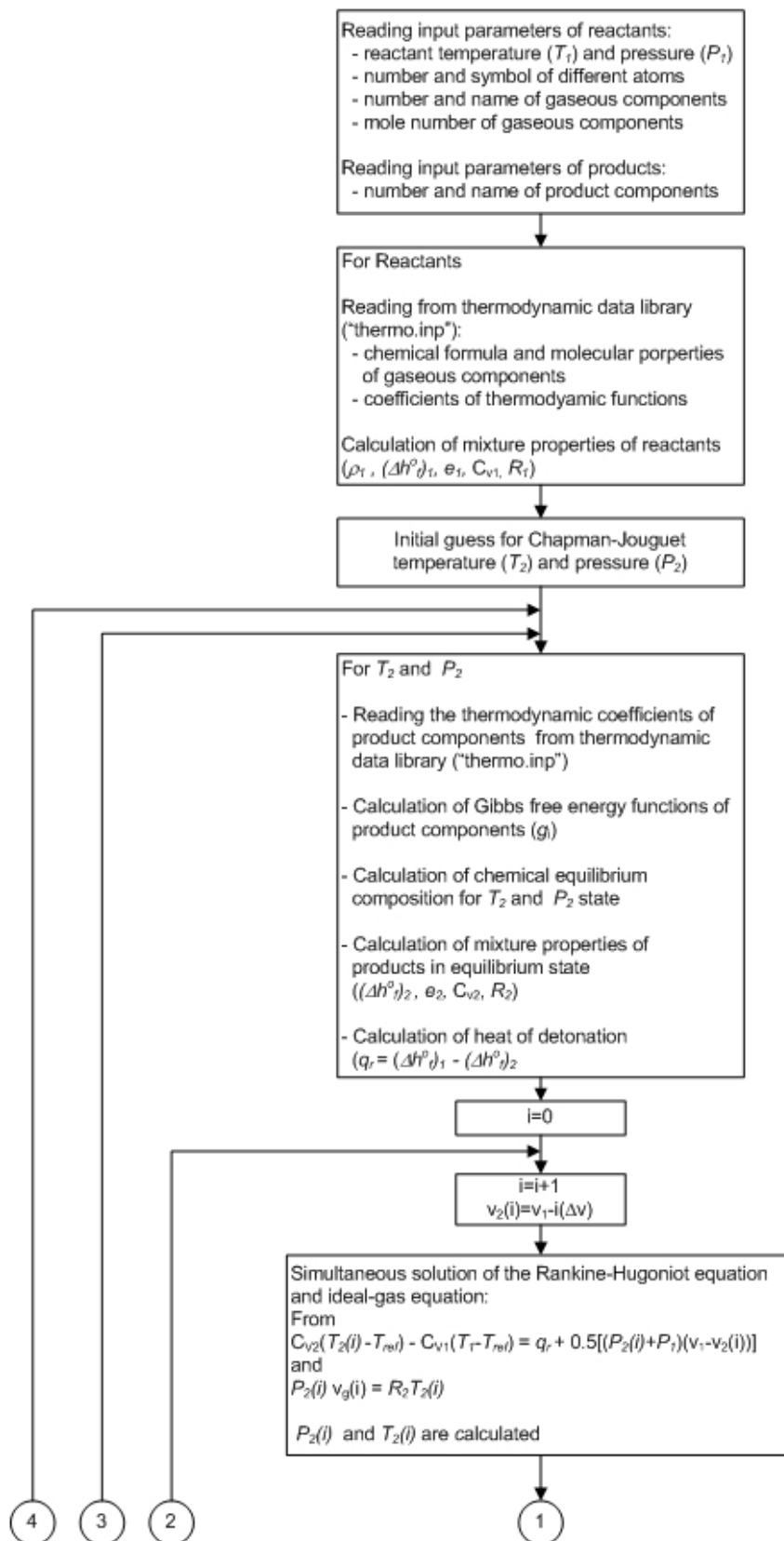


Figure 12. Flow chart of GasPX, continued to next page

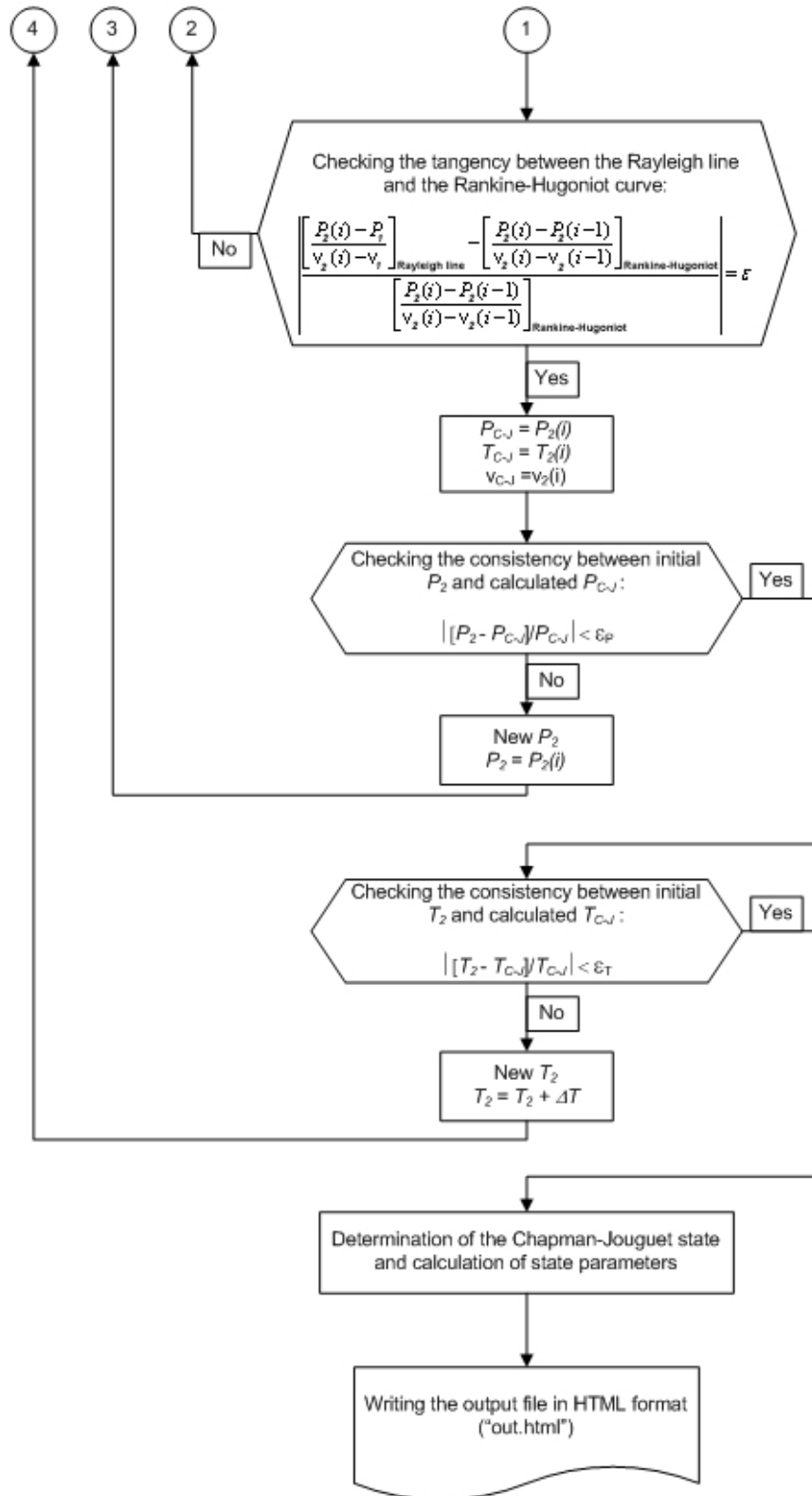


Figure 12. Flow chart of GasPX (Concluded)

3.4.5. Sensitivity Analysis for GasPX

Since GasPX performs the computation of the Chapman-Jouguet detonation point in an iterative manner, the optimum convergence factors, according to which the consistency of the computed parameters are checked, should be determined to obtain adequately precise results. The optimum convergence factors are determined according to an experimental case [56] of the detonation in acetylene-oxygen gaseous composition given in Table 7.

Table 7. Experimental detonation velocity for acetylene-oxygen gaseous mixture [56]

Reactant composition, % (by mole)	C ₂ H ₂	20
	O ₂	80
Experimental Detonation velocity, m/sec	2191.62	

First, the sensitivity analysis should be performed to determine the optimum pressure convergence factor, ε_P , (Step 12 in Section 3.4.4). All computations are performed according to experimental case given in Table 7. Also, while the computations performed for different pressure convergence factors, the other convergence factors and the initial values should be constant. These parameters kept constant are given in Table 8. The detonation pressure and detonation velocity computed according to different pressure convergence factors are given in Table 9. Since there is no distinctive difference between the computed detonation velocities, the computed detonation pressures are compared for different pressure convergence factors. In fourth column of Table 9, each computed detonation pressure is compared with previous computation. Hence, the change of the deviation between pressures according to ε_P can be easily evaluated. In order to observe the deviations between the computed pressures better, they are given in unit of Pascal (Pa).

Table 8. Constant parameters used in the computations performed for the sensitivity analysis of the pressure convergence factor (ε_P)

Initial pressure, bar	0.1
Temperature convergence factor, ε_T	1×10^{-4}
Initial temperature, K	1000
Tangency convergence factor, ε	1×10^{-4}

Table 9. Comparison of the computed Chapman-Jouguet detonation parameters by GasPX for the sensitivity analysis of the pressure convergence factor

ε_P	Calculated detonation pressure, Pa	Calculated detonation velocity, m/sec	Deviation of pressure*, %
1×10^{-8}	2666909.96	2194.96	-
1×10^{-7}	2666909.92	2194.96	1.50×10^{-6}
1×10^{-6}	2666910.03	2194.96	4.12×10^{-6}
1×10^{-5}	2666910.96	2194.96	3.48×10^{-5}
1×10^{-4}	2666906.58	2194.96	1.64×10^{-4}
1×10^{-3}	2666889.81	2194.96	6.29×10^{-4}

* - Absolute value of deviation between computed pressure and computed one for previous pressure convergence factor.

As seen in Table 9, while ε_P increases, the deviation between computed pressures naturally increases. However, there is no drastic change in computed pressures. Lower values of ε_P may result in divergence since the iteration loop may not satisfy the pressure convergence factor for the different cases. And the higher values of ε_P may cause the precision of the results poorly. Therefore, the optimum value of ε_P is determined as 1×10^{-5} .

The effect of initial guess for the detonation pressure values (Step 1 in Section 3.4.4) is also analyzed. A wide range of initial pressures are traced. And the results

are given in Table 10. Third column contains the absolute value of deviation between currently computed pressure and computed pressure for previous initial pressure. Initial pressures are given in unit of 'bar' and the computed detonation pressures are given in unit of Pascal.

Table 10. Effect of initial pressure values on computations

Initial pressure, bar	Calculated detonation pressure, Pa	Deviation of pressure*, %
0.001	2666910.84	-
0.01	2666909.88	3.60×10^{-5}
0.1	2666910.96	4.05×10^{-5}
1	2666909.65	4.91×10^{-5}
10	2666910.53	3.30×10^{-5}
100	2666912.03	5.62×10^{-5}

* - Absolute value of deviation between computed pressure and computed one for previous initial pressure.

Considering the results in Table 10, it can be deduced that GasPX is insensitive to the initial pressure. The initial value of pressure is determined as 0.1 bar in computations of GasPX code.

Similar sensitivity analysis is performed for temperature. The optimum temperature convergence factor, ε_T , (Step 13 in Section 3.4.4) should be determined. As it is made in the determination of the optimum pressure convergence factor, the parameters, given in Table 11, other than the temperature convergence factor are kept constant.

Table 11. Constant parameters used in the computations performed for the sensitivity analysis of the temperature convergence factor (ε_T)

Initial pressure, bar	0.1
Pressure convergence factor, ε_P	1×10^{-5}
Initial temperature, K	1000
Tangency convergence factor, ε	1×10^{-4}

For different ε_T values, the detonation temperature and detonation velocities are computed for the comparison. The results are given in Table 12. Since the calculated temperatures are primarily affected by ε_T , the comparison is performed according to them. Fourth column of Table 12 contains the absolute value of deviation of the computed temperature for current ε_T from the computed temperature for previous ε_T .

Table 12. Comparison of the computed Chapman-Jouguet detonation parameters by GasPX for the sensitivity analysis of the temperature convergence factor

ε_T	Calculated detonation temperature, K	Calculated detonation velocity, m/sec	Deviation of temperature*, %
1×10^{-5}	3907.40	2194.91	-
1×10^{-4}	3907.40	2194.96	0.0
1×10^{-3}	3907.50	2195.00	0.003
1×10^{-2}	3924.00	2198.80	0.422

* - Absolute value of deviation between computed temperature and computed one for previous temperature convergence factor.

Considering the comparisons in Table 12, the temperature convergence factor is determined as 1×10^{-4} for GasPX code. For 3907.4 K, the difference of temperature becomes: $|T_2 - T_{C-J}| = (1 \times 10^{-4}) \times (3907.4 \text{ K}) = 0.39074 \text{ K}$. And this relatively small

difference can be easily considered adequately enough for temperature to reach the accurate results.

The effect of initial temperatures (Step 1 in Section 3.4.4) on computations is also evaluated. The computed detonation temperatures for different initial temperatures are given in Table 13. Third column contains the absolute value of deviation between currently computed temperature and previously computed temperature.

Table 13. Effect of initial temperature values on computations

Initial temperature, K	Calculated detonation temperature, K	Deviation of temperature*, %
500	3907.38	-
1000	3907.40	5.12×10^{-4}
1500	3907.39	2.60×10^{-4}
2000	3907.38	5.10×10^{-4}
3000	3907.40	5.12×10^{-4}
4000	3907.40	0.0

* - Absolute value of deviation between computed temperature and computed one for previous initial temperature.

Considering the results in Table 13, it can be deduced that GasPX is insensitive to initial temperature. The initial value of temperature is determined as 1000 K in the computations of GasPX code.

Last, the optimum tangency convergence factor, ε , (Step 11 in Section 3.4.4) should be determined. Since the basic performance parameter is the detonation velocity and the tangent point gives the Chapman-Jouguet detonation state, the optimum convergence factor is determined according to computed detonation velocities for different convergence factors. In order to obtain relevant results, the parameters other than the tangency convergence factor should be kept constant (Table 14).

Table 14. Constant parameters used in the computations performed for the sensitivity analysis of the tangency convergence factor (ε)

Initial pressure, bar	0.1
Pressure convergence factor, ε_P	1×10^{-5}
Initial temperature, K	1000
Temperature convergence factor, ε_T	1×10^{-4}

The computed detonation velocities and comparisons for different ε values are given in Table 15. Third column contains the absolute value of deviation between currently computed detonation velocity and previously computed detonation velocity.

Table 15. Comparison of the computed Chapman-Jouguet detonation velocities by GasPX for the sensitivity analysis of the tangency convergence factor

ε	Calculated detonation velocity, m/sec	Deviation of detonation velocity*, %
1×10^{-6}	2194.95	-
1×10^{-5}	2194.86	7.15×10^{-3}
1×10^{-4}	2194.96	7.77×10^{-3}
1×10^{-3}	2200.42	2584.07×10^{-3}

* - Absolute value of deviation between computed velocity and computed one for previous convergence factor.

Up to 1×10^{-4} of ε , there is no significant deviation in detonation velocity. However, the deviation between the computed detonation velocities for 1×10^{-4} and 1×10^{-3} of ε shows a dramatic increase. Considering the results given in Table 15 and the computation time, the optimum ε value is determined as 1×10^{-4} . This value of ε can provide the adequately precise detonation parameters.

Therefore, according to all sensitivity analysis, the parameters used in GasPX are given in Table 16.

Table 16. Parameters used in the computations performed by GasPX

Initial pressure, bar	0.1
ε_P	1×10^{-5}
Initial temperature, K	1000
ε_T	1×10^{-4}
ε	1×10^{-4}

3.5. Comparison of the Results

The properties of the Chapman-Jouguet detonation point computed by GasPX are compared with data experimentally measured and data calculated by some investigators using hydrodynamic theory. Besides data given in literature, the predictions of NASA-Lewis code, CEA, are used to consider the accuracy of the GasPX.

3.5.1. Comparison of the Detonation Properties for Hydrogen-Oxygen Mixtures

A critical experimental measurement of detonation velocity on the basis of Chapman-Jouguet Theory was carried out by Lewis and Friauf [19] in 1930. They compared computed detonation velocities with the experimentally determined ones in hydrogen-oxygen mixture, also to which rare gases such as helium, or argon, and diluting gases such as nitrogen were added.

In 1950, similar study was performed by Berets et al. [12]. They conducted experimental measurements of detonation velocity in hydrogen-oxygen mixtures. They measured the detonation velocities by the use of miniature piezoelectric

gages. The velocity measurements were carried out in two stainless steel pipes of 1.2 and 10 cm diameter and both 120 cm long. In order to measure the steady detonation velocity, they divided last 60 cm of tubes into two equal intervals by three gages which were placed at 60 cm, 90 cm and 120 cm far from the initial point. They measured not only the hydrogen-oxygen mixture, but also the mixture of hydrogen-oxygen, to which Helium and Argon were added. In Ref. [12], the experimental detonation velocities and their variation by initial mole fraction of hydrogen were tabulated with respect to the pipe diameter. Also the detonation velocities measured in the first and second half of the last 60 cm of the test tube were presented. Berets et al. also made some calculations of detonation velocities by the Chapman-Jouguet Theory.

The GasPX predictions were compared with the experimental values of detonation velocities by Berets et al. for hydrogen-oxygen and also additional rare gas mixture. In computations, the state of the reactants, which are hydrogen and oxygen, was taken as the reference state at $T= 298.15$ K and $P= 1$ atm.

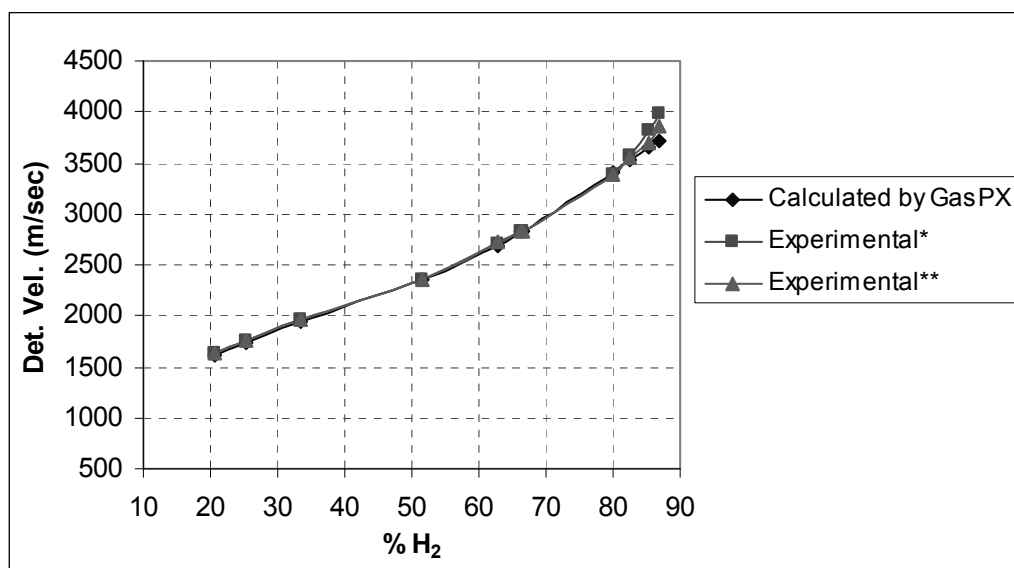
Table 17. Comparison of GasPX predictions with experimental velocities of detonation wave of hydrogen and oxygen mixtures in a 10-cm diameter pipe

Initial % H ₂ *	Experimental 10 cm pipe diameter First 30 cm	Experimental 10 cm pipe diameter Last 30 cm	Calculated Velocity (m/sec)	Deviation** %	Calculated Temperature (K)	Calculated Pressure (bar)
20.5	1644	1635	1608.3	1.902	2358	12.28
25.2	1768	1763	1737.9	1.566	2650	13.67
33.5	1954	1969	1938.0	1.198	3000	15.23
51.5	2360	2365	2364.6	-0.088	3470	17.27
62.8	2703	2728	2692.1	0.861	3640	17.70
66.4	2839	2836	2824.2	0.469	3660	17.99
66.7	2833	2825	2837.9	-0.315	3660	18.06
80.1	3387	3390	3413.5	-0.738	3400	17.13
82.6	3562	3555	3539.3	0.540	3250	16.60
85.2	3825	3695	3658.4	2.703	3050	15.73
86.9	3990	3867	3718.6	5.342	2900	14.85

* Mole fraction

** Deviation from the mean value of the experimental data

The computed results by GasPX are given in Table 17 for different initial hydrogen mole fraction in the reactant mixture. The results are compared with the experimental ones [12]. Second column and third column contains the measured detonation velocities in the first 30 cm and the last 30 cm, respectively, of the last 60 cm of the tube, in which measurements were performed. Fifth column contains the deviation of calculated values by GasPX from the mean value of the experimental results measured in the first 30 cm and the last 30 cm of the last part of the test tube.



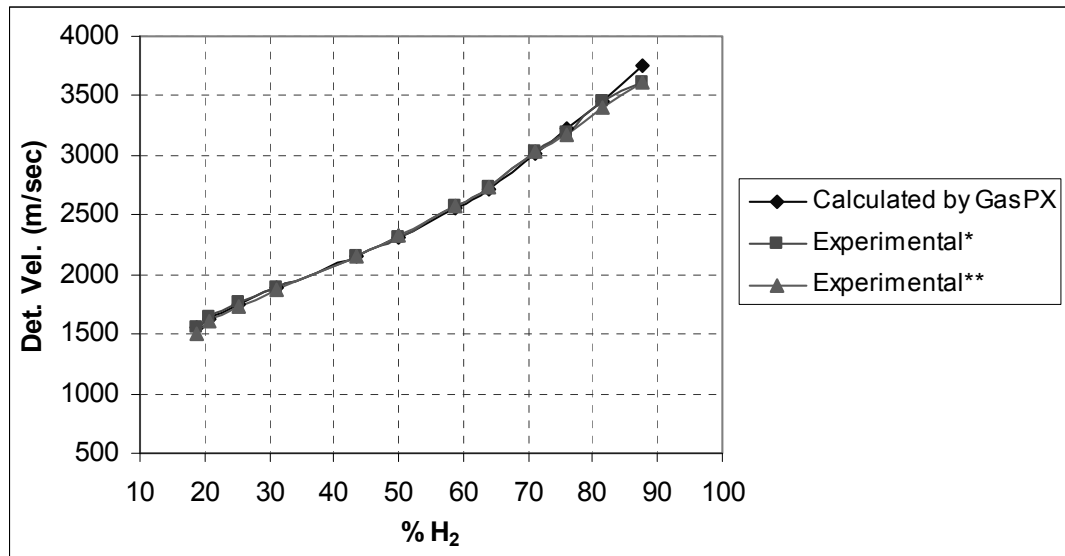
* Measured detonation velocities in the first 30 cm of the last 60cm of the tube
 ** Measured detonation velocities in the last 30 cm of the last 60cm of the tube

Figure 13. Comparison of the calculated and measured velocities of detonation wave for a 10-cm diameter pipe

The maximum deviation in Table 17 is less than 6 %. As a result of this comparison, it can be deduced that the computed results by GasPX for hydrogen-oxygen reactant mixture without any additional gas has a satisfactory agreement with experimental measurements. Also the adequate consistency between GasPX and the experiments can be observed in Figure 13.

The comparison between computed detonation wave velocities and measured values in a 1.2-cm diameter pipe is given in Figure 14. The consistency between the

measured detonation velocities and computed ones by GasPX can be observed in Figure 14. In other words, the agreement in Figure 13 maintains in Figure 14.



* Measured detonation velocities in first 30 cm of the last 60cm of the tube
 ** Measured detonation velocities in last 30 cm of the last 60cm of the tube

Figure 14. Comparison of the calculated and measured velocities of detonation wave for a 1.2-cm diameter pipe

The computed detonation properties, especially wave velocity of detonation, obtained by GasPX are not only compared by the experimental values, but also computed values by NASA-Lewis code, CEA [25]. Berets et al. performed measurements of detonation velocities for reactant mixture containing hydrogen, oxygen and helium gases. The experimental data and obtained data by means of NASA-Lewis code, CEA, are compared with the computations by GasPX. Due to no experimental data other than detonation velocities, the detonation pressure and temperature computed by GasPX can be compared with only those by NASA-Lewis code. All comparisons are given in Table 18.

Table 18. Calculated and experimental velocities of detonation wave in hydrogen, oxygen and helium mixtures

Initial Reactant Mixture (by mole)			Method	Detonation Velocity (m/sec)	Detonation Temperature (K)	Detonation Pressure (bar)
% H ₂	% He	% O ₂				
44.4	32.8	22.8	Experimental [12]	3097	-	-
			NASA-Lewis Code, CEA	3199.4	3512	18.868
			GasPX	3192	3457	17.610
			Deviation 1, %	3.00	-	-
			Deviation 2, %	-0.22	-1.60	-6.60
44.4	33.7	21.9	Experimental [12]	3110	-	-
			NASA-Lewis Code, CEA	3244	3508	18.870
			GasPX	3276	3547	18.010
			Deviation 1, %	5.33	-	-
			Deviation 2, %	0.98	1.11	-5.00
24.3	63.2	12.5	Experimental [12]	3395	-	-
			NASA-Lewis Code, CEA	3642	3205	17.70
			GasPX	3662	3183	16.42
			Deviation 1, %	7.30	-	-
			Deviation 2, %	0.55	-0.70	-7.23
24.8	62.7	12.5	Experimental [12]	3307	-	-
			NASA-Lewis Code, CEA	3648	3214	17.70
			GasPX	3652	3225	16.62
			Deviation 1, %	10.40	-	-
			Deviation 2, %	0.11	0.30	-6.10

- Deviation 1 – The percent of difference between data by GasPX and experimental data,
- Deviation 2 – The percent of difference between data by GasPX and data by NASA-Lewis code, CEA.

By addition of helium into the hydrogen-oxygen reactant mixture, the consistency between the computed wave velocities of detonation by GasPX and those measured from experiments degrades. While the helium fraction in reactant mixture increases, the deviation between computations and experiments increases. However, the detonation wave velocities obtained by GasPX differ very little from the results obtained by NASA-Lewis code. At 62.7 percent of helium, the deviation between experimental detonation velocity and that computed by GasPX is 10.4 %, whereas the deviation between GasPX and NASA-Lewis is only 0.11 %.

Considering these results, it can be deduced that GasPX and NASA-Lewis code shows a great agreement on computation of detonation wave velocity. The possible reason for deviation between detonation pressures obtained by GasPX and NASA-Lewis code might be explained by the fact that different methods are used to compute the Chapman-Jouguet detonation point. GasPX uses an iterative calculation procedure in which the iteration loop for pressure runs inside the iteration loop for temperature. On the other hand, NASA-Lewis code uses Newton-Raphson iteration method developed by Zeleznik and Gordon [55]. Also the computation methods of equilibrium composition at Chapman-Jouguet of GasPX and NASA-Lewis are different. As explained in Section 3.4.3, GasPX uses a commercial optimization solver on the basis of minimization of Gibbs free energy subject to mass balance. However, NASA-Lewis uses the modified optimization method developed by White et al. [42].

The detonation properties computed by GasPX for hydrogen, oxygen and helium reactant mixture are compared with those computed by Berets et al. The comparison of the calculated detonation properties and calculated equilibrium compositions are given in Table 19 and Table 20, respectively. It can be seen from Table 19 and Table 20 that detonation properties computed by GasPX have a reasonably good agreement with the calculated ones in the paper [12].

Table 19. Comparison of the calculated velocities of detonation wave in hydrogen, oxygen and helium mixtures

Initial Reactant Mixture (by mole)			Method	Detonation Velocity (m/sec)	Detonation Temperature (K)	Detonation Pressure (bar)
% H ₂	% He	% O ₂				
44.4	22.2	33.3	Calculated [12]	3249	3515	17.90
			GasPX	3215	3440	17.52
			Deviation, %	-1.04	-2.10	-2.10
25.0	12.5	62.5	Calculated [12]	3672	3198	16.46
			GasPX	3659	3175	16.38
			Deviation, %	-0.35	-0.72	-0.50

Table 20. Comparison of the calculated equilibrium compositions

Initial Reactant Mixture (by mole)			Method	Mole Fraction, %					
% H ₂	% He	% O ₂		H ₂ O	H ₂	O ₂	OH	H	O
44.4	33.3	22.2	Calculated [12]	35.2	9.80	3.10	7.20	4.40	2.20
			GasPX	35.6	9.36	2.81	7.86	4.23	1.92
25.0	62.5	12.5	Calculated [12]	21.7	3.90	1.30	2.60	1.30	0.60
			GasPX	21.6	3.76	1.20	2.90	1.24	0.53

All detonation wave velocities calculated by GasPX, NASA-Lewis or methods stated in the reference [12] for the helium added reactant mixtures have discrepancy with experimental data. Berets et al. claimed that incomplete equilibrium state of hydrogen-oxygen mixture with additional helium caused the loss in the useful energy. One can then expect detonation velocities lower than those calculated on the assumption of complete equilibrium reaction because some of the energy is not utilized.

Considering the results obtained by GasPX and taking into account the explanation about the discrepancy between calculated detonation velocities and measured ones for hydrogen-oxygen mixture with additional helium gas, it follows that there is a reasonably successful agreement between the data obtained by GasPX and either experimental data or data calculated by other computer codes.

3.5.2. Comparison of the Detonation Properties for Acetylene-Oxygen Mixtures

The detonation velocities for acetylene-oxygen mixture in varied compositions are computed by GasPX. The state of the reactants, which are acetylene and oxygen, is taken as the reference point at $T= 298.15$ K and $P= 1$ atm. The computed results are compared with the experimental ones conducted by Breton [56], and Kistiakowsky et al. [57].

The comparison between the computed results by GasPX and experimental values measured by Breton is given in Table 21. The Breton's experimental values are given as a plot of detonation velocity changing with acetylene percent in reactant mixture [58]. Breton performed his measurements by means of the method based on Schlieren Photographic record technique [59].

In Table 21, the first column contains the percent of acetylene in reactant mixture and the second column contains the oxygen percent. The third column contains the measured detonation wave velocity by Breton. The experimental values in the third column are representative data deduced from the plot given in [58]. The fourth column gives the computed detonation wave velocity by GasPX. The fifth column gives the percentage deviation between the experimental and calculated values. The sixth and seventh columns give the temperature and pressure, respectively, of the Chapman-Jouguet detonation point.

Table 21. Calculated and experimental velocities of detonation wave in acetylene and oxygen mixtures

Reactants (by mole)		Experimental Velocity (m/s) [56]	Calculated Velocity (m/s)	Deviation %	Calculated Temperature (K)	Calculated Pressure (bar)
% C ₂ H ₂	% O ₂					
5.0	95.0	1643.72	1599.13	-2.71	2599	14.96
6.0	94.0	1691.91	1678.65	-0.78	2829	16.33
9.0	91.0	1854.18	1844.87	-0.50	3300	19.86
16.5	83.5	2095.75	2100.63	0.23	3793	25.12
20.0	80.0	2191.62	2194.96	0.15	3907	26.67
40.0	60.0	2729.69	2719.30	-0.38	4425	38.90
50.0	50.0	2932.73	2937.00	0.14	4509	44.20
60.0	40.0	2516.87	2581.46	2.56	3905	34.74
70.0	30.0	2211.90	2197.00	-0.67	3152	25.00
75.0	25.0	2123.19	1978.00	-6.83	2685	20.56
85.0	15.0	2092.07	1520.20	-27.33	1743	11.93

It can be understood from Table 21 that the calculated detonation velocities in the range of 5 to 70 percent of acetylene differ from the measured velocities of detonation in acetylene-oxygen mixture by a maximum deviation of 2.71 %. However, this satisfactory agreement can not be sustained above 70 percent of acetylene. The discrepancy between detonation wave velocities above 70 percent acetylene can be easily realized in Figure 15. On the side of excess acetylene, the measured velocities of the detonation wave are higher than computed ones.

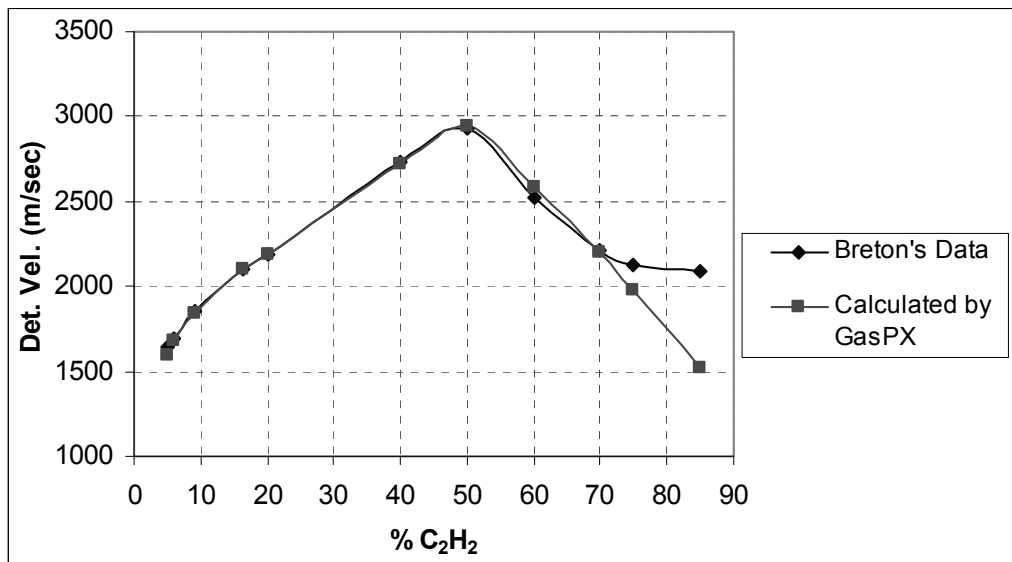


Figure 15. Comparison of the calculated and measured velocities of detonation wave in acetylene and oxygen mixtures

Table 22 gives the calculated detonation composition for the same test cases as given in Table 21. The eleventh column contains the percent of the solid carbon (Cs) and the twelfth contains the percent of carbon vapor (C) in the product (equilibrium) composition. As seen in Table 22, for the reactant mixtures with high amount of acetylene, the residual acetylene after reaction takes up most of the carbon. However, significant solid carbon formation is likely to occur during the detonation of highly acetylene rich mixtures, which is disregarded in the calculation of the Chapman-Jouguet detonation point by GasPX. Absence of the solid carbon formation is probably the cause of the discrepancy for mixture containing acetylene more than 70 percent.

Table 22. Calculated composition of the detonation products at C-J state

Mole Fraction %											
Initial C ₂ H ₂	C ₂ H ₂	H ₂ O	H ₂	OH	H	O ₂	O	CO ₂	CO	Cs	C
5.0	0.00	4.57	0.012	1.013	0.01	83.67	0.53	10.00	0.17	0.00	0.00
6.0	0.00	5.10	0.34	1.93	0.04	79.38	1.34	11.63	0.55	0.00	0.00
9.0	0.00	6.25	0.167	4.70	0.30	66.17	5.00	14.73	3.11	0.00	0.00
16.5	0.00	8.12	0.90	9.77	1.94	38.28	11.20	15.18	14.60	0.00	0.00
20.0	0.00	8.60	1.45	11.14	3.16	28.45	12.79	13.78	20.62	0.00	0.00
40.0	0.00	6.12	9.22	7.45	15.50	1.60	6.48	3.57	50.10	0.00	0.00
50.0	0.02	0.03	18.80	0.024	21.72	0.00	0.02	0.00	59.34	0.00	0.00
60.0	13.48	0.00	22.00	0.00	10.3	0.00	0.00	0.00	54.22	0.00	0.00
70.0	30.42	0.00	21.71	0.00	2.22	0.00	0.00	0.00	45.60	0.00	0.00
75.0	40.00	0.00	19.70	0.00	0.50	0.00	0.00	0.00	40.00	0.00	0.00
85.0	60.90	0.00	13.04	0.00	0.00	0.00	0.00	0.00	26.10	0.00	0.00

The detonation velocity computations by GasPX are repeated above 60 percent acetylene by taking account of the solid carbon formation in detonation products. The results are given in Table 23.

Table 23. Experimental and Calculated velocities of detonation wave after taking solid carbon formation into account

Reactants (by mole)		Experimental Velocity (m/s) [56]	Calculated Velocity (m/s)	Deviation %	Calculated Temperature (K)	Calculated Pressure (bar)
% C ₂ H ₂	% O ₂					
5.0	95.0	1643.72	1599.13	-2.71	2599	14.96
6.0	94.0	1691.92	1678.65	-0.78	2829	16.33
9.0	91.0	1854.18	1844.87	-0.50	3299	19.86
16.5	83.5	2095.75	2100.63	0.23	3793	25.12
20.0	80.0	2191.62	2193.34	0.08	3899	26.95
40.0	60.0	2729.69	2719.30	-0.38	4425	38.90
50.0	50.0	2932.73	2937.00	-0.14	4509	44.20
60.0	40.0	2516.87	2609.00	3.66	3947	35.00
70.0	30.0	2211.90	2431.00	9.91	3687	30.83
75.0	25.0	2123.19	2368.00	11.53	3630	29.00
80.0	20.0	2150.00	2294.00	6.69	3632	28.60
85.0	15.0	2092.07	2216.00	5.92	3527	26.50
91.0	9.0	2195.50	2178.97	0.75	3434	24.25

Including solid carbon formation into the calculation, the deviation at 85 percent acetylene is decreased from 27.33 to 5.92 %, and also the deviation from the experimental value at 91 percent of acetylene is 0.75 %. Even though the deviations show an increase in the range of 60 to 75 percent of acetylene, the drastic discrepancy between measured and calculated detonation velocities above 80 percent acetylene is prevented.

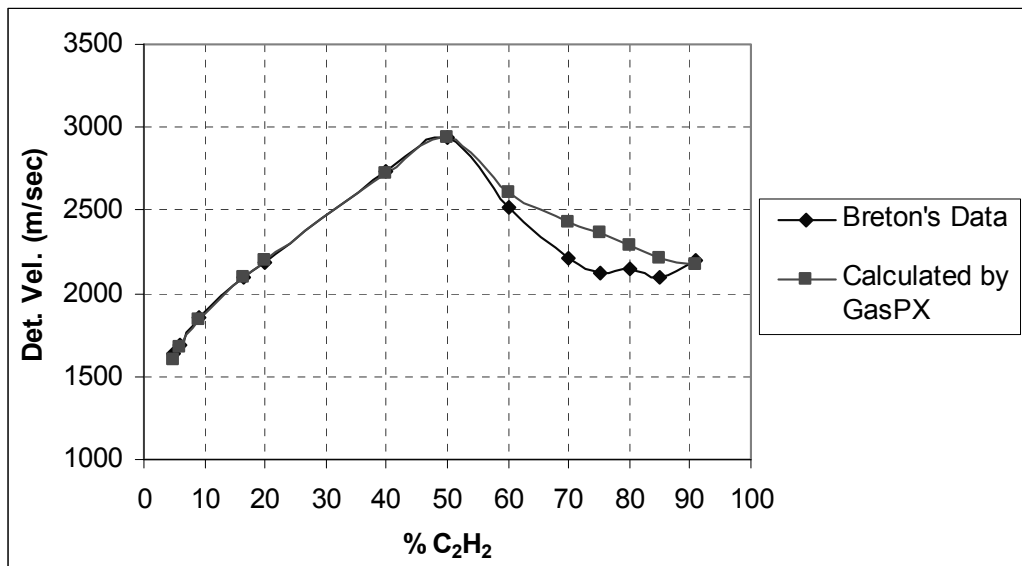


Figure 16. Comparison of the calculated and measured velocities of detonation wave by including the solid carbon formation into computations

The plot of the measured and calculated detonation wave velocity varying with mole fractions of acetylene in the reactant mixture is given in Figure 16. The consistency between measured and calculated detonation wave velocity for notably excess acetylene (above 80 percent of acetylene) in the reactant mixture and also change of product mixture with initial mole fraction of acetylene can be observed in Figure 16 and Table 24. The fraction of the solid carbon (Cs) in the product mixture is given in the eleventh column of Table 24.

Table 24. Calculated composition of the detonation products including solid carbon at C-J state

Mole fraction, %											
Initial C ₂ H ₂	C ₂ H ₂	H ₂ O	H ₂	OH	H	O ₂	O	CO ₂	CO	Cs	C
5.0	0.00	4.57	0.01	1.01	0.01	83.67	0.53	10.00	0.17	0.00	0.00
6.0	0.00	5.10	0.34	1.93	0.04	79.38	1.34	11.63	0.55	0.00	0.00
9.0	0.00	6.25	0.17	4.70	0.30	66.17	5.00	14.73	3.11	0.00	0.00
16.5	0.00	8.12	0.90	9.77	1.94	38.28	11.20	15.18	14.60	0.00	0.00
20.0	0.00	8.60	1.45	11.14	3.16	28.45	12.79	13.78	20.62	0.00	0.00
40.0	0.00	6.12	9.22	7.45	15.50	1.60	6.48	3.57	50.10	0.00	0.00
50.0	0.02	0.03	18.80	0.02	21.72	0.00	0.02	0.00	59.34	0.00	0.00
60.0	10.80	0.00	22.37	0.00	11.00	0.00	0.00	0.00	51.60	4.14	0.00
70.0	8.52	0.00	26.00	0.00	7.40	0.00	0.00	0.00	30.00	26.1	0.00
75.0	7.17	0.00	27.00	0.00	5.70	0.00	0.00	0.00	24.70	35.0	0.00
85.0	2.642	0.00	28.40	0.00	6.10	0.00	0.00	0.00	17.00	45.8	0.00
91.0	2.47	0.00	29.16	0.00	5.02	0.00	0.00	0.00	12.10	51.3	0.00

After Breton's studies on measurement of detonation wave velocity in acetylene-oxygen mixture, Kistiakowsky et al. [57] performed both experimental and computational studies on detonation wave velocities for the same compositions as Breton's.

To obtain steady wave velocities in the mixtures, they used a mixture close to 50-50 acetylene-oxygen initiator mixture at higher than atmospheric pressure. The detonation wave velocities were measured by piezoelectric gages mounted flush in the wall of the tube, as in the experimental study conducted by Kistiakowsky et al. [48].

They observed satisfactory agreement between calculated and measured detonation wave velocities in the range of 7 to 50 percent of acetylene in the

reactant mixture. However, their calculations showed an inconsistency with experimental measurements above 50 percent of acetylene. They represented measured and calculated detonation wave velocities with a plot, Figure 17, in their paper [57]. The plot, Figure 17, also shows the previous experimental detonation wave velocities measured by investigators [16, 56, 60]. At about 60 percent of acetylene in Figure 17, the calculated detonation curve breaks into two curves. The velocities calculated for a heat of sublimation of carbon equal to 171 kcal are shown by upper curve, while the other curve involving a heat of sublimation of carbon equal to 136 kcal is plotted inside the upper one.

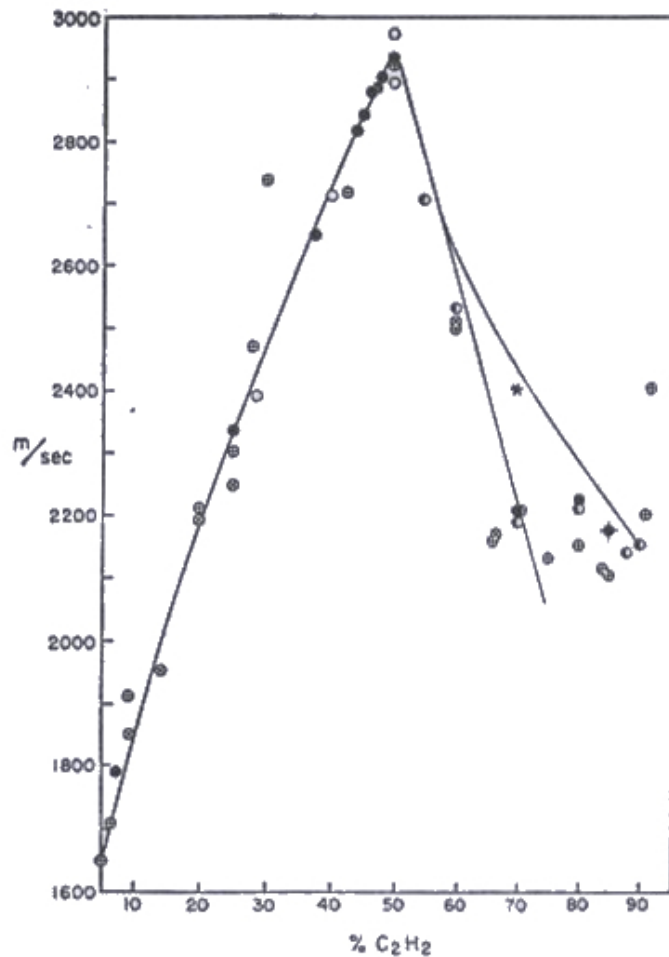


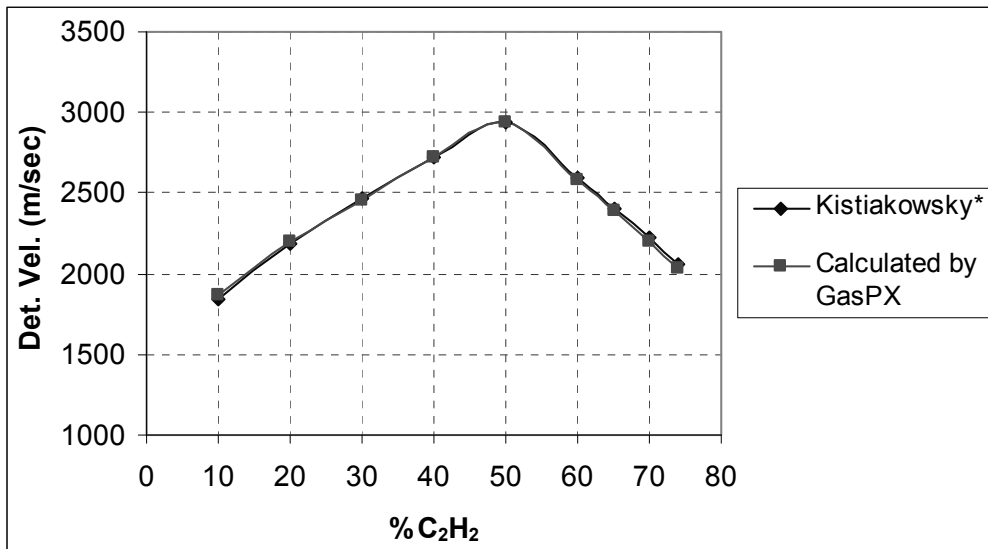
Figure 17. Detonation velocities in acetylene-oxygen mixtures at 1 atm pressure [57]; (•-measured velocities with pure acetylene; solid lines are calculated velocities)

At high heat of sublimation of carbon like 171 kcal, probability of formation of solid carbon in product (equilibrium) mixture increases. So in computations by GasPX, solid carbon formation is included when the results are compared with the upper curve, but not included when the results are compared with the inner curve where the computations performed for the heat of sublimation of carbon equal to 136 kcal.

Without solid carbon formation in product mixture, the computed results by GasPX of detonation in acetylene-oxygen mixture are given in Table 25. The calculated results placed in the third column are representative velocities obtained from Figure 17. Up to 50 percent of acetylene in the reactant mixture, there is a singular curve, but above about 60 percent of acetylene, the inner curve was taken into consideration due to low heat of sublimation of carbon equal to 136 kcal.

Table 25. Comparison of the calculated velocities of detonation wave in acetylene and oxygen mixtures without solid carbon in products

Reactants (by mole)		Calculated Velocity (m/s) [57]	Calculated Velocity (m/s)	Deviation %	Calculated Temperature (K)	Calculated Pressure (bar)
% C ₂ H ₂	% O ₂					
10	90	1844.63	1872.48	1.51	3323	20.07
20	80	2182.49	2194.96	0.57	3907	26.67
30	70	2461.37	2457.00	-0.20	4185	32.76
40	60	2724.86	2719.30	-0.20	4425	38.90
50	50	2934.10	2937.00	0.10	4509	44.20
60	40	2594.32	2581.46	-0.50	3905	34.74
65	35	2409.13	2396.00	-0.54	3559	29.84
70	30	2230.68	2197.00	-1.51	3152	25.00
74	26	2061.76	2029.65	-1.55	2795	21.44



* Calculated velocities [57]

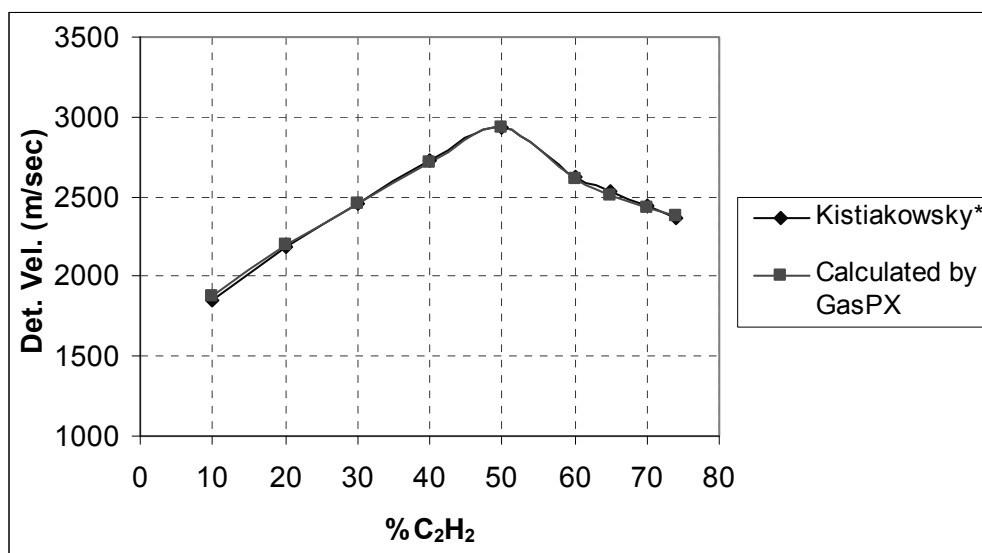
Figure 18. Comparison of the calculated velocities of detonation wave without solid carbon formation into computations

The comparison of the results given in Table 25 is plotted in Figure 18. Without solid carbon formation, there is a perfect agreement between the calculated results given in paper [57] and the results computed by GasPX in Figure 18.

Now taking consideration of the solid carbon formation in computations by GasPX, the results of GasPX are compared with the representative calculated detonation velocities of upper curve in Figure 17, where the heat of sublimation of carbon is equal to 171 kcal. And the comparisons between calculated results are shown in Table 26.

Table 26. Comparison of the calculated velocities of detonation wave in acetylene and oxygen mixtures with solid carbon in products

Reactants (by mole)		Calculated Velocity (m/s) [57]	Calculated Velocity (m/s)	Deviation %	Calculated Temperature (K)	Calculated Pressure (bar)
% C ₂ H ₂	% O ₂					
10	90	1844.63	1872.48	1.60	3323	20.07
20	80	2182.49	2194.96	0.57	3907	26.67
30	70	2461.37	2457.00	0.18	4185	32.76
40	60	2724.86	2719.30	0.20	4425	38.9
50	50	2934.10	2937.00	0.10	4509	44.2
60	40	2626.83	2609.00	0.68	3947	35.0
65	35	2527.36	2509.70	0.70	3784	32.64
70	30	2441.17	2431.00	0.42	3687	30.83
74	26	2369.60	2376.64	0.30	3629	29.38



* Calculated velocities [57]

Figure 19. Comparison of the calculated velocities of detonation wave with solid carbon formation into computations

The comparison between calculated detonation velocities in paper [57] and computed those by GasPX with solid carbon formation in product equilibrium composition is given in Figure 19. This plot shows the very good agreement between the calculated results.

In accordance with these results, it can be deduced that GasPX has generally good agreement with both experimentally measured and previously computed velocity of detonation wave in acetylene-oxygen mixture.

In Figure 17, the maximum value of detonation velocity is observed for 50-50 percent of acetylene-oxygen composition. Also, the same case is observed in the computed detonation velocities (Figure 18 and Figure 19). If one examines Table 25 and Table 26, it can be realized that for equal mole fraction of acetylene and oxygen gases in reactant composition, the reaction takes place at the condition where almost all acetylene and completely all oxygen are consumed after reaction. Also, the highest detonation temperature is observed for the 50-50 % composition of acetylene-oxygen. According to these results, one can expect that the highest heat of detonation (heat of reaction) is observed for the highest C-J temperature which is observed for the 50-50 % composition of acetylene-oxygen. However, in Table 27, the calculated highest C-J temperature does not occur at the highest heat of detonation computed by GasPX. Since the highest temperature along the Rankine-Hugoniot curve is not observed at Chapman-Jouguet point and also the detonation velocity reaches its minimum value along the Rankine-Hugoniot curve at the Chapman-Jouguet point, it can not be deduced that the highest detonation velocity is observed at the highest temperature. Moreover, the computation of the Chapman-Jouguet point depends on the simultaneous solution of the conservation laws and the ideal gas equation of state. Also, the equilibrium composition has a notable influence on the computations. Hence, since there are a lot of parameters taking place in computations, it can not be a common conclusion that the C-J temperature has a proportional effect on detonation velocity and it can not be also a common conclusion that the highest heat of detonation for a reactant mixture is observed for the complete consumption of the reactants.

Table 27. Computed heat of detonation in acetylene and oxygen mixtures with solid carbon in products

Reactants (by mole)		Calculated Temperature (K)	Calculated Heat of Detonation (kJ/kg)
% C ₂ H ₂	% O ₂		
10	90	3323	2758.67
20	80	3907	3590.30
30	70	4185	4170.70
40	60	4425	4673.67
50	50	4509	4987.20
60	40	3947	5200.73
65	35	3784	5493.78
70	30	3687	5773.22
74	26	3629	6001.96

3.5.3. Comparison of the Detonation Properties for Cyanogen-Oxygen Mixtures

Detonation velocities were measured in mixtures of cyanogen (C₂N₂) and oxygen in several tube diameters by Kistiakowsky et al. [48], with a reproducibility of the order of 0.1 percent. Thermodynamic calculations of detonation velocities were carried out for several experimental conditions in their study.

They measured the detonation velocities by piezoelectric gages mounted flush in the wall of the tube. The detonations were started by a spark in a 50-50 acetylene-oxygen initiator mixture. Several gages were located along the tube to provide information on the constancy of the detonation velocity. Considering the fact that the products of detonation wave could not be treated as ideal and the tube diameter effect on detonation velocity, the experimental velocities were corrected to ideal and infinite diameter detonation wave velocities. Besides, the experimental studies, they performed some calculations of detonation properties.

The experimental and calculated properties of detonation in the mixture of cyanogen (C₂N₂) and oxygen by Kistiakowsky et al. [48] are compared with values obtained by GasPX to confirm the accuracy of the code. All computations by GasPX are performed by reckoning the state of the reactants (cyanogen-oxygen mixture) at the reference point at $T_{ref} = 298.15$ K and $P_{ref} = 1$ atm.

The experimental data and computed detonation velocities by GasPX are given in Table 28. Fifth column of the table contains the corrected infinite diameter detonation velocities. The computed values are compared with the corrected experimental detonation velocities. The deviation between GasPX predictions and data from experiments is given in seventh column. Also the experimental data, the corrected experimental data, and results computed by GasPX are plotted with initial molar cyanogen (C_2N_2) fraction in Figure 20.

Table 28. Comparison of the computed detonation wave velocities by experimental and corrected data

Reactants (by mole)			Experimental Velocity (m/s) [48]	Corrected Experimental Velocity (m/s) [48]	Calculated Velocity* (m/s)	Deviation %
% C_2N_2	% O_2	% Ar				
41.19	58.52	0.29	2512	2540	2522.0	-0.71
44.00	55.72	0.28	2618	2628	2626.0	-0.07
49.88	49.87	0.25	2773	2771	2748.4	-0.81
25.00	25.00	50.00	2377	2387	2389.2	-0.09
50.5	49.3	0.2	2768	2766	2734.2	-1.15
51.5	48.3	0.2	2744	2741	2694.9	-1.70
53.5	46.3	0.2	2614	2624	2541.0	-3.10
57.00	42.8	0.2	2410	-	2282.0	-5.31

* Computed detonation wave velocities by GasPX

** Deviation according to non-corrected experimental value

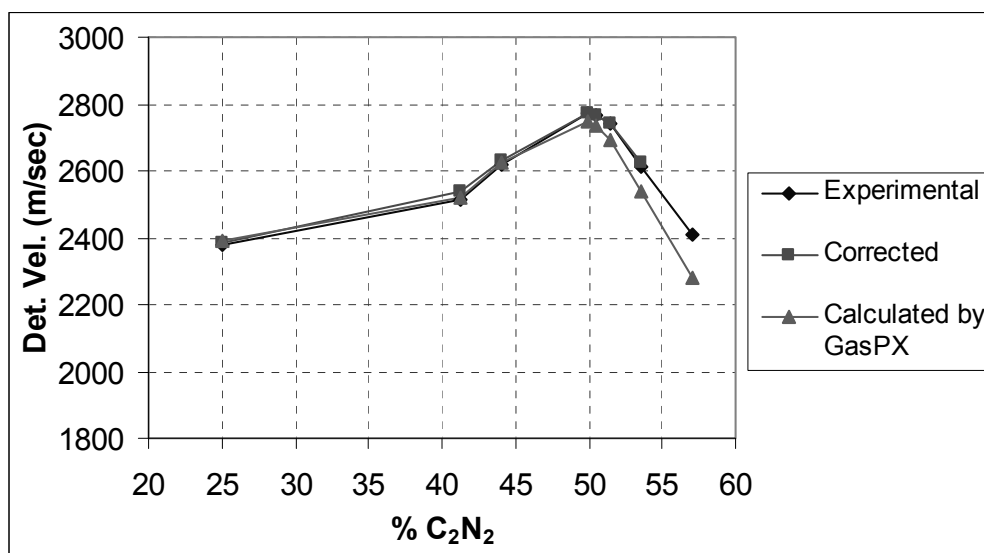


Figure 20. Comparison of the detonation wave velocities computed by GasPX and experimental data

Considering the results presented in Table 28 and Figure 20 it follows that the maximum deviation is less than 6 %. Also the good agreement between results up to 50 % of cyanogen can be verified by Table 28 and Figure 20. However there is a discrepancy between computations and experimental data above 53 percent of Cyanogen. This inconsistency might be resulting from ideality of the Chapman-Jouguet Theory. In order to verify the accuracy of the computations, the computed results by GasPX are compared with those obtained by NASA-Lewis code, CEA, and calculated data given in reference [48].

Table 29. Comparison of the computed detonation wave velocities

Reactants (by mole)			Calculated Velocity* (m/s)	Calculated Velocity** (m/s)	Calculated Velocity*** (m/s)	Deviation 1 %	Deviation 2 %
% C ₂ N ₂	% O ₂	% Ar					
41.19	58.52	0.29	2522.0	2526	2527	-0.16	-0.20
44.00	55.72	0.28	2626.0	2634	2633.6	-0.30	-0.29
49.88	49.87	0.25	2748.4	2756	2749	-0.28	-0.02
25.00	25.00	50.00	2389.2	2389	2388	0.01	0.05
50.5	49.3	0.20	2734.2	2762	2736	-1.01	-0.07
51.5	48.3	0.20	2694.9	2720	2694	-0.92	0.03
53.5	46.3	0.20	2541.0	2602	2542	-2.34	-0.04

* Computed detonation wave velocities by GasPX

** Computed detonation wave velocities by NASA-Lewis

*** Computed detonation wave velocities [48]

Deviation 1 - The percent of difference between data by GasPX and calculated data [48]

Deviation 2 - The percent of difference between data by GasPX and data by NASA-Lewis code, CEA

All computed results are given in Table 29. It can be noted from Table 29 that GasPX has a great agreement with other calculations. Especially, the deviation between GasPX and NASA-Lewis code is not more than 0.5 percent. On the basis of this notably satisfactory agreement it can be deduced that the discrepancy between experimental data and computed results by GasPX may be caused by the ideal assumptions in computations because GasPX has a great consistency with NASA-Lewis code which uses a different computation method than GasPX.

On the other hand, detonation velocities computed by GasPX are compared by experimental data stated in other study performed by Peek and Thrap [22]. They measured the detonation velocity by means of six ionization gages and associated electronic equipment. Also they applied corrections to the experimental data to

compute the infinite diameter detonation velocities. The detonation wave velocities computed by GasPX are compared with the experimental data, which is corrected to the infinite diameter, in Table 30 and Figure 21. These results show that GasPX is in good agreement not only with other computer code and computations method but also with the experimental data to which infinite diameter correction is applied.

Table 30. Comparison of the computed detonation wave velocities with corrected experimental data

Reactants (by mole)			Experimental Velocity (m/s)* [22]	Calculated Velocity (m/s)	Deviation %
% C ₂ N ₂	% O ₂	% Ar			
30.1	69.7602	0.1398	2265	2253.0	0.53
35.2	64.6704	0.1296	2378	2369.0	0.38
40.1	59.7802	0.1198	2511	2491.0	0.80
44.9	54.9898	0.1102	2692	2666.5	0.95
49.9	49.9998	0.1002	2765	2754.2	0.39

* The detonation velocities which are corrected to infinite diameter velocity

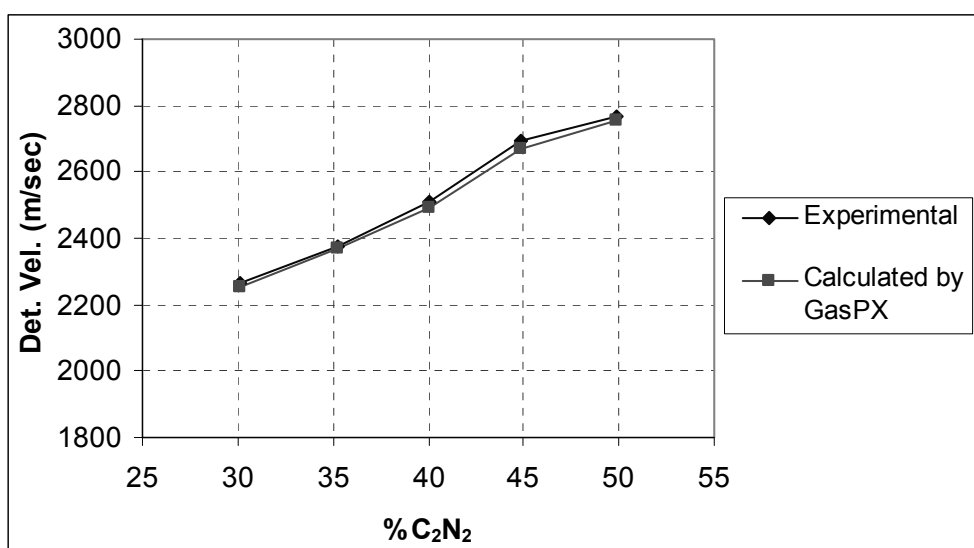


Figure 21. Comparison of the computed detonation wave velocities with corrected experimental data

CHAPTER 4

DETONATION IN CONDENSED PHASE EXPLOSIVES

4.1. One-Dimensional Analysis

As explained previously, the detonation is a shock wave of which propagation is sustained by fast chemical reactions. Consider a distinct shape solid explosive at atmospheric pressure, P_1 , of 1.01325 bar and a specific volume v_1 . Due to the shock wave, the explosive is compressed along the Hugoniot curve (shock adiabat) to a specific volume v_a of the solid explosive while the chemical reaction is initiated and the pressure increases to value P_a . The reaction is completed at the pressure, P_2 , and specific volume, v_2 on the Hugoniot curve for the detonation products. Then, the products of the reaction expand isentropically (the Taylor wave) into the surrounding medium.

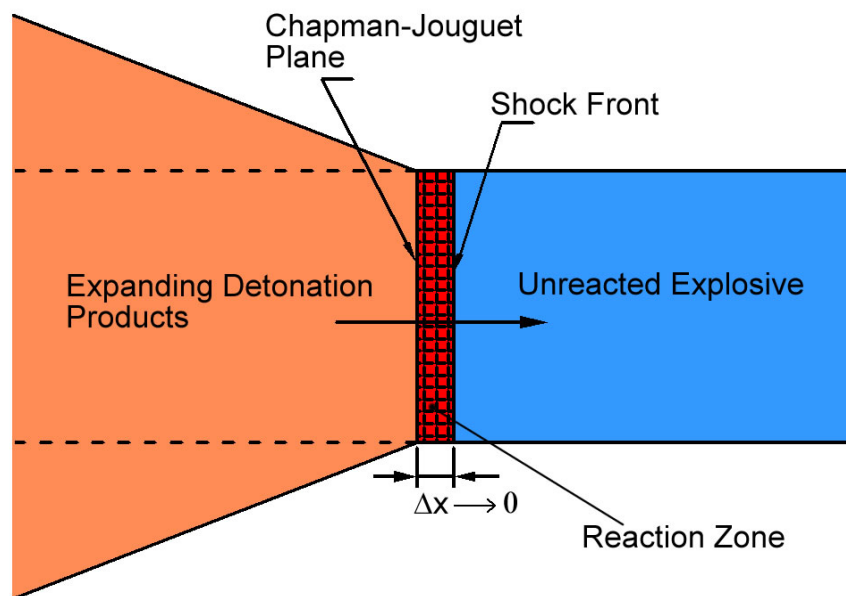


Figure 22. Simplified Presentation of Condensed Phase Explosive Detonation Phenomenon

As seen in Figure 22, the unreacted explosive is compressed by shock front. Then chemical reaction, which generates the heat of detonation, occurs in the reaction zone. After the completion of the reaction, the pressure and specific volume of the product reach the Chapman-Jouguet point on the Rankine-Hugoniot curve. In the rear zone of the Chapman-Jouguet plane, the products expand along the isentrope.

The Chapman-Jouguet Theory provides a comprehensible and satisfactory explanation for detonation in condensed (solid) explosives as it does for gaseous detonation by assuming followings in addition to its main assumptions:

- 1) Because the reaction zone in Figure 22 is infinitely thin, it can be reckoned that the reaction is completed at the shock front,
- 2) The shock front, the reaction zone and the Chapman-Jouguet plane are moving together also with the same velocity which is defined as the detonation velocity, D .

All thermodynamic and hydrodynamic equations, which are applied to the detonation phenomenon in gaseous mixture, are valid for detonation in solid explosives. The Rayleigh line and Rankine-Hugoniot relations have been already derived from the conservation equations (continuity, momentum and energy) in Chapter 2.

The Rayleigh line relation

$$\dot{m}''^2 = \rho_1^2 u_1^2 = \rho_2^2 u_2^2 = \frac{P_2 - P_1}{\frac{1}{\rho_1} - \frac{1}{\rho_2}} \quad (133)$$

The Rankine-Hugoniot equation:

$$C_{v2}(T_2 - T_{ref}) - C_{v1}(T_1 - T_{ref}) - q_R = \frac{1}{2}(P_2 + P_1) \left(\frac{1}{\rho_1} - \frac{1}{\rho_2} \right) \quad (134)$$

where, $q_R = \Delta h_{f1}^o - \Delta h_{f2}^o$ is the heat of detonation, and C_{v1} and C_{v2} are the constant-volume mean specific heats.

4.2. Equation of State

4.2.1. Equation of State for Product Gas Mixture

The Chapman-Jouguet Theory can obtain fairly successful results in gaseous detonation even if ideal-gas equation of state is used. However, the ideal-gas equation of state is insufficient to describe the detonation phenomenon in condensed phase explosives [61].

During the steady-state detonation of condensed phase explosives, the pressure of the detonation products can exceed 20 GPa, supported by the bulk density and the energy of the explosive. Under this high pressure, the product gases can be compressed to 1.5-2.5 times their normal solid densities [62]. Because from the initial state to the detonation point, the density of the product gas mixture changes respectively from dilute gas to very dense gas, the compressibility factor,

$Z \left(= \frac{P\bar{V}_g}{R_u T} \right)$, plays a significant role to describe the state of the product gaseous

mixture. According to [63], Z is on the order of 15 for the product gases of condensed phase detonation. When the loading density of the explosives is high, the intermolecular forces (attractive potential or repulsive potential) result in a remarkable increase of the pressure and the temperature. This non-ideal behavior of product gases is largely determined by the interactions between pairs of gas molecules which can be described as an intermolecular potential [64]. Intermolecular potential parameters are generally obtained empirically by choosing them to be consistent with experimental results.

The compressibility factor of the product gaseous mixture can be written as an infinite series expansion in pressure:

$$Z = 1 + \hat{B}(T)P + \hat{C}(T)P^2 + \hat{D}(T)P^3 + \dots \quad (135)$$

where the coefficients $\hat{B}(T)$, $\hat{C}(T)$, $\hat{D}(T)$... are functions of the temperature only. This expansion can also be expressed in terms of density or molar specific volume \bar{V}_g instead of pressure P ,

$$Z = 1 + \frac{B(T)}{\bar{V}_g} + \frac{C(T)}{\bar{V}_g^2} + \frac{D(T)}{\bar{V}_g^3} + \dots \quad (136)$$

Eqn. 136 is known as *Virial expansions*, and the coefficients B, C, D, \dots are called *Virial coefficients*. The word *virial* stems from the Latin word for force. The virial coefficients arise from the intermolecular forces in a real gas mixture. The virial coefficients can be derived by the methods of statistical mechanics, and their physical significance can be attributed to the coefficients: B/\bar{V}_g , accounts for two-molecule interactions, B/\bar{V}_g^2 accounts for three-molecule interactions, etc. Neglecting the higher than the second order terms, the virial EOS becomes,

$$\frac{P\bar{V}_g}{R_u T} = 1 + \frac{B(T)}{\bar{V}_g} + \frac{C(T)}{\bar{V}_g^2} \quad (137)$$

Defining the $x = \frac{B(T)}{\bar{V}_g}$

The Virial EOS can be written as,

$$\frac{P\bar{V}_g}{R_u T} = 1 + x + \beta x^2 \quad (138)$$

or approximately

$$\frac{P\bar{V}_g}{R_u T} = 1 + x e^{\beta x} \quad (139)$$

Using the repulsive potential of the form $U = A/r^n$, where r is the separation distance between the molecules, Jeans [65] showed that,

$$B = \frac{K}{T^\alpha} \quad (140)$$

where $\alpha = 3/n$ and $K \propto A^{3/n}$.

Thus,

$$x = \frac{K}{\bar{V}_g (T + \theta)^\alpha} \quad (141)$$

where the constant θ prevents the pressure going to infinity as the temperature approaches zero. Hence, for a mixture of detonation products in gas phase, the more common form of the Becker-Kistiakowsky-Wilson (BKW) Equation of State is obtained [33, 49, and 50]:

$$\frac{P\bar{V}_g}{RT} = F(x) = 1 + x e^{\beta x} \quad (142)$$

$$x = \kappa \frac{\sum_i x_i k_i}{\bar{V}_g (T + \theta)^\alpha} \quad (143)$$

where x_i and k_i are respectively mole fractions and covolumes of the gaseous products of the detonation and \bar{V}_g is the molar volume of gaseous products in unit cm^3/mole . The covolume represents the repulsive potential of each gaseous product, sum of which describes the non-ideal behavior of the product gas mixture at high density accompanied by high temperature. The geometrical covolume is defined as the volume in A^3 (cubic Angstrom) occupied by a molecule rotating about 10.46 times its center of mass [35]. The geometrical covolume can be calculated from the molecular dimensions. Also the geometrical covolume of a detonation product can be calibrated or reproduced by using the experimental shock Hugoniot. The covolumes of some detonation products are given in Table 31 [35].

β , κ and α are empirical constants of BKW EOS and can be adjusted iteratively by using the experimental data of Hugoniot. In computer program named FORTRAN BKW developed by Mader [51], two sets of BKW constants were used: the “Best RDX Fit” parameter set for most of explosives, and the TNT set for explosives with large amount of solid carbon in detonation products. These set of BKW constants are given in Table 32 [35].

Table 31. Covolumes of some gaseous detonation products

	H ₂ O	H ₂	O ₂	CO ₂	CO	NH ₃	CH ₄	NO	N ₂
k_i	250	180	350	600	390	476	528	386	380

Table 32. Constants in BKW Equation of State

Parameter Set	β	κ	α	θ
Fitting RDX	0.181	14.15	0.54	400
Fitting TNT	0.09585	12.685	0.50	400
Best RDX Fit	0.16	10.91	0.50	400

4.2.2. Equation of State for Solid Products

The detonation products of explosives can include solid products such as graphite. Although most of solid products are generally assumed to be incompressible, the volume occupied by the solid carbon in the detonation products should be corrected because the detonation velocity is a function of the volume occupied by the detonation products. To describe the state of the solid carbon in detonation products, an equation of state named Cowan and Fickett was developed by Cowan and Fickett [50].

The Cowan and Fickett Equation of State is of the form:

$$P = P_1(v_s) + a(v_s)T + b(v_s)T^2 \quad (144)$$

where P in megabars and T in volts (i.e., in units of 11605.6 K) with

$$\eta = \frac{v_s^o(T^o)}{v_s} = \frac{\rho}{\rho_o}$$
 being the compression of the material relative to its normal crystal

density of $\rho_o = 2.25 \text{ g/cm}^3$. The other parameters in Eqn. 144 are:

$$P_1(v_s) = -2.467 + 6.769\eta - 6.956\eta^2 + 6.040\eta^3 - 03869\eta^4 \quad (145)$$

$$a(v_s) = -0.2267 + 0.2712\eta \quad (146)$$

$$b(v_s) = 0.08316 - 0.07804\eta^{-1} + 0.03068\eta^{-2} \quad (147)$$

The range of applicability of this equation of state is $0.95 < \eta < 2.5$ and $0 < T < 2$.

4.3. Determination of the Chapman-Jouguet Point

Determination of the Chapman-Jouguet point in computations of detonation properties of solid explosives is not different than the procedures applied to the computations in gaseous detonation.

The tangency between the Rayleigh line and the Rankine-Hugoniot curve designates the Chapman-Jouguet point on the shock adiabat. Due to this tangency, the slopes of the two relations must be equal at the Chapman-Jouguet point.

$$\left[\frac{dP_2}{d\left(\frac{1}{\rho_2}\right)} \right]_{\text{Rayleigh line}} = \left[\frac{dP_2}{d\left(\frac{1}{\rho_2}\right)} \right]_{\text{Rankine-Hugoniot}} \quad (148)$$

By using the backward difference method in derivations, the equality of the slope can be solved as below,

$$\left| \frac{\left[\frac{P_2(i) - P_1}{v_2(i) - v_1} \right]_{\text{Rayleigh line}} - \left[\frac{P_2(i) - P_2(i-1)}{v_2(i) - v_2(i-1)} \right]_{\text{Rankine-Hugoniot}}}{\left[\frac{P_2(i) - P_2(i-1)}{v_2(i) - v_2(i-1)} \right]_{\text{Rankine-Hugoniot}}} \right| = \varepsilon \quad (149)$$

where the difference of the slopes goes zero ($\varepsilon \rightarrow 0$) denotes the tangent point which is equal to the Chapman-Jouguet point.

At the Chapman-Jouguet detonation point, the detonation velocity, D , reaches its minimum value along the Rankine-Hugoniot curve.

$$D = \left(\frac{1}{\rho_1} \right) \sqrt{\frac{P_2 - P_1}{\frac{1}{\rho_1} - \frac{1}{\rho_2}}} \quad (150)$$

4.4. Numerical Solution of Steady-State Detonation Properties for Solid Explosives

In order to compute detonation properties of several C-H-N-O based condensed phase explosives, the computer code named BARUT-X, written in FORTRAN language, has been developed on the basis of Chapman-Jouguet Theory. The numerical computation method of the BARUT-X is similar to that of GasPX code which can perform the calculation of the detonation properties in energetic gaseous mixtures. BARUT-X uses double precision type of data in the computations.

In accordance with the BKW Equation of State for product gaseous mixture and the Cowan and Fickett Equation of State for solid carbon in products, BARUT-X

computes the Chapman-Jouguet detonation point on the Rankine-Hugoniot curve, and the state properties of the detonation products at that point under the assumption of thermal and chemical equilibrium.

The detonation point properties, which are detonation velocity, detonation temperature, denotation pressure, specific volume of the products, equilibrium composition at the Chapman-Jouguet point, and the heat of detonation are written into an output file named 'out.html' in HTML format.

The major subroutines of the BARUT-X are READ, REACTCALC, PRODCALC, PRODFINALCALC, EQUILIBRIUM, BKW, and COWAN.

The structure of the subroutines, READ, REACTCALC, PRODCALC, PRODFINALCALC, and EQUILIBRIUM is not notably different than those of GasPX

Subroutine READ reads the molecular properties and the thermodynamic coefficients of each gaseous and condensed phase species by using the library of the thermodynamic data which is given as a data file named "thermo.inp" [53, 54].

Subroutine REACTCALC calculates the thermodynamic properties of the reactant explosives at the reference state ($T_{ref} = 298.15$ K and $P_{ref} = 1$ atm). The only thermodynamic property used in computations is the heat of formation at the reactant state.

Subroutine PRODCALC calculates and arranges the chemical potential of the each product species before equilibrium computation.

Subroutine EQUILIBRIUM performs the chemical equilibrium calculations by means of a commercial optimization solver.

Subroutine PRODFINALCALC calculates the thermodynamic properties of the product gaseous mixture after chemical equilibrium computation in conformity with the BKW EOS, and Cowan and Fickett EOS.

Subroutine BKW computes the pressure and temperature for a given density of the products on the Rankine-Hugoniot curve by satisfying simultaneously Rankine-Hugoniot relation and BKW Equation of State for real gases. Subroutine BKW also

calculates the imperfections of the thermodynamic properties coming from the non-ideal behavior of the product gaseous mixture, and the corrected thermodynamic properties are used by the other subroutines.

Subroutine COWAN performs the computation of the density of the solid carbon as well as the imperfections of the thermodynamic properties for solid carbon by satisfying the Cowan and Fickett Equation of State.

4.4.1. Thermodynamic Functions

4.4.1.1. Thermodynamic Functions for Reactants

Because all explosives are assumed to be at the reference state, thermodynamic functions, other than enthalpy of formation, with respect to the reference state, $P_{ref} = 1$ atm and $T_{ref} = 298.15$ K, are zero.

The only thermodynamic function, which is required for unreacted explosive, is enthalpy of formation, $(\Delta \bar{h}_f^o)_i$, at the reference state, $T_{ref} = 298.15$ K.

4.4.1.2. Thermodynamic Functions for Gaseous Products

In computations of BARUT-X, the ideal thermodynamic functions are calculated as in computations of GasPX.

The ideal specific thermodynamic functions which are specific internal energy, specific entropy and specific Gibbs free energy are calculated with the same procedures explained in detail in Section 3.4.1 by using the thermodynamic data library named "thermo.inp" by NASA Glenn Research Center.

Due to the non-ideal behavior of product gases, the thermodynamic function of the each product gas diverges from the ideal thermodynamic properties. In order to define the corrected thermodynamic functions, the BKW EOS must be considered. Any thermodynamic function includes the imperfection and ideal part,

$$\bar{U} = \bar{U}^* + \bar{U}' \quad (151)$$

where \bar{U} denotes the any extensive property such as thermodynamic functions on molar basis, and superscript ' denotes the imperfection part of the thermodynamic function, whereas superscript * denotes the thermodynamic function of denotation products in ideal-gas condition.

$F(x)$ term in Eqn. 142 is the gas imperfection factor. By considering the imperfection of product gas components, the non-ideal parts of the thermodynamic functions [50] are defined as below,

Imperfection of the internal energy

$$\bar{e}'_g = R_u T \left[\frac{\alpha T (F(x) - 1)}{(T + \theta)} \right] \quad (152)$$

Imperfection of the entropy:

$$\bar{s}'_g = R_u \left[\ln(F(x)) - \frac{e^{\beta \cdot x} - 1}{\beta} + \frac{\alpha T (F(x) - 1)}{T + \theta} \right] \quad (153)$$

Imperfection of the Gibbs function:

$$\mu'_i = -R_u T \left[\ln(F(x)) - \frac{e^{\beta \cdot x} - 1}{\beta} - k_i \frac{(F(x) - 1)}{\sum_g x_i k_i} \right] \quad (154)$$

and

$$\bar{e}_i^*(T) = (\bar{e}(T) - \bar{e}(298))_i \text{ with unit (kJ/K.kmol)}. \quad (155)$$

$$\mu_i^* = \bar{g}_i + R_u T \ln \frac{x_i P}{P_{ref}} \text{ with unit (kJ/kmol)}. \quad (156)$$

The determination of the thermodynamic functions in ideal-gas state has already been presented in Section 3.4.1.

4.4.1.3. Thermodynamic Functions for Solid Products

Because the specific volume or density of the solid carbon formed as graphite in detonation products is corrected by means of the Cowan and Fickett Equation of State, its thermodynamic functions shall be corrected by defining the imperfection terms on the basis of Cowan-Fickett Equation of State.

The specific internal energy, which is consistent with reference [50], is

$$\bar{e}_s(T) = \bar{h}(T) - (\Delta\bar{h}_f^o)_s + \left[-P_{ref} v_s^o + \int_{v_s^o}^{v_s} [b(v)T^2 - P_1(v)] dv \right] MW_s \quad (157)$$

where $b(v)$ and $P_1(v)$ are defined respectively by Eqns. 147 and 145. and $\bar{h}(T) = [\bar{h}(T) - \bar{h}(298.15)] + \Delta\bar{h}_f^o$ with unit, (kJ/K.kmol)

$v_s^o = \frac{1}{\rho_o}$, and ρ_o - the normal crystal density of carbon is equal to 2.25 g/cm³

Imperfection of the chemical potential:

$$\mu'_s = \left[P v_s - P_{ref} v_s^o - \int_{v_s^o}^{v_s} [P_1(v) + a(v)T + b(v)T^2] dv \right] MW_s \quad (158)$$

where $a(v)$ is defined by Eqn. 146 and MW_s is the molar mass of the solid carbon.

The ideal part of the chemical potential of solid carbon has been discussed as solid or condensed phase component in Section 3.4.1,

$$\mu_s^* = \bar{g}_s \text{ with unit, (kJ/kmol)}. \quad (159)$$

4.4.2. Thermodynamic Properties at State of the Detonation Products

For gas phase;

$$n_g = \sum_g n_i \quad (160)$$

where n_i is the mole number of the each species at gas phase, n_g is the total mole number of the gaseous species, and n_s is the mole number of the solid carbon.

Total mole number, n , at the state,

$$n = n_g + n_s \quad (161)$$

Each mole fraction of the gaseous species is,

$$x_i = \frac{n_i}{n_g} \quad (162)$$

The mole fraction of the gaseous mixture is,

$$x_g = \frac{n_g}{n} \quad (163)$$

The mole fraction of the carbon is,

$$x_s = \frac{n_s}{n} \quad (164)$$

Molar weight of the gaseous mixture,

$$MW_g = \frac{\sum n_i MW_i}{n_g} \quad (165)$$

where MW_i (kg/kmol) is the molecular weight of the each gas species in detonation products, and MW_s (kg/kmol) is the molecular weight of the graphite (solid carbon).

Molar weight of the mixture (kg/kmol) at the state,

$$MW = \frac{n_g MW_g + n_s MW_s}{n_g + n_s} \quad (166)$$

Subscript g denotes the gaseous phase and subscript s denotes the solid carbon.

Any extensive property, U , per unit mass (per kg):

$$U = \frac{\sum n_i \bar{U}_i + n_s \bar{U}_s}{n_g MW_g + n_s MW_s} \quad (167)$$

where, \bar{U} , is any extensive properties on molar basis.

Internal energy, heat of formation, and similar extensive properties are computed per unit mass in BARUT-X.

The thermodynamic properties of the products are separated into the ideal and imperfection parts.

For gaseous products, specific internal energy is,

$$\bar{e}_i(T) = \sum_g x_i \bar{e}_i^*(T) + \bar{e}' \quad (168)$$

If Eqn. 168 is expanded, the specific internal energy can be rewritten as

$$\bar{e}_i(T) = \left[\sum_g x_i (\bar{e}(T) - \bar{e}(298.15))_i \right] + R_u T \left[\frac{\alpha T (F(x) - 1)}{(T + \theta)} \right] \quad (169)$$

The thermodynamic properties of the solid carbon are also calculated by considering the imperfection and ideal parts.

Specific internal energy of the solid carbon has been defined previously in Eqn. 157:

$$\bar{e}_s(T) = \bar{h}(T) - \Delta \bar{h}_f^o + \left[-P_{ref} v_s^o + \int_{v_s^o}^{v_s} [b(v)T^2 - P_1(v)] dv \right] MW_s \quad (157)$$

Specific internal energy of the state of the detonation products, e_2 (kJ/kg),

$$e_2 = \frac{\sum_g n_i \bar{e}_i + n_s \bar{e}_s}{n_g MW_g + n_s MW_s} \quad (170)$$

Heat of formation of the state, Δh_f^o (kJ/kg)

$$\Delta h_f^o = \frac{\sum_g n_i (\Delta \bar{h}_f^o)_i + n_s (\Delta \bar{h}_f^o)_s}{n_g MW_g + n_s MW_s} \quad (171)$$

4.4.3. Chemical Equilibrium

BARUT-X computes the chemical-equilibrium composition on the basis of minimization of Gibbs free energy by using a commercial optimization solver which can be run coupled with FORTRAN subroutines. Indeed, the computation principle is exactly the same as that applied in GasPX code.

The minimum value of the Gibbs function is the objective function of the non-linear optimization method ($G \rightarrow \min$).

Gibbs function can be written in terms of chemical potential on molar base,

$$G = \sum_g n_i \mu_i + n_s \mu_s \quad (172)$$

The chemical potential of the gas products can be written in terms of ideal and imperfection parts.

$$\mu_i = \bar{g}_i + R_u T \ln \frac{x_i P}{P_{ref}} - R_u T \left[\ln(F(x)) - \frac{e^{\beta x} - 1}{\beta} - k_i \frac{(F(x) - 1)}{\sum_g x_i k_i} \right] \quad (173)$$

The chemical potential for the solid carbon,

$$\mu_s = \bar{g}_s + \left[P v_s - P_{ref} v_s^o - \int_{v_s^o}^{v_s} [P_1(v) + a(v)T + b(v)T^2] dv \right] MW_s \quad (174)$$

Hence the objective function yields,

$$\sum_g n_i \mu_i + n_s \mu_s \rightarrow \text{MIN} \quad (175)$$

While the objective function, which is the Gibbs free energy of the state, goes to minimum value, the conservation of mass must be satisfied. The total mass of the reactants must be constant after the detonation reaction: The whole computations method has been profoundly discussed in Section 3.4.3.

4.4.4. Algorithm of BARUT-X

The numerical computation model of the BARUT-X depends on the iteration technique similar to that of GasPX except ideal-gas assumption. The computations start with the initial assumptions of the Chapman-Jouguet detonation point. The state properties are then corrected in an iterative manner. The iteration performed for the determination of the pressure is run under the iteration performed for the computation of the temperature. Also, the calculations of the BKW and the Cowan-Fickett Equation of States are iteratively performed.

BARUT-X can compute detonation properties of only C-H-N-O based explosives. Therefore, the different atom numbers in computation is four.

By BARUT-X, the calculation of the detonation parameters is performed as follows:

1. In order to perform the computation, some initial assumptions of the C-J state are needed (Table 33).

Table 33. Initial conditions for computation of BARUT-X

Initial Condition	Value
C-J temperature, T_2	1500 K
C-J pressure, P_2	1 bar
Specific volume of the detonation products, v_2	$4.5 \times 10^4 \text{ m}^3/\text{kg}$
Molecular weight of the gaseous product mixture, MW_g	25 kg/kmol

There are not any initial assumptions for solid carbon in this step. After the first equilibrium computation, the solid carbon formation is included into the computations in the nature of the numerical model.

2. The input file, named REACTIN.FOR, which designates the reactant condition in FORTRAN format, is read.

The reactant may be individual explosive, mixture of several explosives, and mixture of explosives and inert compounds. The reactant is assumed to be at the reference state. The input file includes the temperature of the explosive(s), T_1 , pressure of the explosive(s), P_1 , number of explosive(s), descriptive name of the each compound of the explosive(s), mass percentage of the each compound of the explosive(s), and the density of the explosive(s).

REACTIN.FOR file can be composed by users in free FORTRAN format, Table 34.

Table 34. Free FORTRAN format of "REACTIN.FOR"

Line	Content	Columns
1	Temperature of the explosive(s) in Kelvin, reference state temperature, $T_1 = 298.15$ K	1
	Pressure of the explosive(s) in bar, reference state pressure, $P_1 = 1.01325$ bar	2
2	Number of compound of the explosive(s), limited up to 20	1
3 – [a]	Mass percentage of the each compound of the explosive(s)	1
	Descriptive name of the each compound of the explosive(s)	2
[b]	Density of the explosive(s) (mixture) in kg/m^3	1

a. Line number in which the last compound of the explosive(s) is written

b. Line number starts after a, $b = a + 1$

For example, % 90 HMX and %10 WAX mixture on mass base with the density of 1767 kg/m^3 is entered in "REACTIN.FOR" as below

```

300.0 1.01325 ! TEMPERATURE (K) AND PRESSURE (bar)
2
90 HMX ! MASS PERCENTAGE AND NAME OF EXPLOSIVE(S)
10 WAX
1767      !KG/M3 DENSITY OF EXPLOSIVE(S)
    
```

3. After reading the explosives, the heat of formation and the total number of C, H, N and O atoms in the explosive(s) are calculated by using the explosive data library named "EXPLOSIVE.FOR" in free FORTRAN format. The explosive data library file contains the properties of explosive in each row as given in Table 35.

Table 35. Format of a row in the explosive data library, "EXPLOSIVE.FOR"

Column 1	Representative Name of the explosives (for example, HMX, RDX...)
Column 2	Molecular Mass of the explosives in kg/kmol
Column 3	Heat of formation of explosive, $(\Delta \bar{h}_f^o)$, at 298.15 K in kJ/kg
Column 4	Number of carbon, C, in chemical formula
Column 5	Number of hydrogen, H, in chemical formula
Column 6	Number of nitrogen, N, in chemical formula
Column 7	Number of oxygen, O, in chemical formula
Column 8	Full name or explanation of explosive (for example, Octogen, Hexogen)

The mole numbers of the compounds corresponding to the mass percentages of those are calculated,

$$nr_i = \frac{MP_i}{MWR_i} \quad (176)$$

where nr_i , MP_i and MWR_i are the mole number, the mass percent and the molecular weight of the compound, respectively.

Heat of formation per unit mass (kJ/kg):

$$\Delta h_{f1}^o = \frac{\sum_i [MP_i (\Delta \bar{h}_f^o)_i]}{\sum_i MP_i} \quad (177)$$

Specific internal energy per unit mass (kJ/kg):

$$e_1 = e_1(T_1) - e_1(298.15) \quad (178)$$

Since $T_1 = 298.15$ K, then $e_1 = 0$ (kJ/kg)

4. The input file, named PRODUCTIN.FOR, which the product components are designated within, is read. The product components, which may be formed after detonation reaction, are composed within the PRODUCTIN.FOR in the free FORTRAN format (Table 36). This input file contains the number of the components limited up to 20 species, the descriptive names (commonly

chemical formula) of the components, and the covolume of the gaseous components. The covolume value for the solid carbon is zero.

Table 36. Free FORTRAN format of "PRODUCTIN.FOR"

Line	Content	Columns
1	Number of reactant components limited up to 20	1
2-[a]	Covolume of products	1
	Chemical formula of products	2

a. Final line number depends on the number of components and can not exceed the 21

Example of PRODUCTIN.FOR :

```

10      ! NUMBER OF CHEMICAL COMPONENTS
250    H2O
180    H2
350    O2
600    CO2
390    CO
476    NH3
528    CH4
386    NO
380    N2
0      C(gr)

```

5. After reading the product components, in order to perform the chemical equilibrium calculation, the chemical potential of the each component is calculated. But these chemical potentials must be corrected to real gases and the compressibility of the solid carbon by taking the imperfections into account.

With the corrected chemical potentials, μ , and by means of a commercial optimization solver running coupled with FORTRAN, the equilibrium computation is performed at P_2 and T_2 .

P_2 and T_2 are changed by iteration manner until reaching the C-J detonation point.

The detailed computation method of the chemical-equilibrium is explained in Section 4.4.3.

The commercial optimization solver computes the equilibrium composition by satisfying the minimum value of Gibbs free energy of product composition with the constraint of mass conservation for assumed detonation pressure P_2 , and temperature, T_2 .

$$\sum_g y_i \left[\frac{\mu_i}{R_u T_2} \right] + y_s \left[\frac{\mu_s}{R_u T_2} \right] \rightarrow \text{MIN} \quad (179)$$

where y_i is the mole number of the gaseous product component i and y_s is the mole number of the solid carbon, which will be determined after equilibrium calculation.

6. After determination of the equilibrium composition, the thermodynamic properties of the product mixture are calculated for T_2 and P_2 by using thermodynamic data library, "thermo.inp" file. The specific internal energy per unit mass, enthalpy of formation per unit mass, mean specific heat at constant volume per unit mass are calculated by BARUT-X.

The internal energies, \bar{e}_i , of gaseous species i is corrected to that in real gas condition in accordance with BKW Equation of State.

Also the internal energy, \bar{e}_s , of the solid carbon is corrected according to the Cowan and Fickett Equation of State.

After the specific internal energies on molar base are corrected, the specific internal energy of the mixture per unit mass can be computed.

Specific internal energy per unit mass (kJ/kg):

$$e_2 = \frac{\sum_g y_i \bar{e}_i + y_s \bar{e}_s}{y_g MW_g + y_s MW_s} \quad (180)$$

where y_i is the mole number of the gaseous component and y_s is the mole number of solid carbon.

The constant-volume mean specific heat per unit mass (kJ/kg):

$$C_{v2} = \frac{e_2(T_2) - e_2(298.15)}{T_2 - 298.15} \quad (181)$$

Heat of formation of the state, Δh_f^o (kJ/kg)

$$\Delta h_{f2}^o = \frac{\sum_i y_i (\Delta \bar{h}_f^o)_i + y_s (\Delta \bar{h}_f^o)_s}{y_g MW_g + y_s MW_s} \quad (182)$$

Gas constant of the reactant mixture:

$$R_2 = \frac{R_u \sum_i y_i}{\sum_g (y_i MW_i)} \quad (183)$$

At this step, the heat of reaction, q_R , is calculated per unit mass as well:

$$q_R = \Delta h_{f1}^o - \Delta h_{f2}^o \quad (\text{kJ/kg})$$

7. After determination of the equilibrium composition and thermodynamic properties of the equilibrium mixture, parameters of the state (pressure and temperature) are calculated along the Rankine-Hugoniot curve by increasing the density starting from initial density (density of the unreacted gaseous mixture) to the final density (density of the detonation product mixture) with a certain increment of the density. The determination procedure used in BARUT-X is basically the same as that used in GasPX. Figure 23 adequately depicts the computation procedure along the Rankine-Hugoniot curve (Shock adiabat of the detonation products)

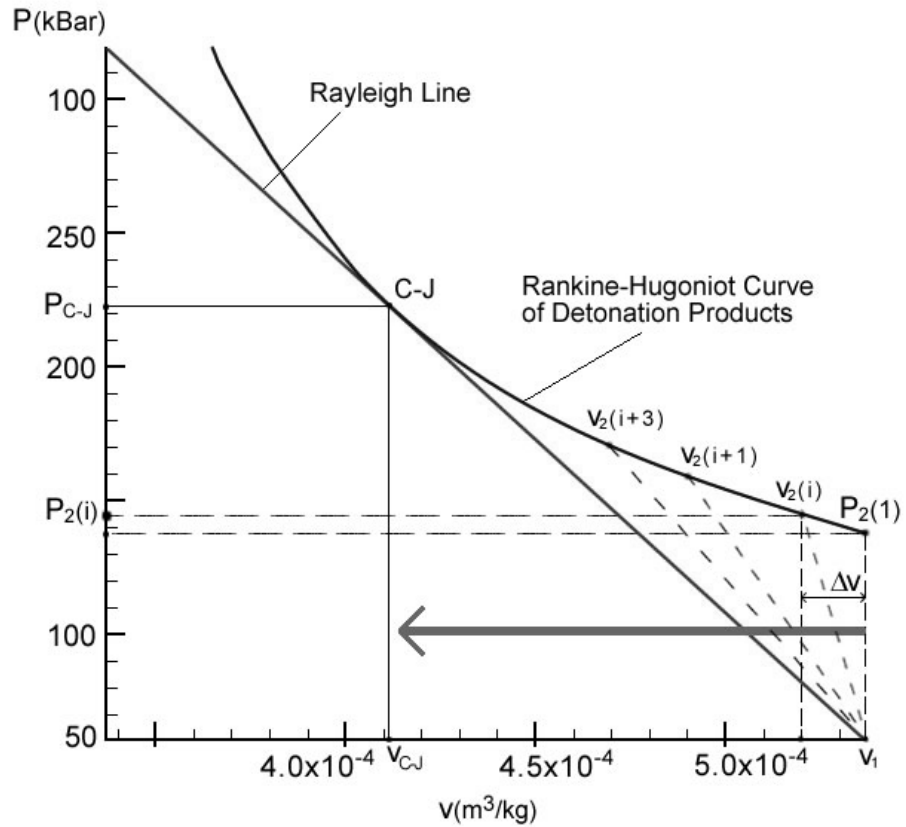


Figure 23. Determination of the Chapman-Jouguet Point on the Rankine-Hugoniot curve by BARUT-X

Calculation of the specific volume for certain increment of density:

$$\rho_2(i) = \rho_1 + i \Delta\rho$$

$$v_2(i) = \frac{1}{\rho_2(i)}$$

and

$$\Delta\rho = 0.1 \text{ (kg/m}^3\text{) for BARUT-X}$$

8. The Chapman-Jouguet point is calculated by solving the Rankine-Hugoniot equation and BKW equations simultaneously. An initial pressure is needed for this calculation, which is assumed to be $P_x = 1 \times 10^5 \text{ Pa}$
9. The temperature of the detonation products for iterated specific volume is computed by using Rankine-Hugoniot Relation.

$$T_2(i) = \frac{q_R + \frac{1}{2}(P_x + P_1)(v_1 - v_2(i)) + C_{V1}(T_1 - T_{ref})}{C_{V2}} + T_{ref} \quad (184)$$

where heat of reaction is in kJ/kg, the pressures are in kPa, the specific heats are in kJ/kg·K and, the temperatures are in K

10. After determination of the temperature, the pressure which corresponds to iterated specific volume on the Rankine-Hugoniot curve is calculated by means of the BKW Equation. Because the BKW Equation of State is applied to just gas phase components and the specific volume of the products includes the specific volumes of both gas and condensed phase components, the specific volume of the gaseous products is calculated as follows.

Due to the compression of the solid carbon, its density can not be reckoned as standard crystal density, 2.25 g/cm³. This crystal density is corrected to real density at given temperature, T_2 and pressure, P_2 by using the Cowan and Fickett Equation of State, Eqn. 144. After determination of the compressed solid carbon density, ρ_s , or the specific volume, v_s , the specific volume of the gaseous products mixture can be calculated as follows,

$$v_g = \frac{v_2(i) \left[\sum_g y_i MW_i + y_s MW_s \right] - v_s y_s MW_s}{\sum_g y_i MW_i} \quad (185)$$

If there is no formation of the solid carbon, the specific volume of the gaseous product becomes,

$$v_g = v_2(i)$$

The gas constant and the temperature of the product mixture were calculated previously (in the step 6 and step 9 respectively).

By solving BKW Equation of State, $\frac{P v_g}{RT} = F(x) = 1 + x e^{\beta x}$,

$$\text{where } x = \kappa \cdot \frac{\sum_i y_i k_i}{(v_g MW_g 1000)(T + \theta)^\alpha}$$

and the pressure is determined from,

$$P_g = \frac{R_2 T_2 F(x)}{V_g} \quad (186)$$

If $|P_g - P_x| \rightarrow 0$ then $P_2(i) = P_g$ and pass through the next step (Step 11).

Else, New $P_x = P_g$ and with this new P_x go to step 9, and repeat all process up to current step.

- 11.** Because the Rayleigh line is tangent to the Rankine-Hugoniot curve at the Chapman-Jouguet point, the difference of their slopes goes to zero. The determination method (Eqn. 149) was explained in Section 4.3 in detail.

If ε goes to zero then define $P_{C-J} = P_2(i)$, $T_{C-J} = T_2(i)$, $v_{C-J} = v_2(i)$, and proceed to the next step (step 12). Else go to step 7 and repeat all steps up to current step by new specific volume defined in step 7.

- 12.** The pressure, P_2 , at which the state of the product composition calculated, is compared with the pressure, P_{C-J} calculated by the determination methods of the Chapman-Jouguet point in step 11. If ε_p goes to zero

where $\varepsilon_p = \left| \frac{P_2 - P_{C-J}}{P_{C-J}} \right|$ then pass through the next step (step 13). Else,

define $P_2 = P_{C-J}$ and go to step 5 and repeat all steps up to current step by new P_2 .

- 13.** The temperature, T_2 , at which the state and the thermodynamic properties of the product composition are calculated, is compared with the temperature, T_{C-J} calculated by Rankine-Hugoniot equation in step 9 and also satisfies the Chapman-Jouguet point in step 11. If ε_T goes to zero

where $\varepsilon_T = \left| \frac{T_2 - T_{C-J}}{T_{C-J}} \right|$ then pass through the next step (step 14). Else,

$T_2 = T_2 + \Delta T$ and go to step 5 and repeat all steps up to current step with new T_2 .

- 14.** The temperature and the pressure, at which all state properties of the detonation composition are calculated, satisfy the Rankine-Hugoniot curve and BKW Equation of State as well as the Rayleigh line. In other words, the Chapman-Jouguet point is determined. Also the properties of the Chapman-Jouguet point can be calculated.

Chapman-Jouguet temperature is T_{C-J} (K),

Chapman-Jouguet pressure is P_{C-J} (Pa),

Specific volume of the product mixture at C-J point is v_{C-J} (m^3/kg),

Density of the product mixture at C-J point is ρ_{C-J} (kg/m^3),

Specific volume of the gaseous detonation product is v_g (m^3/kg),

Specific volume of the solid carbon is v_s (m^3/kg),

Also the composition of the detonation product and the heat of reaction, q_R , at C-J point were already determined.

The detonation velocity, D , can be calculated by Eqn. 79.

Therefore, the computations of the detonation point and detonation properties of condensed explosive(s) are completed.

Flow chart of BARUT-X is given in Figure 24 in accordance with the previously explained algorithm.

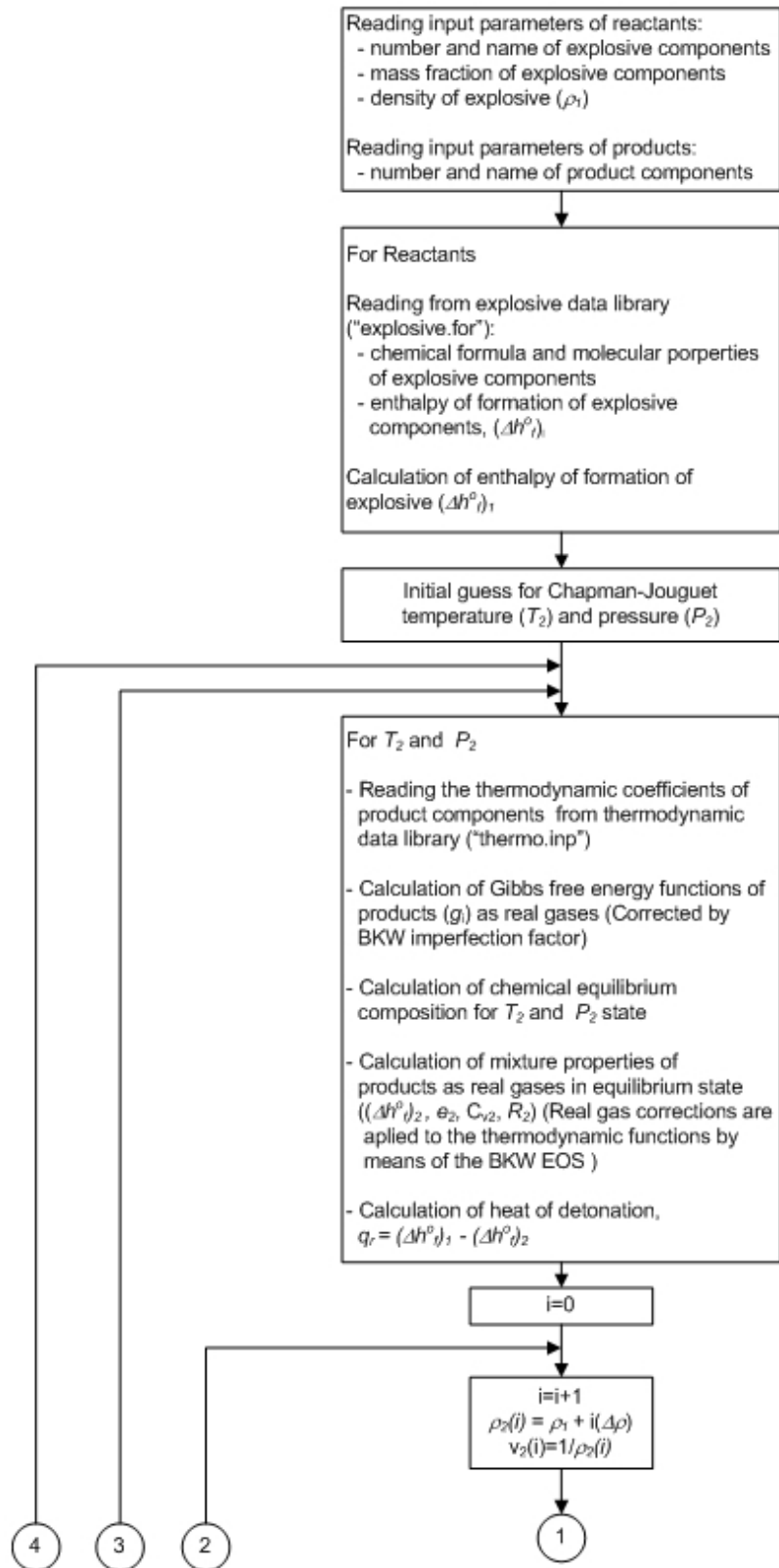


Figure 24. Flow chart of BARUT-X, continued to next page

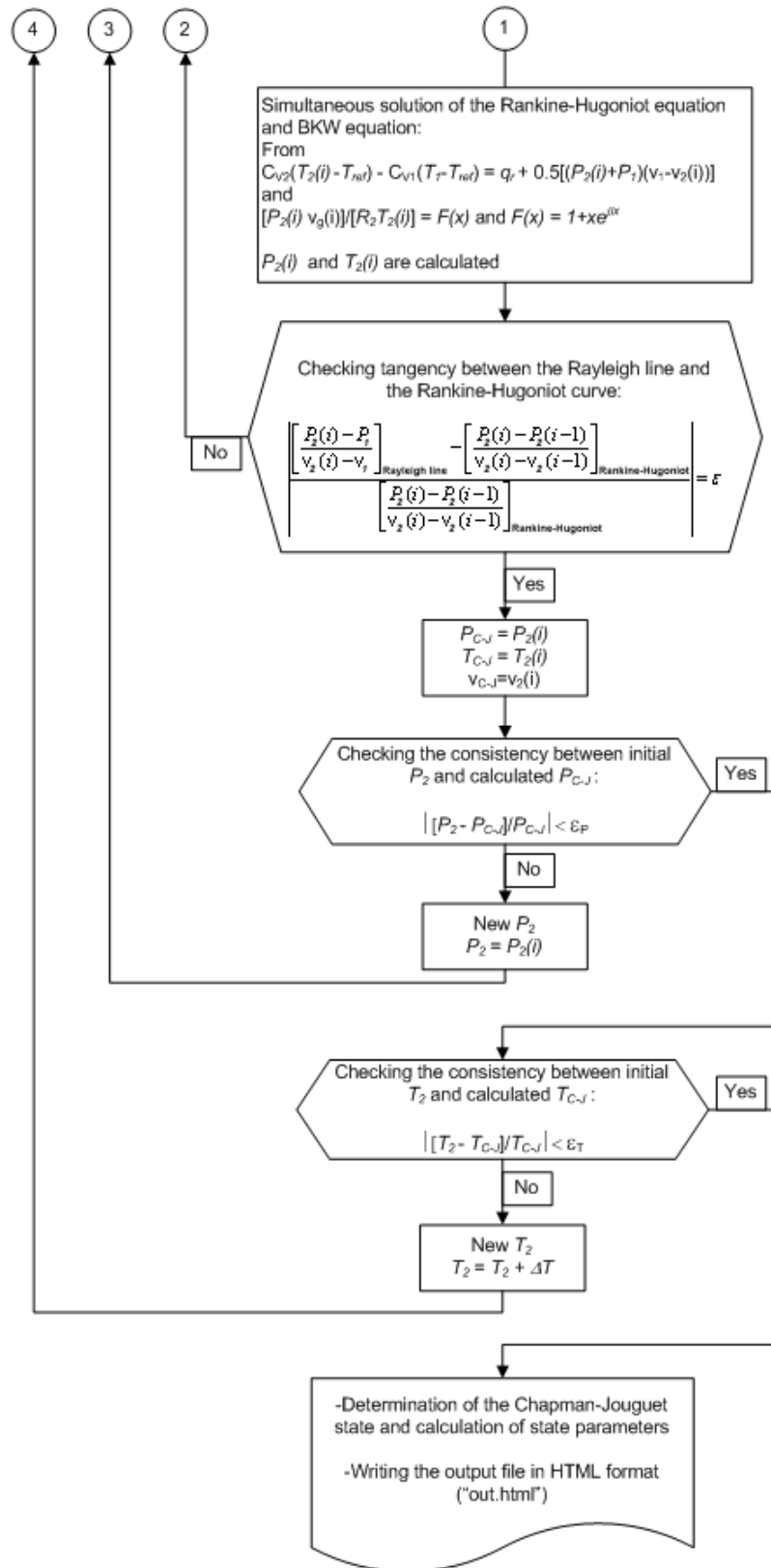


Figure 24. Flow chart of BARUT-X (Concluded)

4.4.5. Sensitivity Analysis for BARUT-X

Similar sensitivity analysis made for GasPX should be performed for BARUT-X since the structure of the numerical model of both codes is similar.

The optimum convergence factors for BARUT-X are determined according to the experimental case of RDX [35] whose details are given in Table 37.

Table 37. Experimental detonation parameters of RDX [35]

Component	RDX
Loading density, kg/m ³	1800
Detonation pressure, Pa	34700000000
Detonation velocity, m/sec	8754

In order to determine the optimum pressure convergence factor, ε_p (Step 12 in Section 4.4.4), the detonation pressures are compared according to different values of ε_p . The convergence factors other than ε_p and the initial values are given in Table 38. The computed detonation pressures are given in Table 39 with computed detonation velocities. Since the computed detonation pressures are primarily affected by the ε_p and there is no distinctive difference between the computed detonation velocities, the comparison is performed according to the computed detonation pressures. In fourth column of Table 39, each computed detonation pressure for current convergence factor is compared with the pressure computed for previous convergence factor. Also, in order to observe the deviations between the computed pressures better, they are given in unit of Pascal (Pa).

Table 38. Constant parameters used in the computations performed for the sensitivity analysis of the pressure convergence factor (ε_P)

Initial pressure, bar	1
Temperature convergence factor, ε_T	1×10^{-4}
Initial temperature, K	1500
Tangency convergence factor, ε	1×10^{-4}

Table 39. Comparison of the computed Chapman-Jouguet detonation parameters by BARUT-X for the sensitivity analysis of the pressure convergence factor

ε_P	Calculated detonation pressure, Pa	Calculated detonation velocity, m/sec	Deviation of pressure*, %
1×10^{-10}	32976817285.20	8737.13	-
1×10^{-9}	32976817284.69	8737.13	1.55×10^{-9}
1×10^{-8}	32976817284.05	8737.13	1.94×10^{-9}
1×10^{-7}	32976817285.96	8737.13	5.79×10^{-9}
1×10^{-6}	32976817344.26	8737.13	1.77×10^{-7}
1×10^{-5}	32976817780.32	8737.13	1.32×10^{-6}

* - Absolute value of deviation between computed pressure and computed one for previous pressure convergence factor.

As seen in Table 39, there is no drastic change in computed pressures. Lower values of ε_P may result in divergence since the iteration loop may not satisfy the pressure convergence factor for the different cases. And the higher values of ε_P may cause the precision of the results poorly. Therefore, the optimum value of ε_P is determined as 1×10^{-8} .

The effect of initial guess for the detonation pressure values (Step 1 in Section 4.4.4) on the computations is also analyzed. A wide range of initial pressures are traced. And the results are given in Table 40. Third column contains the absolute value of deviation between currently computed pressure and computed pressure for

previous initial pressure. Initial pressures are given in unit of 'bar' and the computed detonation pressures are given in unit of Pascal.

Table 40. Effect of initial pressure values on computations

Initial pressure, bar	Calculated detonation pressure, Pa	Deviation of pressure*, %
0.01	32976817283.39	-
0.1	32976817284.79	4.24×10^{-9}
1	32976817284.05	2.24×10^{-9}
10	32976817284.30	7.58×10^{-10}
100	32976817284.65	1.06×10^{-9}
1000	32976817284.48	5.15×10^{-10}

* - Absolute value of deviation between computed pressure and computed one for previous initial pressure.

Considering the results in Table 40, it can be deduced that BARUT-X is insensitive to initial pressure. The initial value of pressure is determined as 1 bar in computations of BARUT-X code.

Similar sensitivity analysis is performed for temperature. The optimum temperature convergence factors, ε_T , (Step 13 in Section 4.4.4) should be determined. As it is made in the determination of the optimum pressure convergence factor, the parameters, given in Table 41, other than the temperature convergence factors are kept constant.

Table 41. Constant parameters used in the computations performed for the sensitivity analysis of the temperature convergence factor (ε_T)

Initial pressure, bar	1
Pressure convergence factor, ε_P	1×10^{-8}
Initial temperature, K	1500
Tangency convergence factor, ε	1×10^{-4}

For different ε_T values, the detonation temperature and detonation velocities are computed for the comparison. The results are given in Table 42. Since the calculated temperatures are primarily affected by ε_T , the comparison is performed according to them. Fourth column of Table 42 contains the absolute value of deviation of the computed temperature for current ε_T from the computed temperature for previous ε_T .

Table 42. Comparison of the computed Chapman-Jouguet detonation parameters by BARUT-X for the sensitivity analysis of the temperature convergence factor

ε_T	Calculated detonation temperature, K	Calculated detonation velocity, m/sec	Deviation of temperature*, %
1×10^{-5}	2500.6	8737.13	-
1×10^{-4}	2500.6	8737.13	0.0
1×10^{-3}	2500.6	8737.13	0.0
1×10^{-2}	2510.4	8738.01	0.39
1×10^{-1}	2557.3	8741.30	1.87

* - Absolute value of deviation between computed temperature and computed one for previous temperature convergence factor.

Considering the comparisons in Table 42, temperature convergence factor is determined as 1×10^{-4} for BARUT-X code. For 2500.6 K, the difference of temperature becomes: $|T_2 - T_{C-J}| = (1 \times 10^{-4}) \times (2500.6 \text{ K}) = 0.25006 \text{ K}$. And this

relatively small difference can be easily considered adequately enough for temperature to reach the accurate results.

The effect of initial temperatures on computations is compared in Table 43. The computed detonation temperatures for different initial temperatures are given in the table. Third column contains the absolute value of deviation between currently computed temperature and previously computed temperature.

Table 43. Effect of initial temperature values on computations

Initial temperature, K	Calculated detonation temperature, K	Deviation of temperature*, %
500	2501.3	
1000	2500.6	0.028
1500	2500.6	0.0
2000	2500.6	0.0
3000	2499.3	0.052
4000	2500.6	0.052

* - Absolute value of deviation between computed temperature and computed one for previous initial temperature.

Considering the results in Table 43, it can be deduced that BARUT-X is insensitive to initial temperature. The initial value of temperature is determined as 1500 K in the computations of BARUT-X code.

Last, the optimum tangency convergence factor, ε , (Step 11 in Section 4.4.4), should be determined. Since the basic performance parameter is the detonation velocity and the tangent point gives the Chapman-Jouguet detonation state, the optimum convergence factor is determined according to computed detonation velocities for different convergence factors. In order to obtain relevant results, the parameters other than the convergence factor of the tangency should be kept constant (Table 44).

Table 44. Constant parameters used in the computations performed for the sensitivity analysis of the tangency convergence factor (ε)

Initial pressure, bar	1
Pressure convergence factor, ε_P	1×10^{-8}
Initial temperature, K	1500
Temperature convergence factor, ε_T	1×10^{-4}

The computed detonation velocities and comparisons for different ε values are given in Table 45. Third column contains the absolute value of deviation between currently computed detonation velocity and previously computed detonation velocity.

Table 45. Comparison of the computed Chapman-Jouguet detonation velocities by BARUT-X for the sensitivity analysis of tangency convergence factor

ε	Calculated detonation velocity, m/sec	Deviation of detonation velocity*, %
1×10^{-6}	8737.01	-
1×10^{-5}	8736.99	2.52×10^{-4}
1×10^{-4}	8737.13	15.57×10^{-4}
1×10^{-3}	8737.91	89.95×10^{-4}
1×10^{-2}	8738.91	114.20×10^{-4}

* - Absolute value of deviation between computed velocity and computed one for previous convergence factor.

Above 1×10^{-4} of ε , the deviation shows a relatively great increase but also it is in reasonably acceptable limits. Considering the results given in Table 45 and the computation time, the optimum ε value is determined as 1×10^{-4} . This value of ε can provide the adequately precise detonation parameters.

Therefore, according to all sensitivity analysis, the parameters used in BARUT-X are given in Table 46.

Table 46. Parameters used in the computations performed by BARUT-X

Initial pressure, bar	1
ε_P	1×10^{-8}
Initial temperature, K	1500
ε_T	1×10^{-4}
ε	1×10^{-4}

4.5. Comparison of the Results

The detonation velocity of solid explosives is the basic performance parameter and its measurement is easier than the measurement of other detonation performance parameters. High quality electrical switch or pin measurements have been possible to measure the detonation velocity since the late 1940s at the Los Alamos National Laboratory [31]. In this method, the switches are placed within explosive at discrete points along the stick (cylinder shaped explosive) length. The times at which the detonation front reaches these points are determined by using the high conductivity or pressure at the detonation front to close the electrical switch or pin. The detonation velocity can be calculated from the measured distances and times.

The most commonly used values for detonation pressure (C-J pressure) are from experiments in which the pressure has been inferred from its measured effects in other materials [31]. The C-J pressure is usually obtained by measuring the shock or free-surface velocity of inerts of varying thickness and density in contact with the detonating explosive. The flash gap technique first used by Deal [26] has been carried out for determining the initial free surface velocity of the inert material. And the C-J pressure has been obtained from the free surface velocity and the geometry of the explosive.

The C-J state temperature is the least information of the C-J state. The temperatures are measured experimentally from the brightness of the detonation front as it proceeds toward a detector [35].

Several high explosives, for which experimental data for detonation parameters have been reported in the literature [35, 66, 67, 68], were chosen to test the BARUT-X code. The detonation parameters are calculated for these explosives applying different sets of the constants: RDX, TNT, and BKWR set. The set of constants are given in Table 47.

Table 47. Values of constants in BKW Equation of State

BKW Parameters	β	κ	α	θ
RDX [35]	0.160	10.910	0.50	400
TNT [35]	0.09585	12.685	0.50	400
BKWR [66]	0.176	11.80	0.50	1850

The results calculated by BARUT-X are given for different loading densities of explosives in Tables 48 - 51 with the results calculated by EXPLO5 and the experimental data for explosives, HMX, TNT, RDX, and PETN, respectively. Also the comparisons between BARUT-X, EXPLO5 and experiments are given in these tables. The properties of the explosives are given in Appendix A. Unless otherwise specified, the results calculated by EXPLO5 and experimental data are according to M. Sućeska [66] in Tables 48 - 51. In these tables, second column contains the different loading densities of the explosives, third column contains the determination method of the detonation parameters, fourth column contains the experimentally obtained and calculated detonation velocities in different densities of explosives, and fifth column contains the experimentally obtained and calculated detonation pressures in different densities of explosives. "Deviation 1" denotes the percentage of difference between results calculated by BARUT-X and data obtained experimentally. And "Deviation 2" denotes the percentage of difference between results calculated by BARUT-X and those by EXPLO5. The detonation performance parameters correspond to the Chapman-Jouguet state properties. For some

explosives and some detonation parameters, different BKW parameters can be used in computations of both EXPLO5 and BARUT-X. The type of BKW parameters used in computations is indicated below the tables.

The extended analysis of the results given in the Tables 48 - 51 are also shown in plots for each explosive. The detonation velocities calculated by BARUT-X and EXPLO5 are compared with the experimentally obtained data in Figure 25, Figure 27, Figure 29, and Figure 31 for HMX, TNT, RDX, and PETN, respectively. The calculated and experimental detonation pressures are compared in Figure 26, Figure 28, Figure 30, and Figure 32 complying with the tables as well.

Table 48. Comparison of calculated and experimental values of detonation parameters for different densities of HMX

Explosives	Density g/cm ³	Method	Detonation Velocity (m/sec)	Detonation Pressure (GPa)
HMX	1.89	Experimental [66]	9110	39.0
		EXPLO5 [66]*	9110	38.9
		BARUT-X**	9106	37.0
		Deviation 1, %	-0.04	-5.13
		Deviation 2, %	-0.04	-4.88
	1.6	Experimental [66]	7910	28.0
		EXPLO5 [66]*	7980	26.3
		BARUT-X**	7965	25.3
		Deviation 1, %	0.70	-9.64
		Deviation 2, %	-0.19	-3.80
	1.2	Experimental [66]	6580	16.0
		EXPLO5 [66]*	6640	14.8
		BARUT-X**	6653	13.8
		Deviation 1, %	1.11	-13.75
		Deviation 2, %	0.20	-10.14

* - RDX-type of parameters in BKW Equation is used by EXPLO5 [66].

** - RDX-type of parameters in BKW Equation is used by BARUT-X.

Deviation 1 – The percent of difference between data by BARUT-X and experimental data.

Deviation 2 – The percent of difference between data by BARUT-X and data by EXPLO5.

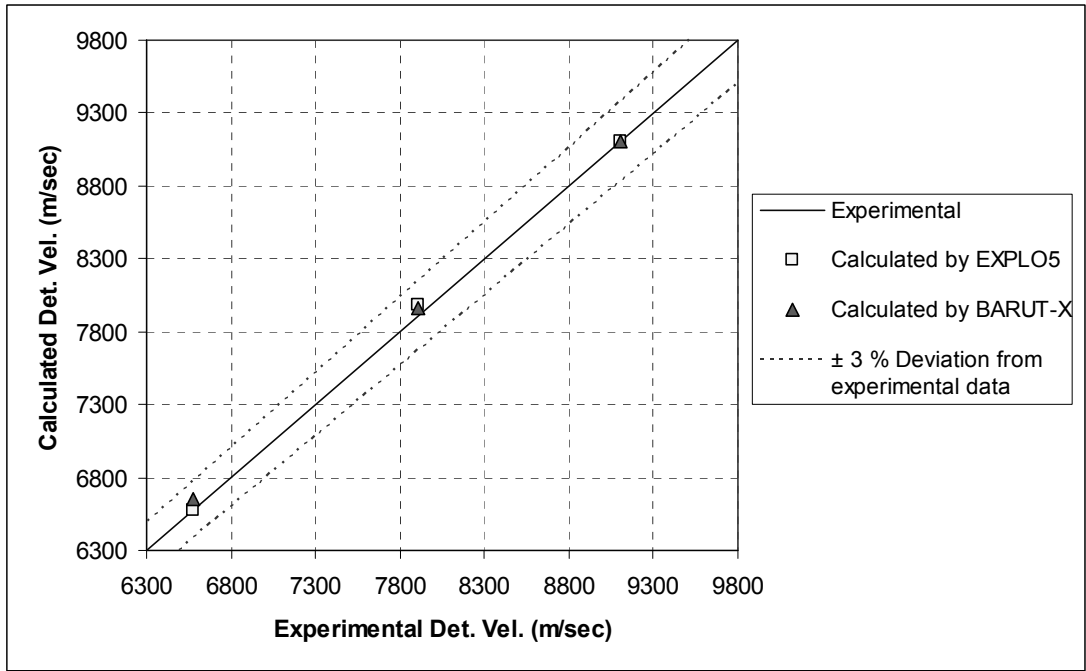


Figure 25. Comparison of calculated and experimental values of detonation velocity for different densities of HMX

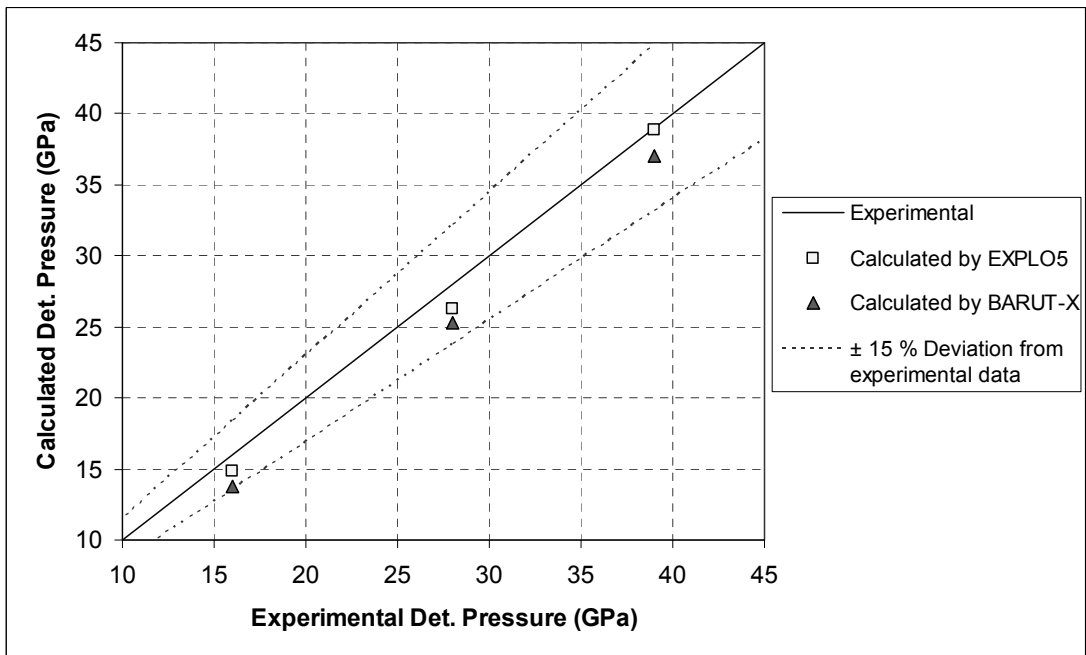


Figure 26. Comparison of calculated and experimental values of detonation pressure for different densities of HMX

Table 49. Comparison of calculated and experimental values of detonation parameters for different densities of TNT

Explosives	Density g/cm ³	Method	Detonation Velocity (m/sec)	Detonation Pressure (GPa)
TNT	1.640	Experimental [66]	6950	21.0
		EXPLO5 [66]*	6940	20.5
		BARUT-X**	6948	18.7
		Deviation 1, %	-0.03	-10.95
		Deviation 2, %	0.12	-8.78
	1.632	Experimental [66]	7070	20.5
		EXPLO5 [66]*	6920	20.4
		BARUT-X**	6921	18.50
		Deviation 1, %	-2.11	-9.76
		Deviation 2, %	0.01	-9.31
	1.533	Experimental [66]	6810	17.10
		EXPLO5 [66]*	6620	17.70
		BARUT-X**	6618	16.20
		Deviation 1, %	-2.82	-5.26
		Deviation 2, %	-0.03	-8.47
	1.00	Experimental [66]	5000	6.70
		EXPLO5 [66]*	5130	7.70
		BARUT-X**	5096	7.00
		Deviation 1, %	1.92	4.48
		Deviation 2, %	-0.66	-9.09

* - TNT-type of parameters in BKW Equation is used by EXPLO5 [66].

** - TNT-type of parameters in BKW Equation is used by BARUT-X.

Deviation 1 – The percent of difference between data by BARUT-X and experimental data.

Deviation 2 – The percent of difference between data by BARUT-X and data by EXPLO5.

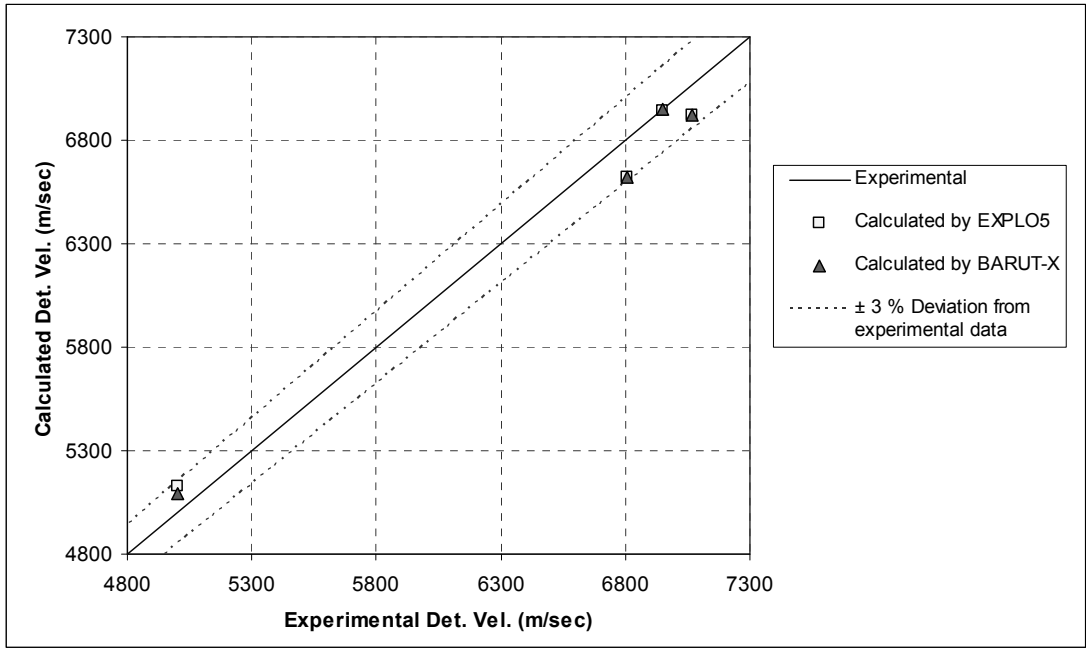


Figure 27. Comparison of calculated and experimental values of detonation velocity for different densities of TNT

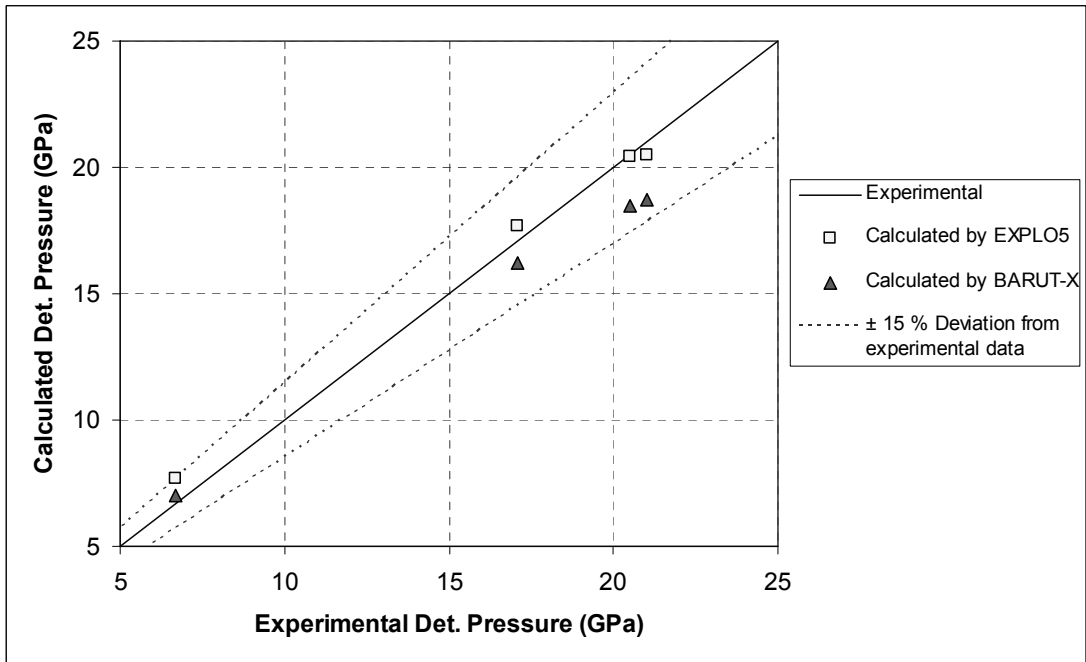


Figure 28. Comparison of calculated and experimental values of detonation pressure for different densities of TNT

Table 50. Comparison of calculated and experimental values of detonation parameters for different densities of RDX

Explosives	Density g/cm ³	Method	Detonation Velocity (m/sec)	Detonation Pressure (GPa)
RDX	1.80	Experimental [66]	8750	34.7
		EXPLO5 [66]*	8750	34.6
		BARUT-X**	8737	33.0
		Deviation 1, %	-0.15	-4.98
		Deviation 2, %	-0.15	-4.71
	1.66	Experimental [66]	8240	29.3
		EXPLO5 [66]*	8210	28.7
		BARUT-X**	8189	27.5
		Deviation 1, %	-0.62	-6.14
		Deviation 2, %	-0.26	-4.18
	1.20	Experimental [66]	6770	15.2
		EXPLO5 [66]*	6660	14.7
		BARUT-X**	6655	14.0
		Deviation 1, %	-1.70	-7.89
		Deviation 2, %	-0.08	-4.76
1.00	Experimental [66]	6100	8.90***	
	EXPLO5 [66]*	6070	10.70	
	BARUT-X**	6046	10.20	
	Deviation 1, %	-0.89	14.61	
	Deviation 2, %	-0.40	-4.67	

* - RDX-type of parameters in BKW Equation is used by EXPLO5 [66].

** - RDX-type of parameters in BKW Equation is used by BARUT-X.

*** - This detonation pressure value is according to M. Hobbs and M. Baer [67]

Deviation 1 – The percent of difference between data by BARUT-X and experimental data.

Deviation 2 – The percent of difference between data by BARUT-X and data by EXPLO5.

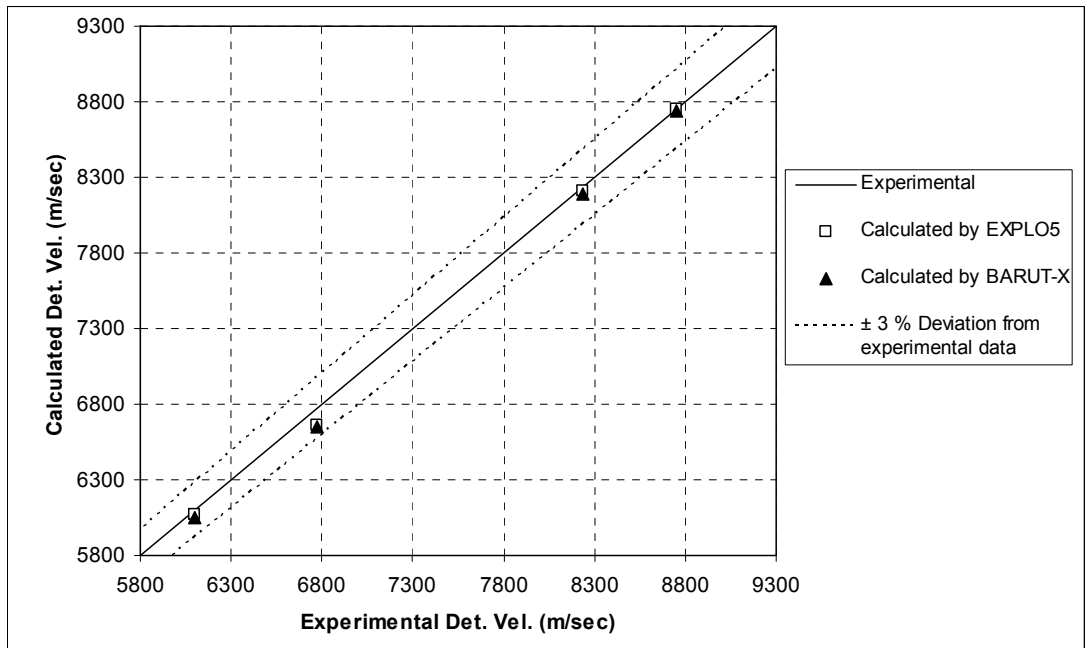


Figure 29. Comparison of calculated and experimental values of detonation pressure for different densities of RDX

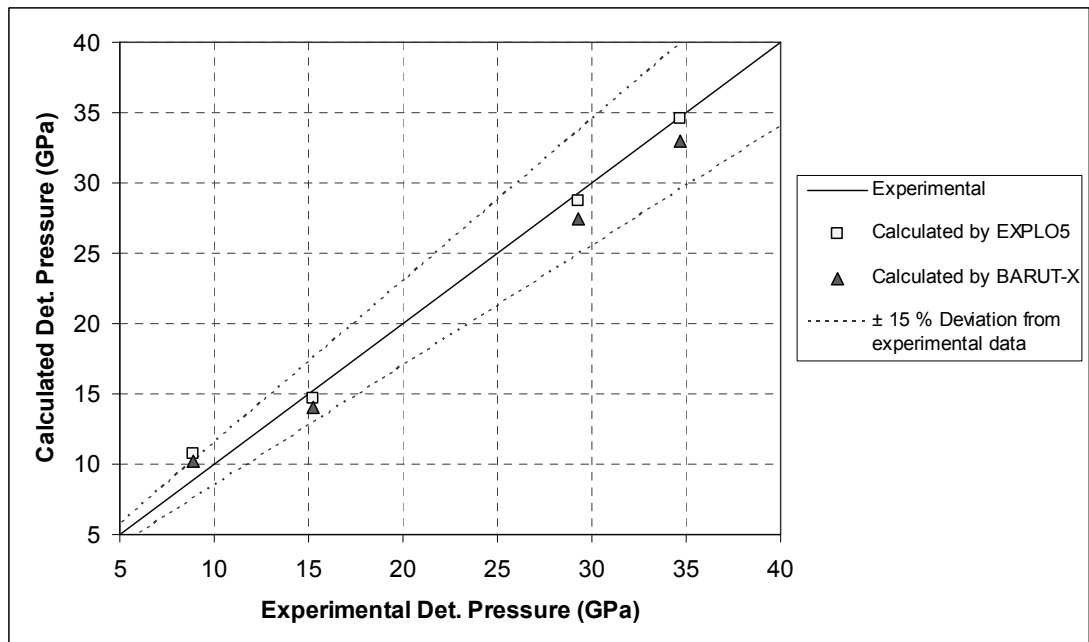


Figure 30. Comparison of calculated and experimental values of detonation pressure for different densities of RDX

Table 51. Comparison of calculated and experimental values of detonation parameters for different densities of PETN

Explosives	Density g/cm ³	Method	Detonation Velocity (m/sec)	Detonation Pressure (GPa)
PETN	1.763	Experimental [66]	8270	31.5
		EXPLO5 [66]*	8650	32.7
		BARUT-X**	8356	30.5
		Deviation 1, %	1.04	-3.17
		Deviation 2, %	-3.40	-6.73
	1.60	Experimental [66]	7750	26.6
		EXPLO5 [66]*	7990	26.2
		BARUT-X**	7768	24.7
		Deviation 1, %	0.23	-7.26
		Deviation 2, %	-2.78	-5.84
	1.503	Experimental [66]	7480	24.0
		EXPLO5 [66]*	7630	22.8
		BARUT-X**	7437	21.6
		Deviation 1, %	-0.57	-9.92
		Deviation 2, %	-2.53	-5.18
	1.263	Experimental [66]	6590	16.0
		EXPLO5 [66]*	6760	15.8
		BARUT-X**	6706	15.4
		Deviation 1, %	1.76	-3.75
		Deviation 2, %	-0.80	-2.53

* - RDX-type of parameters in BKW Equation is used by EXPLO5 [66].

** - RDX-type of parameters in BKW Equation is used by BARUT-X.

Deviation 1 – The percent of difference between data by BARUT-X and experimental data.

Deviation 2 – The percent of difference between data by BARUT-X and data by EXPLO5.

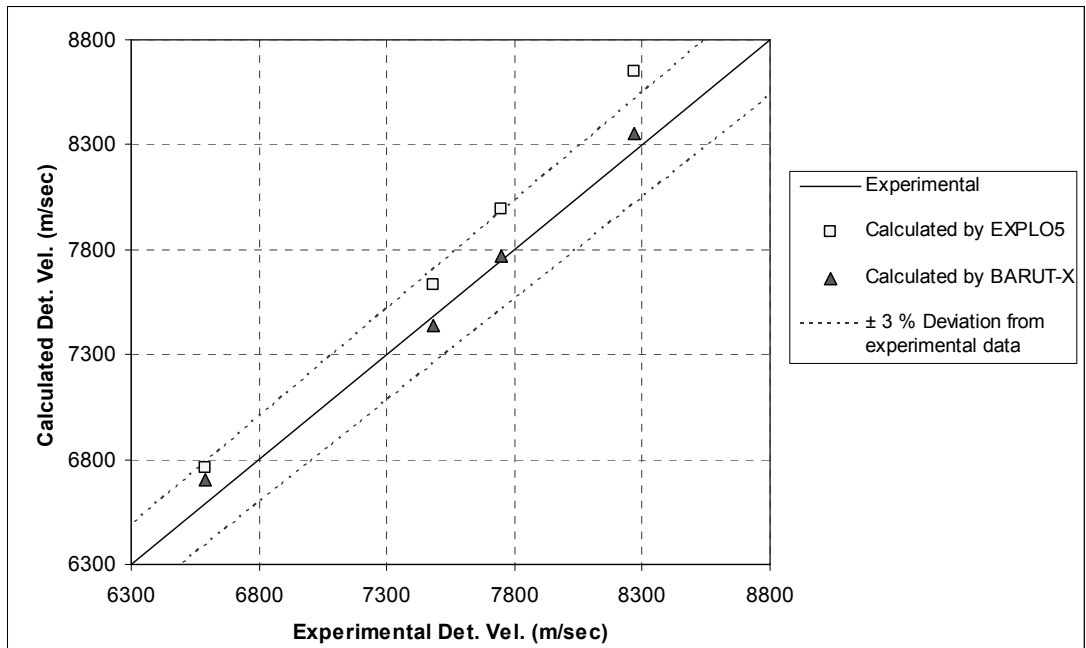


Figure 31. Comparison of calculated and experimental values of detonation pressure for different densities of PETN

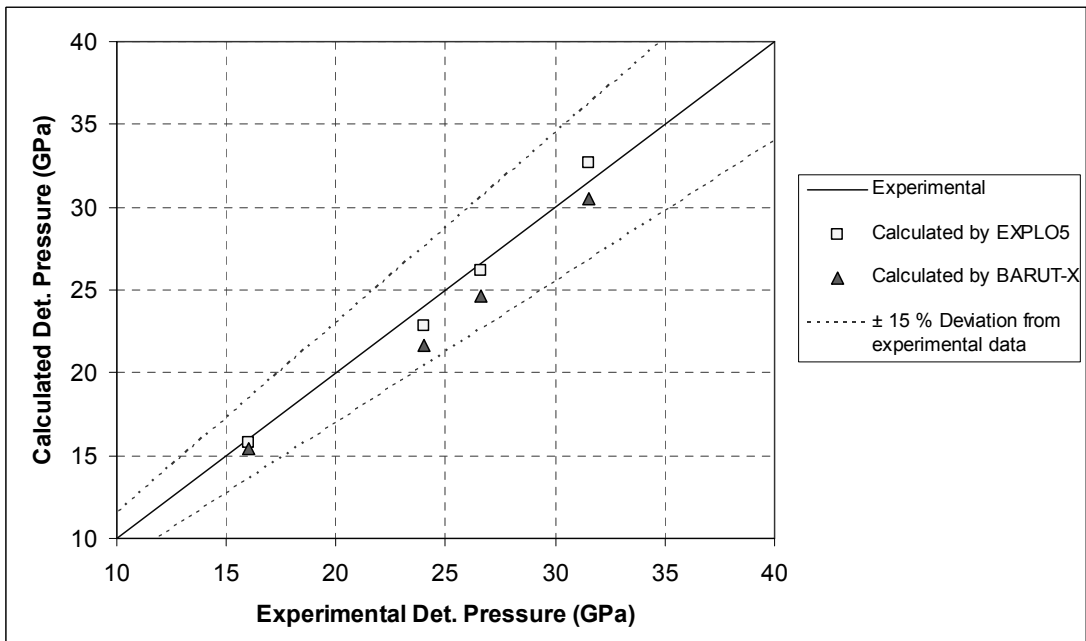


Figure 32. Comparison of calculated and experimental values of detonation pressure for different densities of PETN

If the results calculated by BARUT-X, and experimental data in Table 48 are compared by means of Figure 26, the maximum deviation between BARUT-X and experiments is observed in the detonation (C-J) pressure by about 15%. The deviation in detonation pressure between results of BARUT-X and experimental data shows an increase with the decrease of loading density of HMX. Also the maximum deviation in detonation pressure between BARUT-X and EXPLO5 is observed for the minimum density in the table. However, except the minimum density, the deviation between BARUT-X and EXPLO5 does not exceed 5 %. On the other hand, considering Figure 25 it can be inferred that BARUT-X has a great agreement in detonation velocity with both EXPLO5 and experiments. The calculated detonation velocity by BARUT-X differs from the experimental data by less than 3 %.

Different from the other explosives, due to the high carbon/oxygen ratio in the chemical formula of the TNT, TNT type BKW parameters are used. The maximum deviation is observed between BARUT-X and experiments in detonation pressure with difference of 10.95 % (Table 49) for TNT, whereas the difference in detonation velocity is less than 3 %. Also, BARUT-X and EXPLO5 are in good agreement for detonation velocity (Figure 27).

If Figures 29 and 30 for RDX, and Figures 31 and 32 for PETN are analyzed, the similar case is observed that while there is a discrepancy between the calculated detonation pressure by BARUT-X and experimental ones, the calculated and experimental detonation velocity has a reasonably satisfactory agreement. Also, the same consequence can be deduced for EXPLO5 despite the better agreement in detonation pressure with experimental ones than BARUT-X.

For Mader [35], the reason of the discrepancy observed between calculated and experimental detonation pressures (C-J pressure), while there is a great agreement in detonation velocity, is the nonsteady-state nature of the detonation wave. He states that real detonations are not steady-state and chemical equilibrium may not be necessarily achieved, which could result in a larger error (up to 20 %) on calculated detonation pressures and temperatures than on the calculated detonation velocities (up to 10%). For engineering purpose, however, these errors obtained using BKW EOS could be considered adequate. Also according to Mader [35], the

variation of the density and the composition of the products in a wide range should be taken into account for bearing out the validity of the previous assertion.

BARUT-X uses the BKW Equation of State which has been also applied to the FORTRAN BKW by Mader [51]. The maximum difference between calculated pressures by BARUT-X and experimental detonation pressures is below 10 % for TNT, and PETN. For HMX and RDX, the maximum difference is about to 15 % for detonation pressures. On the other hand, the difference between calculated detonation velocities by BARUT-X and experimental velocities does not exceed 3 %. These results are in the limits of adequate equation of state according to Mader. Therefore, it can be deduced that BARUT-X performs the calculations of detonation parameters in acceptable engineering approach.

The results of BARUT-X are compared with not only experimental data but also those computed by EXPLO5 developed by Sućeska. BARUT-X and EXPLO5 uses the same BKW set of constants in computations. The maximum difference between two programs is observed in computed detonation pressure by about 10 %, however the difference between calculated detonation velocities is below 1% for HMX, TNT and RDX. For PETN, maximum deviation in velocities is about 3% but BARUT-X has better agreement with experiments than EXPLO5. The difference between the two computer codes may be caused by the differences in the numerical models. The basic differences between the two programs are,

1. Determination of the Chapman-Jouguet point is performed according to tangency between Rankine-Hugoniot curve and Rayleigh line at Chapman-Jouguet point by BARUT-X. But, EXPLO5 uses the minimum detonation velocity along the Rankine-Hugoniot curve to determine the Chapman-Jouguet point as does FORTRAN BKW,
2. BARUT-X uses a commercial optimization solver coupled with FORTRAN to calculate the equilibrium composition at Chapman-Jouguet point, however, EXPLO5 performs the chemical equilibrium calculations according to the method developed by White et al. [42],
3. The thermodynamic data libraries used by two computer codes are completely different. BARUT-X uses the thermodynamic data library [53, 54] developed by NASA Glenn Research Center,

4. EXPLO5 may apply some correction equations other than BKW and Cowan & Fickett Equation of States.

In order to test BARUT-X for detonation parameters different than pressure and velocity, the heats of detonation for some explosives calculated by BARUT-X are compared with those calculated by EXPLO5 in Table 52. Both programs use the BWKR type of parameters (Table 47) in BKW Equation of State for calculations of heat of detonation. The calculated results by EXPLO5 given in third column are the heats of detonation values of the explosives with the inclusion of solid carbon formation, of which enthalpy of formation is equal to zero.

The maximum difference between two programs is less than 3 % in Table 52. According to these results it can be inferred that there is an obvious consistency between two computer codes in terms of heats of detonation. The heat of detonation principally depends on the mole numbers of the detonation products for the same enthalpy of formations. So, this consistency also shows the agreement in chemical equilibrium computations of two programs. Because EXPLO5 and FORTRAN BKW use the similar equilibrium routine to calculate the detonation composition, there shall be an agreement between BARUT-X and FORTRAN BKW. Considering Table 53, the prefect agreement in computations of detonation composition can be confirmed. Also this result yields that BARUT-X accurately performs the calculation of equilibrium composition.

Table 52. Comparison of calculated values of detonation heat

Explosive	Density (g/cm ³)	Heats of detonation calculated by EXPLO5 [68] (kJ/kg)	Heats of detonation calculated by BARUT-X (kJ/kg)	Deviation %
HMX	1.89	-6214	-6144	-1.13
	1.20	-5666	-5580	-1.51
HNS	1.649	-5520	-5429	-1.64
	1.017	-4662	-4533	-2.76
PETN	1.735	-6269	-6168	-1.62
	1.496	-5897	-5912	0.25
	1.34	-5895	-5797	-1.65
TNT	1.533	-5247	-5147	-1.91

Table 53. Comparison of calculated mole numbers of detonation products per mole of explosive at C-J point

Product*	HMX $\rho_1 = 1.90 \text{ g/cm}^3$		TNT $\rho_1 = 1.64 \text{ g/cm}^3$		RDX $\rho_1 = 1.80 \text{ g/cm}^3$	
	F. BKW** [35]	BARUT-X	F. BKW** [35]	BARUT-X	F. BKW** [35]	BARUT-X
H ₂ O	4.00	4.00	2.50	2.50	3.00	3.00
H ₂	0.00	0.00	0.00	0.00	0.00	0.00
O ₂	0.00	0.00	0.00	0.00	0.00	0.00
CO ₂	2.00	2.00	1.66	1.66	1.49	1.49
CO	0.008	0.008	0.188	0.18	0.022	0.022
NH ₃	0.00	0.00	0.01	0.00	0.00	0.00
CH ₄	0.00	0.00	0.00	0.00	0.00	0.00
NO	0.00	0.00	0.00	0.00	0.00	0.00
N ₂	4.00	4.00	1.50	1.50	3.00	3.00
Cs	2.00	2.00	5.15	5.16	1.49	1.49

* Mole number of products per mole of explosive (mole / per mole of explosive)

** FORTRAN BKW code by Mader [35]

CHAPTER 5

SUMMARY and CONCLUSIONS

5.1. Summary and Conclusions

The earliest and simplest theory, which interprets the detonation phenomena in a successful manner even today, is the Chapman-Jouguet Theory. The theory discusses the expanding gases behind the reaction zone in thermodynamic equilibrium after instantaneous chemical reaction. Also the theory assumes that the flow is steady-state, inviscid, adiabatic, and one dimensional with negligible body force and shaft work.

On the basis of Chapman-Jouguet Theory, GasPX and BARUT-X, which are computer codes written in FORTRAN language, have been developed to determine the Chapman-Jouguet detonation state parameters. The computations are performed in the assumptions of steady-state and chemical equilibrium conditions.

In order to compute equilibrium composition at the detonation point, a chemical equilibrium code has been developed. This code has an improved algorithm than the other computer codes (CEA, FORTRAN BKW and EXPLO5) which generally use the method developed by White et al. [42]. A commercial non-linear optimization solver coupled with FORTRAN has been adapted to the computation of chemical equilibrium. An objective function, which is a non-linear equation, is derived from Gibbs free energy function of the final state. This non-linear equation defined as an objective function is solved to determine the minimum value of Gibbs function by the commercial optimization solver while the mass balance is satisfied.

GasPX is a computer code which can calculate the detonation point properties in detonation of energetic gaseous mixtures. Examining the compressibility of the product gaseous mixture, the ideal gas equation of state is reckoned adequate to describe the gaseous products. GasPX calculates thermodynamic properties of the reactants and products by using the thermodynamic data library file named "thermo.inp" developed by NASA Glenn Research Center. Detonation parameters of

several gaseous mixtures in different composition ratios have been performed by GasPX. The results are compared with the experimental data and results obtained by NASA-Lewis CEA code and by other theoretical calculations. The calculated detonation velocities of hydrogen-oxygen reactant gas mixtures have displayed adequate agreement with experimental measurements. With the addition of helium into the hydrogen-oxygen mixture, the calculated detonation velocities by GasPX are within the 10 % of measured values however, the same difference is observed between the results computed by NASA-Lewis CEA code, and experimental data. GasPX shows a satisfactory agreement with the calculations in the reference [12] for detonation pressures, temperatures and velocities with a difference less than 3 %. The similar comparisons are performed for acetylene-oxygen mixture to test the accuracy of the GasPX. Considering the formation of the solid carbon in the product for acetylene-oxygen reactant mixture, the calculated results by GasPX become reasonably consistent with the experimental measurements. The comparisons of the results of GasPX with the calculated results in the reference [57] show the great agreement (less than 2% difference) for detonation velocity and pressure. A similar satisfactory agreement between GasPX and experimental data as well as the computations in the reference [48] is obtained for the cyanogen-oxygen mixture. According to these comparisons, it can be concluded that GasPX performs the computations of the detonation parameters with adequate accuracy for detonation in gaseous mixture.

The other code, BARUT-X, has been developed to compute the detonation parameters of C-H-N-O based solid explosives in accordance with Chapman-Jouguet Theory and in chemical equilibrium condition. Since the ideal-gas assumption is not adequate to describe the state of detonation products at high density and high pressure, the BKW Equation of State is applied to the BARUT-X code. The detonation products of explosives can include solid products such as graphite. Although most of solid products are generally assumed to be incompressible, the volume occupied by the solid carbon in the detonation products is corrected using Cowan & Fickett Equation of State. The ideal part of product mixture is computed by means of thermodynamic data library developed by NASA Glenn Research Center. The computer code BARUT-X is tested by the comparison of the computed values for the detonation parameters to the experimental values for some explosives with different loading densities. There is a good agreement

between BARUT-X predictions and the experimental data in terms of the detonation velocities, for which deviation does not exceed 3 %. However, significant deviation is observed in the detonation pressure within 15 % of the experimentally measured values. These results are consistent with the explanation made by Mader. For him [35], the reason of the notable deviation observed between calculated and experimental detonation pressures (C-J pressure) while there is a great agreement in detonation velocity, is the nonsteady-state nature of the detonation wave. Also the detonation heat and product composition computed by BARUT-X are compared with results computed by the EXPLO5 and FORTRAN BKW computer programs. For these detonation parameters, BARUT-X displays a satisfactory agreement with the computer programs, with a difference less than 3%. Considering the good agreement of the calculated results with the experimental measurements and the results of other codes, BARUT-X can be considered a successful prediction tool for the detonation of solid explosives. However, since there is a significant deviation between computations and experiments for detonation pressure in different loading densities of explosives, the numerical model of BARUT-X needs to be improved.

5.2. Future Work

The calculations of Chapman-Jouguet detonation point parameters are successfully performed by GasPX for gaseous reactants. In solid explosives, BARUT-X displays an adequate agreement with the experimental measurements. Although the deviation of the calculated detonation pressures from the experiments is in the limits defined as the satisfactory for numerical models by Mader, the computations of the detonation pressure should be improved. The future work should attempt to handle and optimize the numerical model of BARUT-X for improving the consistency between computations and measurements for pressure.

The BKW Equation of State for the gaseous products is used in BARUT-X. This equation of state has optimized adjustable parameters to provide good agreement with C-H-N-O based ideal explosives. In order to obtain better agreement in nonideal explosives, which would exhibit nonsteady and time dependent behavior, JCZ equation of state, should be implemented in BARUT-X code while the BKW Equation of State should be operable on demand. The success of JCZ equation of

state in BARUT-X should be validated for either ideal or nonideal explosives by comparing the results with experimental data.

The expansion isentrope calculation should be implemented within BARUT-X. After determination of the Chapman-Jouguet point, the isentropic expansion of the products gaseous mixture into the surrounding medium should be computed by adding a calculation routine within BARUT-X. And thanks to commercial optimization solver, parameters in JWL [69] (Jones-Wilkins-Lee) equation should be derived from the computed isentropic expansion curve by BARUT-X. After execution of these future intentions, the experimental studies on determination of the detonation and expansion parameters should be conducted later on.

REFERENCES

1. Berthelot, M., and Vielle, P., *On The Velocity of Propagation of Explosive Processes in Gases*, Compt. Rend. Acad. Sci., Paris, **93**, 18 (1881).
2. Mallard, E., and Le Chatelier, H., *On the propagation velocity of burning in gaseous explosive mixtures*, Compt. Rend. Acad. Sci., Paris, **93**, 145 (1881).
3. Berthelot, M., and Vielle, P., *On Explosive Waves*, Compt. Rend. Acad. Sci., **94**, 149, 822 (1882)
4. Le Chatelier, H., "Sur le développement et la propagation de l'onde explosive" Compt. Rend. Acad. Sci., Paris, **130**, 1755 (1900)
5. Bone, W. A., and Townend, D. T. A., *Flame and Combustion in Gases*, Longmans, Green, London, 1927.
6. Chapman, D. L., *On the Rate of Explosion in Gases*, Phil. Mag. [5] 47, 90 (1899)
7. Jouguet, E., *On the Propagation of Chemical Reactions in Gases*, J. Mathématique, p. 347 (1905); "Mécanique des Explosifs," O. Doin, Paris, 1917; see also, L. Crussard, Bull.Soc. Ind. Minérale St.-Etienne 6, 109 (1907).
8. Becker, R., *Impact Waves and Detonations*, Z. Physik, **8**, 321 (1922) (English translation: NACA TM 505 and TM 506, Mrach 1929); Z. Elektrochem. 42, 457 (1936).
9. Zel'dovich, Ya. B., Kompaneets, A. S., *Theory of Detonation*, Academic Press, New York, 1960.
10. Zel'dovich, Ya. B., Raizer, Yu. P., *Physics of Shock Waves and High-Temperature Hydrodynamic Phenomena*, Volume I, Academic Press, New York, 1966.

11. Fickett, W., Davis, W. C., *Detonation: Theory and Experiment*, Dover Publications; Unabridged Edition (March 2, 2001).
12. Berets, D. J., Greene, E. F., and Kistiakowsky, G. B., *Gaseous Detonations. I. Stationary Wave in Hydrogen-Oxygen Mixtures*, Journal of the American Chemical Society, vol. **72**, 1080 (1950).
13. Laffitte, P., *Sur la formation de l'onde explosive*, *Comptes Rendues*, **176**, 1392, 1923.
14. Wendlandt, R., *Z. physik. Chem.*, **116**, 227, 1925.
15. Payman, W. and Walls, J., *The Rate of Detonation in Complex Gaseous Mixtures*, *J. Chem. Soc.* vol. **123**, p. 420 (1923).
16. Dixon, H. B., *Bakerian Lecture: The Rate of Explosion in Gases*, *Phil. Trans. Roy. Soc.* **A184**, 97 (1893).
17. Dixon, H. B., *On the Movements of the Flame in the Explosion of Gases*, *Phil. Trans. Roy. Soc.* **A200**, 315 (1903).
18. Bone, W. A., Fraser, R. P., and Wheeler, W. H., *Phil. Trnas. Roy. Soc.*, **A235**, 29 (1936).
19. Lewis, B., and Friauf, J. B., *Explosions in Detonating Gas Mixtures. I. Calculation of Rates of Explosions in Mixtures of Hydrogen and Oxygen and the Influence of Rare Gases*, *J. Am. Chem. Soc.*, Vol. **52**, p. 3905, 1930.
20. Duff, R. E., Knight, H. T., and Rink, J. P., *Precision Flash X-Ray Determination of Density Ratio in Gaseous Detonations*, *Phys. Fluids*, **1**, 393 1958.
21. Edwards, D. H., Jones, T. G., and Price, B., *Observation on Oblique Shock Waves in Gaseous Detonations*, *J. Fluid Mech.*, **17**, 21, 1963.
22. Peek, H. M., and Thrap, R. G., *Gaseous Detonations in Mixtures of Cyanogen and Oxygen*, *Journal of Chemical Physics*, **26**, 740, 1957.

23. White, D. R., *Turbulent Structure of Gaseous Detonation*, Phys. Fluids, **4**, 465, 1961.
24. Freedman, E., *BLAKE-A Thermodynamics Code based on TIGER: Users' guide and manual*, Technical Report ARBRL-TR-02411, Ballistic Research Laboratory, Aberdeen Proving Ground, Maryland (1982).
25. Gordon, S., and McBride, B. J., *Computer Program for Calculation of Complex Chemical Equilibrium Compositions and Applications, I. Analysis, II. Users Manual and Program Description*, NASA Reference Publication 1311, 1994.
26. Deal, W. E., *Measurement of Chapman-Jouguet Pressure for Explosives*, Journal of Chemical Physics, **27**, 796. 1957.
27. Rivard, W. C., Venable, D., Fickett, W., and Davis, W. C., *Flash X-Ray Observation of Marked Mass Points in Explosive Products*, In Fifth Symposium (International) on Detonation, pp.3-11, Washington, D.C.: Office of Naval Research – Department of the Navy (ACR-184) 1970.
28. Davis, W. C., and Venable, D., *Pressure Measurements for Composition B-3*, In Fifth Symposium (International) on Detonation, pp. 13-21. Washington, D.C.: Office of Naval Research – Department of the Navy (ACR-184), 1970.
29. Mader, C. L., and Craig, B. G., *Nonsteady-State Detonations in One-Dimensional Plane, Diverging, and Converging Geometries*, Los Alamos Scientific Laboratory Report LA-3720, 1975.
30. Davis, W. C., *Magnetic Probe Measurements of Particle Velocity Profiles*, In Sixth Symposium (International) on Detonation, pp. 637-641. Washington, D.C.: Office of Naval Research – Department of the Navy (ACR-221), 1976.
31. Edited by Mader, C. L., Johnson, J. N., Crane, S. L., *Los Alamos Explosives Performance Data*, University of California Press, Berkeley, California, 1982.
32. Volk, F., Bathelt, H., *Application of the Virial Equation of State in Calculating Interior Ballistic Quantities*, Propellants, Explosives, Pyrotechnics, **1**, 7, 1976

33. Kistiakowsky, G. B., and Wilson, E. B., *The Hydrodynamic Theory of Detonation and Shock Waves*, US Office of Scientific Research and Development Report OSRD-114 (1941).
34. Cowperthwaite, M., and Zwisler, W. H., *Proceedings of the Sixth Symposium (International) on Detonation*, Coronada, CA (Office of Naval Research ACR-221,1976)), pp. 162.
35. Mader, C. L., *Numerical Modeling of Explosives and Propellants*, 2nd edition, CRC Press, Boca Raton, FL, USA (1998).
36. Levine, H. B. and Sharples, R. E., *Operator's Manual for RUBY*, Lawrence Livermore National Laboratory, UCRL-6815, 1962.
37. Hobbs, M. L., Baer, M. R., *Nonideal Thermoequilibrium Calculations Using A Large Product Species Data Base*, *Shock Waves*, **2**, 177, 1992
38. Fried, L., Souers, P., *CHEETAH: A Next Generation Thermochemical Code*, Lawrence Livermore National Laboratory, UCRL-ID-117240, 1994.
39. Sućeska, M., *Calculation of the Detonation Properties of C-H-N-O Explosives, Propellants, Explosives, Pyrotechnics*, **16**,197, 1991.
40. Kamlet, M. J., and Jackobs, S. J., *Chemistry of Detonations. I. A Simple Method for Calculating Detonation Properties of C-H-N-O Explosives*, *Journal of Chemical Physics*, **48**, 23, 1968.
41. Rothstein, L. R., and Petersen, L., *Predicting High Explosive Detonation Velocities from their Composition and Structure*, *Propellants, Explosives, Pyrotechnics*, **4**, 56, 1979.
42. White, W. B., Johnson, S. M., and Dantzig, G. B., *Chemical Equilibrium in Complex Mixtures*, *The Journal of Chemical Physics*, **28**, 751, 1958.
43. Kenneth Kuan-yun Kuo, *Principles of Combustion*, John Wiley & Sons, Singapore, pp. 231-284, 1986.

44. Turns, S. R., *An Introduction to Combustion, Concepts and Applications*, Second Edition, McGraw-Hill, Singapore, pp. 599-620, 2000.
45. Scoria, R. L., *On the Thermodynamic Theory of Detonation*, Journal of Chemical Physics, **3**, 425, 1935.
46. Moran, M. J., Shapiro, H. N., *Fundamentals of Engineering Thermodynamics*, 3rd edition, John Wiley & Sons, New York, USA, 1998.
47. Obert, E. F., *Concepts of Thermodynamics*, McGraw-Hill, New York, 1960.
48. Kistiakowsky, G. B., Knight, H. T., and Malin, M. E., *Gaseous Detonations. III. Dissociation Energies of Nitrogen and Carbon Monoxide*, The Journal of Chemical Physics, **20**, 876, 1952.
49. Kistiakowsky, G. B., and Wilson, E. B., *Report on the Prediction of Detonation Velocities of Solid Explosives*, US Office of Scientific Research and Development Report OSRD-69 (1941).
50. Cowan, R. D., and Fickett, W., *Calculation of the Detonation Properties of Solid Explosives with the Kistiakowsky-Wilson Equation of State*, The Journal of Chemical Physics, **24**, 932, 1956.
51. Mader, C. L., *FORTTRAN BKW: A Code for Computing the Detonation Properties of Explosives*, Los Alamos Scientific Laboratory of The University of California, LA-3704, 1967.
52. Borg, R. A. J., Kemister, G., and Jones, D. A., *Chemical Equilibrium Calculations for Detonation Products*, Defense Science and Technology Organization, DSTO-TR-0226, 1995.
53. McBride, B. J., Zehe, M. J., and Gordon, S., *NASA Glenn Coefficients for Calculating Thermodynamic Properties of Individual Species*, Glenn Research Center, NASA/TP-2002-211556, Ohio, 2002.
54. Zehe, M. J., Gordon, S., and McBride, B. J., *CAP: A Computer Code for Generating Tabular Thermodynamic Functions from NASA Lewis Coefficients*, Glenn Research Center, NASA/TP-2001-210959/REV1, Ohio, 2002.

55. Zeleznik, F. J., and Gordon, S., *Calculation of Detonation Properties and Effect of Independent Parameters on Gaseous Detonation*, ARS J., **32**, 605-615, 1962.
56. Breton, J., *Ann. office natl. combustibles liquids*, **11**, 487, 1936; Thésés Faculté des Sciences, Univ. Nancy, 1936.
57. Kistiakowsky, G. B., Knight, H. T., and, Malin, M. E., *Gaseous Detonations. IV. The Acetylene-Oxygen Mixtures*, The Journal of Chemical Physics, **20**, 884, 1952.
58. Lewis, B., Von Elbe, G., *Combustion, Flames and Explosions of Gases*, 3rd Edition, Academic Press Inc., Hartcourt Brace Jovanovich Publishers, Orlando, 1987.
59. Toepler, A., *Optische Studien nach der Methode der Schlieren Beobachtung*, Poggendorff's Ann. **131**, 33, 1867.
60. Le Chatelier, H., *Ann. Chim.*, **20**, 15, 1900.
61. Fickett, W., *On Detonation Properties of Condensed Explosives Calculated with an Equation of State Based On Intermolecular Potential*, LA-2712, Los Alamos Scientific Laboratory of The University of California, Los Alamos, New Mexico, May 1962.
62. Wang, S. Y., Butler, P. B., and Krier, H. *Non-Ideal Equations of State for Combusting and Detonating Explosives*, Progress In Energy and Combustion Science, **11**, 311, 1985.
63. Wescott, B. L., Stewart, D. S., and Davis, W. C., *Equation of State and Reaction Rate for Condensed-Phase Explosives*, 98, 053514, Journal of Applied Physics, 2005.
64. White, A., Zerilli, F.J., and Jones, H. D., *Ab Initio Calculation of Intermolecular Potential Parameters for Gaseous Decomposition Products of Energetic Materials*, DSTO-TR-1016, DSTO Aeronautical and Maritime Research Laboratory, 2000.
65. Jeans, J., *The Dynamical Theory of Gases*, Dover Publications, New York, page 134 (1925).

66. Sućeska, M., *EXPLO5-Computer Program For Calculation of Detonation Parameters*, Proc. of 32nd Int. Annual Conference of ICT, July 3-6, Karlsruhe, German, 2001, pp. 110/1.
67. Hobbs, M. L., Baer, M. R., *Calibration of the BKW-EOS With a Large Product Species Data Base and Measured C-J Properties*, Proc. of the 10th Symp. (International) on Detonation, ONR 33395-12, Boston, MA, July 12-16, 1993. pp. 409-418.
68. Sućeska, M., *Calculation of Detonation Heat by EXPLO5 Computer Code*, Proc. of 30th Int. Annual Conference of ICT, June 29-July 2, Karlsruhe, German, 1999, pp. 50/1.
69. Lan, I. F., and Hung, S. C., *An Improved Simple Method of Deducing JWL Parameters from Cylinder Explosion Test*, Propellants, Explosives, Pyrotechnics, **18**, 18, 1993.

APPENDIX A: Properties of Explosives

Name of Explosives	Full Name of Explosives	Formula	Formula Weight kg/kmol	Enthalpy of Formation at 298.15 K (kJ/kg)
HMX	Octogen	$C_4H_8N_8O_8$	296.15	253.06
RDX	Hexogen	$C_3H_6N_6O_6$	222.11	277.10
TNT	Trinitrotoluene	$C_7H_5N_3O_6$	227.13	-276.50
HNS	Hexanitrostilbene	$C_{14}H_6N_6O_{12}$	450.23	174.0
PETN	Pentrit	$C_5H_8N_4O_{12}$	316.14	-1708.4
TATB	1,3,5-triamino-2,4,6-trinitrobenzene	$C_6H_6N_6O_6$	258.15	-598.46
DATB	1,3-diamino-2,4,6-trinitrobenzene	$C_6H_5N_5O_6$	243.20	-406.28
TETRYL	2,4,6-trinitrophenylmethylnitramine	$C_7H_5N_5O_8$	287.15	68.10
NG	Nitroglycerin	$C_3H_5N_3O_9$	227.10	-1674
NM	Nitromethane	CH_3NO_2	61.04	-1852